

**INVESTIGATION INTO CORROSION PROTECTION
BY COATINGS USING THE ELECTROCHEMICAL
NOISE METHOD**

Thesis submitted in part fulfilment of the requirements for

The Degree of Doctor of Philosophy

2000

**Work was conducted at University College Northampton
(Degree awarded by University of Leicester)**

Stephen J. Mabbutt

UMI Number: U140631

All rights reserved

INFORMATION TO ALL USERS

The quality of this reproduction is dependent upon the quality of the copy submitted.

In the unlikely event that the author did not send a complete manuscript and there are missing pages, these will be noted. Also, if material had to be removed, a note will indicate the deletion.



UMI U140631

Published by ProQuest LLC 2013. Copyright in the Dissertation held by the Author.
Microform Edition © ProQuest LLC.

All rights reserved. This work is protected against
unauthorized copying under Title 17, United States Code.



ProQuest LLC
789 East Eisenhower Parkway
P.O. Box 1346
Ann Arbor, MI 48106-1346

ACKNOWLEDGEMENT

I would like to express my gratitude to my supervisor Dr. Douglas Mills for his guidance and support throughout the period of this work. I am also grateful for the advice and input of my second supervisor Dr. Stuart Lyon of the University of Manchester Institute of Science and Technology (UMIST).

In addition I would like to thank Dr. N. F. Boutle (Head of School, Technology and Design) for his role as part of my supervisory team and additionally for his support of all my academic studies and development since I started at the College.

I am also grateful to the College for its support of my academic and staff development throughout the course of this work.

Kirsty Saunders deserves a special thank you for giving up her evenings to help me compile the thesis and assist with the word processing.

GLOSSARY OF ABBREVIATIONS

<u>Term</u>	<u>Definition</u>
ENM	Electrochemical noise method
EIS	Electrochemical impedance spectroscopy
LPR	Linear polarisation resistance
DC	Direct current
V_n	Potential noise
I_n	Current noise
R_n	Noise resistance
R_{dc}	DC resistance
R_{sn}	Spectral noise resistance
R_p	Polarisation resistance
R_{po}	Pore resistance
R_c	Coating resistance
R_l	Resistance from Nyquist plot
C_{dl}	Double layer capacitance

Investigation into Corrosion Protection by Coatings Using the Electrochemical Noise Method

S. J. Mabbutt

The Electrochemical Noise Method (ENM) monitors the small potential and current fluctuations that occur naturally in electrochemical cells. It is the least intrusive of all electrochemical techniques in common use. This work uses the Electrochemical Noise Method to investigate the corrosion protection afforded by organic coatings. A parameter called Noise Resistance (R_n) is derived from an Ohm law relationship using the potential noise (V_n) and current noise (I_n) values. The noise on the current and potential data sets is calculated as the standard deviation value. The work is divided into three areas. The first looked at coating systems in the intact state on the substrate. In general this part of the work has corroborated previous work where R_n values of $>1 \times 10^7$ ohms-cm² indicated protection of the substrate, correlating with DC resistance values of the coating. The second area of work investigated scribed coatings on the substrate. An important property of organic anti-corrosive coatings is the ability to protect the substrate at a break in the coating. In the scribed work the level of protection afforded at exposed metal by the coating was related to the Noise Resistance value. The third area of this investigation looked at novel ENM techniques to investigate organic coatings. Detached intact coatings were examined in a "U" tube test cell that can be used to simulate different conditions that may be encountered in service. Also a new technique was devised for obtaining ENM data from corrosion cells, this does not require the two separate substrate elements necessary for the more established methodology. The new technique has been called the Single Substrate (SS) technique to reflect this useful property. The technique could be used for in-situ monitoring of structures and it could be adapted for investigation of other situations such as reinforcement bars in concrete.

CONTENTS

1.	CHAPTER 1. Introduction and background	1
1.1	Corrosion Reactions	1
1.2	Corrosion Dynamics	2
1.3	Coatings	2
1.3.1	Oil Based Coating	3
1.3.2	Oils and Fatty Acids	3
1.3.3	Alkyd Resin	5
1.3.3.1	Water-borne Alkyd Resin	5
1.3.3.2	Epoxy Resins	5
1.4	Water-based Two-pack Epoxy Coating	6
1.5	Ionic Resistance as corrosion Protection	7
1.6	Pigments	8
1.7	Coating Performance	9
1.8	Electrochemical Methods	10
1.8.1	The D.C. Resistance Method	10
1.8.2	Electrochemical Impedance Spectroscopy (EIS)	11
1.8.3	Application of EIS	13
1.8.4	Disadvantages of EIS	15
1.9	Electrochemical Noise Measurement (ENM)	16
2.	CHAPTER 2. Literature Review (Electrochemical Noise Monitoring)	17
2.1	Electrochemical Noise Measurement (ENM)	17
2.2	Potential Fluctuations in Corrosion Cells	17
2.2.1	Potential Noise	17
2.3	Potential Noise from Localised Corrosion Mechanisms	22
2.4	ENM Applied to Stress Corrosion Cracking	22
2.4.1	ENM Applied to Pitting Corrosion	24
2.5	Current Noise Monitoring	25
2.6	Current and Potential Monitoring	27
2.7	Characterisation of Noise	27

2.7.1	White Noise and Coloured Noise	28
2.7.2	Measurement in the Frequency Domain	28
2.7.3	Power Spectra and Corrosion Mechanism	29
2.7.4	Higher Order Measures for the Analysis of Electrochemical Noise	30
2.7.5	Fractal Analysis of Noise Data	30
2.8	Noise from Other Sources	31
2.9	Electrochemical Noise Resistance (R_n)	32
2.9.1	Derivation of Noise Resistance (R_n)	33
2.9.2	Applications of Noise Resistance	35
2.10	Relationship Between Resistance Noise (R_n) and Parameters Derived from Electrochemical Impedance Spectroscopy (EIS)	36
2.11	Relationship Between Resistance Noise R_n and D.C. Resistance Measurement R_{dc} on Coated Substrates	39
2.12	Area Effects of Coated Substrates on R_n	40
2.13	Standardisation of Electrochemical Noise Measurement	41
2.14	Experimental Investigation (NDSU Project): Characterisation of Corrosion Under Marine coatings by Electrochemical Noise Methods	42
2.14.1	Overview of the NDSU Report	43
2.14.2	Continuation of ENM Research	50
2.14.3	Publications from the North Dakota Research Project	50
2.15	Publications from Early Work at University College Northampton	50
2.16	Preliminary Published Work Presented at Conference	50
2.16.1	EuroCorr 96	51
2.16.2	EuroCorr 97	52
2.17	Justification of Present Work	53
3.	CHAPTER 3. Experimental - Methodology for General Electrochemical Experiments	54
3.1	Instrumentation	54
3.2	Computer	54
3.3	Zero Resistance Ammeter (ZRA)	55
3.3.1	Software	56
3.4	Electrodes	57
3.4.1	Evaluation of Electrode Noise	54

3.5	Evaluation of Instrument Noise	58
3.6	System Noise	59
3.7	Specimen Materials and Preparation	59
3.7.1	Substrate	59
3.7.2	Coatings	60
3.7.3	Coating Application	60
3.7.4	Blanking	60
3.7.5	Detached Coating	61
3.7.6	Preparation and Removal of Detached Coatings	61
3.8	Experimental set-up	62
3.8.1	Three Electrode System	62
3.8.2	Working Electrodes	62
3.8.3	Reference Electrodes	62
3.9	Experimental Arrangements	63
3.9.1	The Beaker Method	63
3.9.2	Bridge Method	64
3.9.3	Salt Bridge Preparation	65
3.9.4	Effects of Slat Bridge Diameter on Ionic Conduction	65
3.10	Solutions	67
3.10.1	Testing Solutions	67
3.10.2	Ionic Conduction	68
3.11	Experimental Parameters	68
3.12	Data Gathering	69
3.13	Test Protocol	69
3.13.1	Test Length	70
3.13.2	Sample Interval	71
3.14	Shielding	72
3.15	Calculated Parameters	73
3.16	Repeatability of Experiments	74
3.17	Other Techniques - D.C. Resistance Tests on Systems	75
3.18	Other Techniques - Electrochemical Impedance Spectroscopy (EIS)	75
3.18.1	The Nyquist Plot	78

4.	CHAPTER 4. Novel Developments of the Electrochemical Noise Method	79
4.1	Introduction - Questions and Problems of ENM	79
4.2	Detached Coatings	80
4.3	Data analysis of Potential and Current for Frequency Distribution	82
	4.3.1 Kurtosis (4 th Order Moment)	83
	4.3.2 Application of Kurtosis to Real Data	86
	4.3.3 Skewtosis (3 rd Order Moment)	87
	4.3.4 Bi-modal or Non-normal Distribution	90
4.4	Alternative configuration - The Single Substrate Technique	90
5.	CHAPTER 5. Intact Anti-corrosive coating	95
5.1	Introduction and Aims	95
5.2	Coatings and Electrolyte	97
5.3	Testing Procedure	97
5.4	Preliminary Experiment Using Solvent Based Alkyd (Carrs) on Steel and Aluminium Substrate	98
	5.4.1 Preliminary Experiments on Solvent Based Alkyd to Establish Parameters for Testing	99
	5.4.2 Sample Interval Experiment Using Solvent Based Alkyd	99
	5.4.3 Sample Interval Experiment Using Waterborne Alkyd	100
5.5	Intact Water-borne Coatings on Fe	101
	5.5.1 Neocryl Results	101
	5.5.2 Haloflex Results	102
	5.5.3 Comparison of Results from Neocryl and Haloflex	102
	5.5.4 Observations on Water-borne Haloflex and Neocryl Experiments	103
5.6	Waterborne Amine - 2 Pack Epoxy Unpigmented 148 and 152	105
	5.6.1 Elevated Temperature Testing of 148 and 152 Epoxy	106
5.7	Main Experiments on Solvent Systems	107
	5.7.1 Intact 2 Pack Epoxy system (CM) and Intact Solvent Based Alkyd	107
	5.7.2 Additional Testing of Intact 2 Pack Epoxy (CM)	108
5.8	Intact Sealed Red Lead	110
5.9	Interim Conclusions - Justification for Work in Chapter 6	111

6.	CHAPTER 6. Investigation of Scribed Organic Coating	114
6.1	Introduction	114
6.2	Aims	115
6.3	Experimental	115
6.3.1	Scribe Production (Mechanical Coating Removal)	116
6.3.2	Scribe Production (LASER Ablation of Coating)	117
6.3.3	Data Collection	118
6.4	Results	119
6.4.1	Effect on ENM of Potassium Dichromate Inhibitor with Fe in Sulphuric Acid	119
6.4.2	Effects of Leached Inhibitor in Harrison's Solution - (3.5% (NH ₄) ₂ SO ₄ + 0.5% NaCl) Diluted to 0.5%	121
6.4.3	Scribed Waterborne Haloflex and Neocryl in Harrison's Solution	123
6.4.4	Scribed Solvent Based Organic coating in Harrison's Solution - (3.5% (NH ₄) ₂ SO ₄ + 0.5% NaCl) Diluted to 10%	124
6.4.5	Solvent Based CM and RH Results	125
6.4.6	Observations on CM 2 Pack Epoxy and RH Alkyd in 10% Harrison's Solution	126
6.5	Scanning Microscopy Investigation of Corrosion Product at CM Scribes from Immersion in Harrison's Solution (3.5% (NH ₄) ₂ SO ₄ + 0.5% NaCl) Diluted to 10%	128
6.5.1	EDX Analysis of the CM Coating and Scribe Exposed to 10% Harrison's Solution	130
6.6	Scribed CM 2 Pack Epoxy in 0.4% NaCl Solution	131
6.6.1	SEM Analysis of CM Scribe corrosion Product from NaCl Immersion	133
6.6.2	EDX Analysis of CM Scribe Corrosion Product from NaCl Immersion	134
6.7	Conclusion	135
6.8	Investigation of Scribed Red Lead	135
6.8.1	Single Coat Red Lead on Fe in 10% Harrison's Solution	135
6.8.2	Single coat Red Lead Sealed with Non-pigmented Alkyd	136
6.9	Interim conclusion on ENM for Monitoring Inhibition	138
6.10	Mechanistic Information from Data Analysis	139

7.	CHAPTER 7. Results from New Techniques	140
7.1	Introduction	140
7.2	Frequency Distribution Analysis of Time Domain Data Sets	141
7.2.1	Frequency Distribution Analysis of Time Domain Data from Non-pigmented Control Coating	143
7.2.2	Scribed Epoxy Data Analysis	144
7.3	Results from Using the Single Substrate Technique	147
7.3.1	Results from a Preliminary Experiment Comparing the Bridge Method and the Single Substrate Technique Using Solvent Based Alkyd	148
7.3.2	Results from a Comparison of the Single Substrate Technique and the Bridge Method Using CM Epoxy	150
7.3.2.1	Combinations of Cells to Identify Failed Coating Area	152
7.3.3	Results from the Single Substrate Technique compared to the Bridge Method Using RH Alkyd	153
7.4	ENM Results on Detached Coatings	155
7.4.1	Results from Detached Waterborne 152 Compared to "On the Substrate" Values	156
7.4.2	Results of Detached and Attached Pigmented CM Epoxy in Harrison's Solution	157
7.4.3	results from Detached and Attached Solvent Based Alkyd in Harrison's Solution	158
7.4.4	General Observations on Detached coating Investigation by ENM	159
8.	RESULTS 8. Conclusions and Further Work	160
8.1	Conclusions from Chapter 5	160
8.2	Conclusions from Chapter 6	160
8.3	Conclusions from Chapter 7	163
8.4	Further Work	164

REFERENCES

Appendix 1	Data for chapter 4 graphs
Appendix 2	Data for chapter 5 graphs
Appendix 3	Data for chapter 6 graphs
Appendix 4	Data for chapter 7 graphs
Appendix 5	List of co-author publications and presentations 1997 - 2000

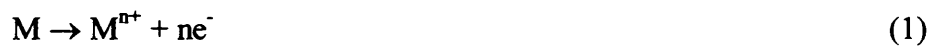
CHAPTER 1

Introduction and Background

1.1 Corrosion Reactions

The corrosion of metals in an aqueous environment constitutes the majority of corrosion processes (Mayne, 1987). For corrosion to take place a transfer of charge between the metal and electrolyte must take place. This is an electrochemical process consisting of two simultaneous but separate reactions.

At the anode the reaction takes the form



Applying this to steel gives:

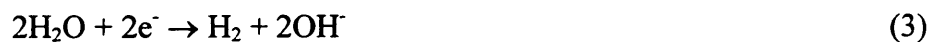


The reactions at the cathode are reduction reactions.

In acid or neutral solutions containing dissolved oxygen the reduction of oxygen is observed.



Where no other reduction reactions prevail water will be reduced



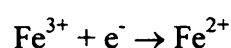
and in acid solutions hydrogen ions are reduced in the reaction



Corrosion cells by their nature contain oxidised ions. These can be reduced in redox reaction



Applied to the iron ion Fe^{3+} the cathodic redox reaction gives



1.2 Corrosion Dynamics

The nature of the surface oxide formed by the reactions outlined in 1.1 greatly affects the resistance of the metal to further corrosion. Many metals form a dense homogenous oxide which is relatively impervious to aqueous solutions. As these oxides form the rate of surface oxidation reduces to a point where the metal is considered resistant to general corrosion and are thereby defined as passive in the particular environment. Non-ferrous metals fall into this category. In conditions favourable to the formation of ferrous oxide plain carbon steels form a complex series of oxides which are easily hydrated and permeable. The effect of this is continued oxidation of the underlying metal and the reason such effort is made to prevent corrosion of steel.

Corrosion can be prevented if the anodic or cathodic reactions on the surface can be stopped or reduced to a very slow rate (Jones, 1996).

1.3 Coatings

Traditionally the most common method of achieving corrosion protection on steel has been the employment of surface coatings. Although not exclusively, coatings of organic origin are used for this purpose. For corrosion to proceed oxygen and water need to be present at the surface of the steel ($O_2 + 2H_2O \rightarrow 4OH^-$). Corrosion rate will be governed by the slower of the diffusion processes. Low rates of corrosion under organic coating have been observed where oxygen diffusion is very low ($\sim 2.5 \text{ mg / cm}^2$ per year) when compared to water permeability which was up to 750 times higher (Guruviah, 1970). Baumann calculated the amount of water which must be present at the metal coating interface. Giving a water permeability rate of just $0.003 - 0.06 \text{ mg / cm}^2$ / per day to give a corrosion rate of $0.02 - 0.35 \text{ mg Fe cm}^2$ /per day. Although oxygen permeation is lower (and in some cases sufficiently low to prevent corrosion) it is the presence of water and oxygen that facilitates corrosion if other aggressive species are present (Haagen and Funke, 1975). The permeability of anions such as Cl^- and $(SO_4)^-$ is therefore important and can be rate determining. Many coatings prevent the migration of

these ions to an extent that they cannot be detected. In cases where failure is by loss of adhesion water permeability can be rate determining with respect to mechanical failure of the system. It has been shown that organic coatings are too permeable to totally prevent corrosion by this mechanism; the cathodic reaction (Mayne, 1987). The anodic reaction can be prevented by inhibitive pigments supplying sufficient electrons to the steel surface to prevent production of Fe^{++} , thus providing cathodic protection. Without cathodic protection the coating must prevent the process by another mechanism. Because the anodic and cathodic sites are spatially situated on the surface of the steel, for the corrosion process to function electrons must flow from anode to cathode through the metal and ions must pass through the coating from cathode to anode to complete the path of conduction. Coatings rely on high ionic resistance to prevent the corrosion process by acting as a barrier to ions, which have a diffusion rate through organic coatings several orders of magnitude less than the diffusion rate of oxygen or water (Mayne, 1987). Coatings which prevent corrosion by this mechanism are termed barrier coatings. Good barrier coatings to O_2 will slow the corrosion rate once it has started but will not prevent corrosion. Inert pigments are often used to enhance this property (Carter, 1987) (section 1.5).

Organic coatings consist of three main constituents; resin, solvent and pigmentation. The resin will be discussed in detail (section 1.3), but essentially it is the final matrix of the solid film that holds the pigments and contributes mainly to the mechanical properties of the coating. The solvent maintains the resin and pigmentation as a liquid to enable application of the coating and dispersion of the pigments within the resin. During curing the solvent portion of the coating will evaporate leaving a solid film. Solvents can be volatile hydrocarbons or with environmental pressure to reduce volatile organic compound emissions water based. Pigments are used for a variety of reasons including; aesthetics, such as colouring or enhanced surface finish. Pigments can be an inert "filler" material to give bulk to the coating and reduce costs by reducing content of more expensive constituents. In the role of primers for steel and anti-corrosive coatings, pigments are added to the coating to help prevent or reduce the corrosion

reactions. These pigments can be organic or non-organic, active or non-active and will be described in detail (1.6).

Most often an organic coating is classified by the resin binder (Lambourne, 1987), e.g. An alkyd coating. The coating may also be classified by the method of prevention of anodic and / or cathodic reactions and categorised by the mechanism of protection (Scantlebury, 1984).

1.3.1 Oil Based Coating

Alkyd resin produced by chemically combining oil derived fatty acids into a polyester polymer structure and was one of the first applications of synthetic polymer synthesis used in surface coatings. Despite this, short oil alkyds are still commonly used in automotive and general industrial applications where they combined melamine/formaldehyde as hardening resins in stoving formulations. Alkyd formulations are defined by the term oil length which refers to the percentage weight of oil in the final formulation. Short oil formulations contain less than 67 % oil which decreases drying time and produces hard coating at the expense of flexibility. Long oil formulations contain more than 67 % oil, these are slower to dry but the coating is more flexible. The long oil formulation is commonly used as an undercoat and for exterior varnish.

1.3.2 Oils and Fatty acids

The oils are mixed glycerol esters of the long chain monocarboxylic acid, the general term for this group is fatty acids. The chains are usually contain 18 carbon atoms C_{18} which terminate in a carboxyl (COOH). The oils can be grouped into drying, semi-drying or non-drying and this is determined by the ability of the un-modified oil to oxidise and cross-link into a film. The ability of the oil to cross-link depends on the nature of the bonds contained in the fatty acid chain. If the fatty acid chain contains no double bonds it is termed saturated, where one double bond is present it is said to be unsaturated. Where two or more double bonds are present in the fatty acid chain it said to polyunsaturated. For an oil to be classed as drying it must contain at least 50 % polyunsaturated fatty acids. Typical fatty acids include; Lauric

[CH₃ (CH₂)₁₀ COOH], Stearic acid [CH₃ (CH₂)₁₆ COOH], Linoleic acid [CH₃ (CH₂)₄ CH=CH CH₂ CH=CH (CH₂)₇ COOH] and Linolenic acid [CH₃ CH₂ CH=CH CH₂ CH=CH CH₂ CH=CH (CH₂)₇ COOH]. Linseed oil, commonly used in alkyd coating is considered a drying oil and contains in excess of 60 % of polyunsaturated linoleic and linolenic acids. Polymerisation of oils is believed to involve the movement of the double bonds in the autoxidative crosslinking process (Bentley,1987).

1.3.3 Alkyd Resin

Oils are not readily reactive with polyester and as such require modification before they can be used in the alkyd coating. This involves reacting the oil with glycerol to form monoglyceride or one of several other techniques depending on whether long or short oil alkyd is being produced.

1.3.3.1 Water-borne Alkyd resin

In an attempt to limit the amount of volatile organic compounds (VOCs) released to the atmosphere every year a move towards coatings with lower or no content of VOCs has seen the emergence of water-borne anti-corrosive coatings. This has included the emulsification of unsaturated dehydrated castor oil - based epoxyester resin (Jochems *et al.*, 1999).

1.3.3.2 Epoxy Resins

The epoxide hydrocarbon group,



react with Carboxyl, hydroxyl, phenol and amine to create useful epoxy resins (Lambourne, 1987). The reactions are exothermic so require no stoving to improve properties. The most common epoxide materials use pre-formed epoxy resins from the reaction between propane

and epichlorhydrin. These are termed Bisphenol epoxide resins. Resins can be graded by chain length or the number of repeat units in the molecule. This effects the viscosity of the resin and melting point. Liquid grade resin can be modified into higher molecular weight resin by chain extenders which is done by reaction with diphenylol propane.

In particular, amine an aromatic molecule of carbon atoms is used to react with epoxy in two-pack compositions as polyamines or polyamide. The advantage of this coating is extremely good chemical resistance and despite high hardness, retained flexibility, good abrasion resistance and good adhesion properties.

1.4 Water-based Two-pack epoxy coating

More recent development of two-pack epoxy coating along with environmental concerns has lead to decreasing use of volatile organic compounds (VOCs) as solvents for coatings towards more environmentally friendly alternatives. Although low solvent high solids systems has seen significant development, the area which has seen the biggest advances has been that of water-borne coatings (Colstee and Waalwijk, 1997).

Water-borne two-pack epoxy coating can be divided into two distinctly different systems (Cook, *et al.*, 1999). Type I systems use the water-borne epoxy curing agent to emulsify the resin immediately the resin and the curing agent are mixed together. These systems often contain no VOCs as excellent emulsions are formed without the use of co-solvents. Films exhibit high gloss, hardness and excellent adhesion.

The type II system water-based epoxy is based on higher molecular weight epoxy resin. Because the higher molecular weight resins are solid with melting temperatures in excess of 75 °C they are pre-dispersed. The curing agent in this case does not need to emulsify the resin, rather it exists as a separate phase in the system. Solidification of these systems occur when enough water or co-solvent have evaporated. Co-solvents are required in type II systems to improve coalescence and improve film properties. A common problem of type II formulations is a heterogeneous film morphology. If not accounted for this can lead to areas of high amine

retention that produce higher hydrophobicity and accelerated water transport relative to other areas of the film. The advantages of type II formulation are improved pot life but also improved mechanical properties of improved adhesion, corrosion protection and flexibility.

Both solvent based and water-borne epoxy coating systems have been used in this work. The former an industrial grade pigmented with zinc phosphate and the latter as a control coating system which was un-pigmented.

Solvent and water-borne alkyd primers containing pigmentation have also been investigated as supplied by manufactures.

1.5 Ionic Resistance as Corrosion Protection

Coating systems which block or act as a barrier, prevent the migration of ions to the substrate. It has been shown that intact barrier coatings on clean steel can give as good if not better performance than soluble inhibitive pigments (Mendoza and Sykes, 1990). The electrical resistance of the coating relates to the ionic transport rate of the coating and has been shown to be an important indicator for the ability of a coating to protect against corrosion. Work by Bacon, Smith and Rugg (Bacon *et al.*, 1948), used over 300 organic coatings in simulated sea water. The work showed that coatings with electrical resistance values $> 1 \times 10^8$ ohm-cm² provided good protection against corrosion. Where electrical resistance was $< 1 \times 10^6$ ohm-cm² the corrosion protection afforded was poor, at intermediate values of resistance protection was borderline. Without a path of conduction ionic transport through the coating between the anode and cathode corrosion cannot take place. It can be seen that protection provided to the substrate by apparently simple coatings can be a complex interaction of several different mechanisms (Mills, 1974).

1.6 Pigments

Development of improved coating systems as a method of protection has led to the use of pigments. Pigments can be divided into two types: inert pigments, typically mica and iron oxide which enhance the barrier properties of the coating by introducing much longer routes which impede migrating ions and active pigments.

Zinc at concentrations greater than 95% by mass protect by galvanic or cathodic protection of the steel by the adjacent zinc which acts as an anode in a corrosive environment. It is claimed (Wranglen, 1972), that this exerts a distance effect protecting the substrate from corrosion at defects, additionally plugging of defects by corrosion products of the zinc are maintained to help prevent further corrosion.

Other active pigments rely on chemical inhibition as a mechanism of corrosion protection. Dissolution of inhibitive pigments from the coating into the water as it migrates through the coating produce a passive surface on the substrate by formation of stable compounds. In the case of Chromate containing wash primer this involves the reduction of Cr(vi) to Cr(iii) and the formation of a chromium-polyvinyl- butyral complex (Camina, 1986). The solubility of the pigment required for effective inhibition needs to be 0.1 to 1.0 g per litre.

It has also been postulated that there is formation of complex substances by reactions with the binder. These substances react with corrosion products to form an adherent passive layer on the substrate (Hernandez *et al.*, 1998).

Certain chromates, red lead and zinc phosphate protect by formation of insoluble ferric compounds. The cation can complex with cathodically produced peroxide ions which increase their power of oxidation (Mayne and Burkill, 1995). Zinc Phosphate containing coating has been found to deposit considerable quantities of zinc on the metal surface which precipitates zinc hydroxide once corrosion has started (Camina *et al.*, 1990). This slows the cathodic reaction and gave typical cathodic inhibition characteristics when subjected to Electrochemical impedance spectroscopy. The main effect is a strong Warburg effect which does not “roll

over". Both chromate and phosphate also exhibit some degree of ionic barrier effect in addition to chemical inhibition. This was demonstrated by higher D.C. resistance values for the pigmented alkyd films compared to clear film.

Adhesion of the coating to the substrate is an important constituent in corrosion protection. If the coating is easily disbonded from the substrate water permeation through the coating will allow corrosion product to lift and thus spread the corroding area (Sykes, 1987).

Because the overall performance of the coating is dependent on the binder much work has been focused on reducing degradation of the resin. One of the major causes of degradation is ultraviolet light. This degrades the polymer by breaking the links in the polymer chains causing chalking (Balfore, 1990). A pigment which has been successfully used in preventing this problem is Titanium dioxide (Balfore, 1996). Titanium dioxide of two crystal forms Anatase and most commonly rutile has a high refractive index which disperses and absorbs short wave ultra violet light protecting the underlying polymer. The success of the pigments in modern coatings is very sensitive to their dispersion through out the polymer. Much work has been done on production processes to give pigmentation that does not flocculate or agglomerate (Reck and Richards, 1997). This is important as the effectiveness of the pigment is a function of surface area and spacing. Much of the drive has been put into the investigation of crystal structure and atomic packing of potential pigment substances produce finer crystals (Howarth, 1998).

1.7 Coating performance

Coatings are assessed by different criteria. These can be mechanical tests such as those contained in standards (American Standards for Testing Materials {ASTM}, 1989), which measure adhesion. This is an important property and considerable research has been done on adhesion and the effect of adhesion on resistance to corrosion. Disbondment can occur by oxide lifting (Jones, 1996), where anodic reaction at a defect causes undercutting of the coating where anodic corrosion products serve to lift the coating by a mechanism that occurs

through wet and dry cycling. Continuous immersion does cause oxide lifting. Cathodic disbondment (Darwin and Scantlebury, 1995), (Gowers and Scantlebury, 1983) can be seen in immersion conditions and is caused by the alkalinity of the cathodic reaction products reacting with the organic polymer by a process called saponification. Typically oxygen and water must migrate through the coating to support the cathodic reaction and this is associated with an anodic site in close proximity (Jones, 1996). Other standards (ASTM, 1992) give visible estimation and numerical rating of coating resistance to corrosion performance. These include the performance of the coating at a scratch or holiday which simulate damage in service. Testing is often accelerated by the use of high temperature cyclic tests developed to simulate months or even years of service in the external environment (ASTM, 1987). Even under accelerated conditions the tests are time consuming and methods of quickly establishing the effectiveness of a particular coating to a particular application is the aim of much present research.

1.8 Electrochemical Methods

As the corrosion process is of an electrochemical nature, assessment and monitoring of anti-corrosive coating performance lends itself to study by electrochemical techniques (Thomas and Bernie, 1987).

1.8.1 The D.C. Resistance Method

Bacon, Smith and Rugg (Bacon *et al.*, 1948) were at the fore front of the use of electrochemical methods. Their work with the DC resistance technique published back in 1948 indicated which coatings would afford good corrosion resistance and those that would not. Using 300 coating systems exposed to artificial sea water the coatings were monitored using D.C. measurements through the coating systems. The DC resistance technique still finds use for assessing coatings but has the disadvantage that to indicate a resistance a current must pass through the coating. Passing a current requires a high impressed voltage that can be in

excess of 1V and this can induce paths of conduction in the system. It is postulated that this can leave paths of weakness in the coating structure which then act as conduction paths for aggressive ions, accelerating degradation of the coating. Using D.C. resistance monitoring as a continuous process is therefore not possible. The technique also does not give mechanistic data of any corrosion processes. Also, DC resistance only gives a single point-in-time value. Results from some modern water-borne coating systems have been anomalous (Mabbutt and Mills, 1997), with the D.C. resistance value being low but little or no corrosion evident. So in the last fifty years more sophisticated techniques have been developed which give mechanistic information on processes of corrosion and coating degradation. A technique which has become well established over the past decade is Electrochemical Impedance.

1.8.2 Electrochemical Impedance Spectroscopy (EIS)

Electrochemical Impedance Spectroscopy has developed over the past twenty years as a useful laboratory technique in the analysis of corrosion mechanisms and corrosion rate (Skully, 2000), this recent work has validated the use of impedance spectroscopy derived values of polarisation resistance and shown correlation with other techniques. The technique has found applications for assessing protection afforded by anti-corrosive coatings (Turgoose and Cottis, 1991). Under conditions of an applied alternating current an organic coating behaves as a capacitor (Hughes and Jeffrey, 1981). The reason for this is the fact that different processes at the surface absorb electrical energy at different frequencies causing a time lag and hence change in phase angle that is measurable. This also applies to the interface between coating and substrate and corrosion product.

Ohm's law under A.C. conditions becomes $E = I.Z$, where Z is the resistance caused by all elements that impede flow. The resistance value comprised of inductors and capacitors is dependent on the frequency of the alternating current. The Electrochemical Impedance Spectroscopy technique uses vector analysis of an impressed A.C. signal from the corrosion circuit to calculate the impedance value (Baboian, 1985), (Jones, 1996). The aim of EIS is to

model the corrosion process in terms of circuit elements and then to draw conclusions about the corrosion process. Measurements can be taken at the corrosion potential, therefore demonstrating the state of the system in its equilibrium state. By recording data at different frequencies a profile of the corrosion cell can be produced. This is represented graphically by two common techniques (Scantlebury and Ho, 1979).

Data can be interpreted by the use of a Nyquist plot where the imaginary impedance values are plotted against real component of impedance as a function of frequency.

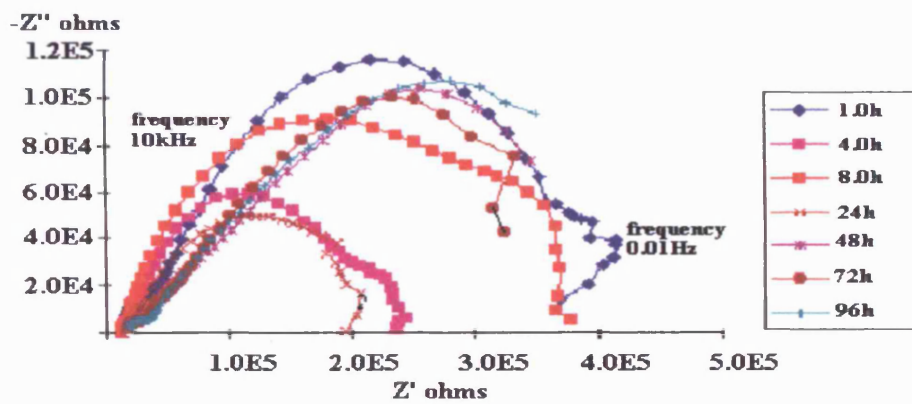


Figure 1.1 Typical Nyquist plots over time for a Scribed Alkyd Coating in Diluted Harrison's solution

This indicates clearly the relationship between resistive and capacitive components of the corrosion cell. For a corrosion cell under charge transfer control the resulting Nyquist plot will be a semi-circle. Where the end points of the semi-circle bisect the x - axis the polarisation resistance (R_p) can be read off of the x - axis scale as the value between the two points. The distance between the high frequency (left hand side) bisection of the x - axis and the y axis represents the ohmic value of the solution (R_s). Work investigating polarisation resistance when applied to coated substrates (Scantlebury and Ho, 1979), used EIS and the changes in both resistance and capacitance with time were clearly shown using the Nyquist plot. Water take-up was established as the main factor influencing the change in capacitance of the coating as it remained constant after one day's immersion.

Bode plots can also be used to interpret impedance data, Figure 1.2. The Bode plot takes the capacitance value of the coating or element under investigation, plotted as a function of frequency.

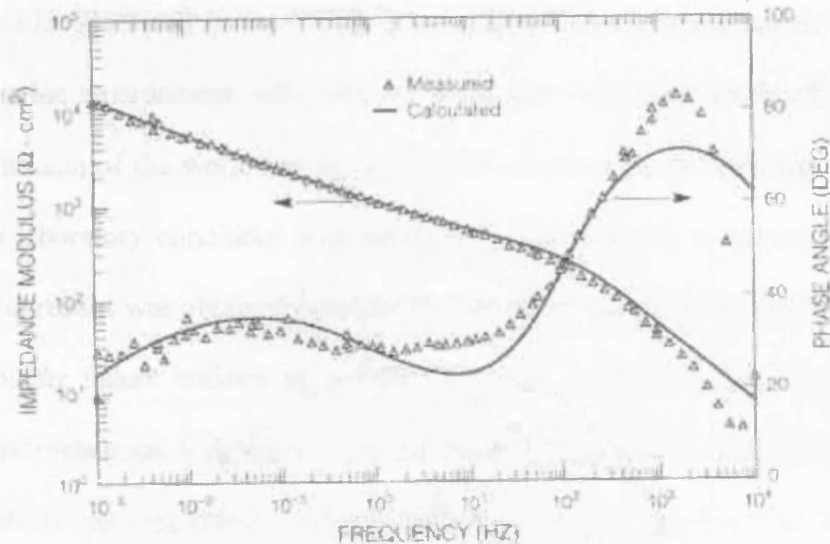


Figure 1.2 Typical Bode plot showing impedance modulus with frequency and phase angle

(Example taken from D. A. Jones, Principles and Prevention of Corrosion)

A coating will give a straight line response to the increase in frequency when plotted on a log / log scale of frequency against capacitance until a point on the capacitance scale equivalent to the coating D.C. value. This point, where the capacitance ceases to be proportional shows a marked decrease in slope on the graph and is termed the “roll-off” frequency. Good correlation with the D.C. resistance value of coatings has been seen (Jeffcoate, *et al.*) (Li *et al.*, 1994).

1.8.3 Applications of EIS

Recent work (Thompson and Campbell, 1995) has applied the technique to on-site applications using portable equipment with the advantage of a non contact probe. This obviates the need to remove sound coating to assess the condition of on-site coating systems.

The novel probe consists of two 30mm graphite rods mounted on a plate 120 mm apart and separated by a permanent magnet. The magnet serves to attach the assembly firmly to the coating surface and good electrical contact between the probes and the coating are ensured by using conductive ultrasound couplant gel.

Results obtained correlated with those obtained using a conventional contact probe. Other work using EIS (Barbucci *et al.*, 1995), has conducted parallel experiments in the laboratory and in a marine environment with stressed specimens containing artificially created coating defects. The aim of the work was to develop an insight into the meaning of the EIS result obtained in laboratory conditions compared with what happens in natural exposure. Good correlation in results was obtained between the laboratory and external exposure tests.

Because coating failure initiates as a local event interest has developed in identifying these areas by electrochemical techniques. Electrochemical Impedance techniques are no exception to this. Defects can result from chemical heterogeneities in the resin (D areas) or physical defects such as bubbles, under-film deposits, or pin holes. The ability to detect and map coating heterogeneity and as well as make quantitative in-situ measurements will help identify the source of failure (i.e. coating chemistry, method of application, cure schedule) and provide insight into the mechanisms of coating degradation. Whittman and Taylor used a 5 electrode arrangement to perform local electrochemical impedance spectroscopy (LEIS) on coated steel substrates (Whittman and Taylor, 1995). Using single frequency measurements, LEIS could successfully detect and map both artificially produced chemical heterogeneity and physical defects such as sub-surface bubbles, under-film deposits and pinholes.

Other workers (Geenen, 1990), have found EIS data capable of allowing a “most probable equivalent circuit” to be established in the study of the degradation of unmodified epoxy coating. The physical meaning of the components were in part verified by monitoring effects of electrolyte concentration, aeration and coating defect size. Coating defects were produced by a novel method of laser ablation which gave more reproducibility. This methodology has been adopted for part of the work in this project.

More recent work (Hernandez *et al.*, 1998) has used EIS in conjunction with traditional accelerated tests, salt spray and humidity chamber tests and adhesion testing to investigate paints pigmented with different contents of micronised zinc phosphate. EIS was able to determine the best formulation for the coating which correlated with results from other testing methods.

1.8.4 Disadvantages of EIS.

Despite finding acceptance over recent years EIS has some negative points which should be appreciated if it is to be compared with other potential techniques for assessing corrosion protection.

The nature of the spectroscopy process involves taking data readings across a wide frequency range, typically 0.05 Hz or lower if required to 50 kHz, for coating systems. The equipment performs the operation dividing each decade of frequency into a number of steps (typically seven) and taking data at each. Because of this necessary process a typical test run can take around 40 minutes, with the overall time being dominated by the time taken to record the low frequency data. This presents two immediate problems; Firstly the physical time constraint if multiple samples are being assessed. Secondly and more important experimentally, is that over the time interval of the test the kinetics of the system can change. In the early stages of testing this may be of importance, but in long term testing it will not necessarily be a problem.

Another criticism of EIS is that it imposes an external voltage on the system and as such cannot be regarded as truly non-intrusive testing. Some evidence that EIS testing can influence the data response of delicate systems has been seen (Mills and Mabbutt, 1997), when the imposed current appeared to induce an early decrease in the resistance of the system when compared to data obtained from ENM. In this situation the performance of mildly inhibitive coatings were being assessed at artificially produced defects.

EIS cannot be regarded as non-intrusive, and as such applications as a continuous monitoring method are not appropriate. Where continuous monitoring of a system is required an

electrochemical technique that is non-intrusive and does not impose a voltage on the system under examination is preferred. Methods of monitoring systems in the field that meet this criteria are rare, but in recent years a method which has been shown to be of use has evolved.

1.9 Electrochemical Noise Measurement (ENM)

Electrochemical noise can be described as fluctuations in potential and current around a mean value in an electrochemical cell. The fluctuations in potential and consequently current are a natural phenomena and with improved instrumentation it has been found possible to exploit these changes using the Electrochemical Noise Measurement method.

CHAPTER 2

Literature Review (Electrochemical Noise Monitoring)

2.1 Electrochemical Noise Measurement (ENM)

Electrochemical noise can be described as naturally occurring fluctuations in potential and current around a mean value in an electrochemical cell (Bertocci *et al.*, 1997) (Dawson, 1996).

2.2 Potential Fluctuations in corrosion cells.

Monitoring of potential fluctuations of bare metal and coated substrates against time was carried out as long ago as 1949. Investigations around this time (Wormwell and Brasher, 1949), looked at different surface finishes of steel and their effect on potential with time when immersed in artificial sea water. It was found that the potentials measured against a SCE were more noble in the case of pickled and shot-blasted, phosphate-dichromate dipped compared to emiered or ground; -0.45 V to -0.51 V respectively. This was extended to coated substrates using two typical marine coatings. One coating was based on iron oxide, minor pigments such as titanium oxide in a resin / linseed-oil medium, the second pigmented with basic lead sulphate, white lead and Burntisland red was a modified phenol-formaldehyde-resin / stand-oil. It was seen in tests carried out over a forty five day period that the potential values peaked at around twenty days. It is stated that the drop-off in these peaks to a more negative value corresponded with the appearance of rust spots and other visual indications of deterioration and that this period is the significant observation. There was also an initial drop in potential before recovery and formation of the "hump"; this was attributed to slight attack on the metal surface leading to plugging of micro-pores by corrosion product. Dr. J. E. O. Mayne, suggested that a more probable cause was partly or wholly the inhibitive action of certain

constituents of the paint. Although the potential time curves did correlate with observed breakdown the technique was very qualitative and gave no prior warning of coating failure.

Fluctuations in potential over small time periods were often blamed on instrumentation and much work has been done to remove the effects of fluctuating voltages and currents in monitoring instruments. It has now been recognised that the source of the fluctuations shown by modern instruments is from the corrosion cell being monitored. Laboratory equipment has also been sited as the source of electrical noise, particularly when dynamic corrosion studies are in progress and needs to be considered where appropriate (Malo and Velazco, 1996).

2.2.1 Potential Noise

The fluctuations are now termed electro-potential noise. Iverson reported in Nature 1967, cited (Iverson, 1968) that “hollow whiskers” formed by the action of slightly acidified potassium ferricyanide and ferrocyanide solutions on metals and alloys appeared to indicate that corroding metals produce bursts of metal ions from point anodes. He also observed that the bursts were of a sporadic nature and postulated that there could be transient fluctuations of electrical charge on the metal surface. Further work (Iverson, 1968) investigated these observations using a variety of metal working electrodes consisting of pure aluminium, aluminium alloys (2025 and 7075), magnesium ribbon, iron, mild steel (1010) and zinc. Auxiliary electrodes were platinum foil strips with potential fluctuations measured using a high impedance voltmeter. Only potential fluctuations were measured for this work and it was concluded that each metal studied had a characteristic potential amplitude and frequency. The frequency of the aluminium, aluminium alloys and the magnesium were generally rapid at 1 - 2 Hz and higher with an amplitude greater than 100 mV. Iverson connected his instrumentation to a loud speaker and was able to listen to a wide range of fluctuations in the audio range.

This indicated that there were considerable higher frequency components within the signal beyond the range of the instrumentation.

Potential fluctuations from the corroding iron, steel and zinc were much slower 1 - 3 or less per 5 minute interval and with amplitudes of less than 50 - 60 mV. It was found that the potential fluctuations from the steel in 0.1 NaCl disappeared when sufficient sodium nitrite inhibitor was added to the solution. Aluminium exhibited similar behaviour when nitrates were added to inhibit corrosion. This was attributed to the inhibitor causing corrosion to cease and indicated that the measured fluctuations in potential had their origin in the corrosion process.

When corroding working electrodes were replaced with platinum there were no measurable fluctuations. The conclusions from this very early work were that monitoring potential fluctuations showed much promise for the detection and study of corrosion processes. It was also suggested that the technique would be of use in the study of inhibitors.

This has come to fruition in certain circumstances particularly where physical inspection of inhibitor performance is not possible (Mickalonis *et al.* 1996). Typical field applications being measurement of systems in oil processing and monitoring of experimental conditions at remote sites. Not only is the plant physically inaccessible but corrosion problems in processing tend to be internal because of the media being processed. Recent developments in remote monitoring have seen control of on-site computers using modems and telephone system data transmission enabling a computer in the laboratory to mimic exactly the one on site. This has been used successfully (Xiao *et al.*, 1997) to establish electrochemical impedance data and electrochemical noise analysis on 13 different polymer coatings from experiments at remote coastal sites. The data correlated well with parallel experiments in the laboratory. The important point in this work is that the raw data is not transmitted through the telephone system media before being processed. If this were the case it would be highly probable that the signals on the data would be degraded and interfered with by noise on the telecommunication

system. By remotely controlling the computer the transmitted data becomes virtually a transmitted file which can be transmitted without corruption by different media. In the oil industry mixtures of oil and water containing CO₂ and sulphide with pH values between 1 and 5 present monitoring problems that are internal. This media is corrosive and also has high ionic resistance presenting further complications for established monitoring techniques (Gusmano *et al.* 1998).

A phenomena with potential noise is that although it is higher on corroding metal, where organic coatings are being monitored the potential noise is higher when the coating is preventing corrosion and offering high resistance (Skerry and Eden, 1989).

Studies of corrosion of iron in sulphuric acid containing inhibitors and using ENM have also concentrated on the monitoring of potential noise. The noise power spectra was used with harmonic analysis to determine the rate of corrosion and these were found to be in agreement with the polarisation resistances in the low frequency range 0 to 100 mHz. At these frequencies the Stern-Geary equation can be used to give a good approximation for corrosion rate (Meszaros *et al.*, 1996). The simplified Stern-Geary equation (2.1), states that the corrosion current (and hence corrosion rate) is inversely proportional to the polarisation resistance (R_p) and dependant on the constant B, which is a proportionality constant.

$$I_{\text{corr}} = B / R_p \quad 2.1$$

The constant B is a number which represents the proportionality between the slopes of the straight line portion of the anodic and cathodic polarisation curves when plotted on a linear potential / log current graph. These are termed Tafel slopes which are explained in section 2.9.1.along with the proportionality constant.

More recent work (Scully, 2000), has verified this and correlated R_{SN} and R_n to polarisation resistance values from traditional linear polarisation techniques and impedance spectroscopy. The data from Iverson's work provided only qualitative characterisation of the metals or alloys and the on-set of corrosion, but the technique had been identified. What was of particular interest was the ability for instantaneous detection of the on-set of corrosion, showing changes in system kinetics before any visual observation was possible.

Work that followed Iverson's also concentrated on potential fluctuations. The nature of noise has been characterised (Betts, 1970) and can be used to establish mechanistic information. Work at UMIST and ICI between 1979 and 1985 concentrated on electrochemical potential noise (EPN) from freely corroding electrodes (Skerry and Eden, 1987) (Skerry and Eden, 1989). These were used in conjunction with more conventional electrochemical methods such as linear polarisation resistance and electrochemical impedance to obtain information relating to corrosion rate, corrosion mechanisms and assessment of anti-corrosive coating performance.

Potential Noise has also been used in isolation to study inhibitor effects of polymerisation of silicate when used on aluminium. (Hirozawa and Turcotte, 1991). Electrochemical Potential Noise was used in conjunction with Electrochemical Impedance Spectroscopy and was found to complement well the evaluation of E_{corr} and R_p as tools for investigating inhibitor interaction with metal surfaces. It was found that the use of nitrate (contrary to that reported by Iverson) and silicates individually did not protect aluminium, but by combining them corrosion protection was greatly improved. This was shown by significant reduction in electrochemical noise and correlated with similar improvement in E_{corr} values and polarisation resistance values. The ratio of SiO_2 to Na_2O was found to be critical regarding the interaction of the silicate with the aluminium surface. The optimum ratio was 1.8 - 2.0 which gave the oxide layer optimum resistance to penetration by chloride.

2.3 Potential Noise from Localised Corrosion Mechanisms

The use of potential noise has found application in the study of corrosion mechanisms which are non-uniform or localised in nature, these include stress corrosion cracking, hydrogen embrittlement and pitting corrosion. Investigations have also been carried out using potential noise for indicating temper embrittlement (Donohoe, 1995), which has been found to be indicative for steels within a limited embrittled range.

2.4 ENM applied to stress corrosion cracking

Investigations into the electrochemical noise generation during stress corrosion cracking was reported (Cottis and Loto, 1986), for steel, aluminium and brass. To induce stress corrosion cracking the brass was tested in Mattsson's solution (a hydrogen sulphide containing solution that accelerates stress corrosion), Aluminium-Zn-Mg in 3.5 % NaCl and 0.95 % C steel in 3.5 % NaCl acidified with H₂SO₄ to pH 2. Stress was applied using a C-ring set-up for both brass and aluminium with a bend beam arrangement applied to the steel. Where localised corrosion is active power spectra show peaks that correspond with actual localised corrosion events.

Various techniques are used for the interpretation of electrochemical noise data (Cottis *et al.*, 1997). Data from localised corrosion studies in laboratories are often transformed into the frequency domain to obtain the power spectra (Bertocci *et al.*, 1997). Information can be obtained from frequency domain plots that cannot be separated from time domain plots such as the power of the signal at low frequency or high frequency. Cottis's work concluded the corrosion mechanism of the brass specimens to be a combination of film rupture and anodic dissolution, with the aluminium considered to be cracking by the same process. The steel

cracking was caused by hydrogen embrittlement. In this work failure of the steel was catastrophic initiated by hydrogen evolution and accompanied by surface etching.

With the steel specimens, the noise spectra had a very consistent level until a single peak corresponding with the fast fracture event.

Behaviour of brass and aluminium showed a reduction in noise with crack progress. This was attributed to a shielding effect by the bulk material as the crack penetrated. A peak when the crack began to yawn was considered good evidence that the process was controlling the noise emission.

Further work on potential noise generation during stress corrosion cracking of alpha-brass (Loto and Cottis, 1987), was conducted under the same conditions, but potential noise was monitored at various frequencies between 1 Hz to 120 mHz. Initial high noise values were attributed to the formation of a surface oxide layer Cu_2O , which as it formed caused a reduction in noise levels. A further increase was attributed to the film break down and the onset of pitting. The specimens were compared to non-stressed specimens under the same conditions and these showed different behaviour in the form of general corrosion. The formation of cracks in the stressed specimens that originated at surface corrosion pits visible at 4 hours, produced peaks in the data. With the non-stressed specimens these peaks were not present which was attributed to the fact that no stress corrosion cracking occurred. The results from work on aluminium AA 7075 - T6 alloy (Loto and Cottis, 1989), analysed by the same techniques also showed that when the highest amplitudes in noise were seen, these were associated with the specimen cracking. Also observed was that higher potential noise indicated increased corrosion rate, again typical of bare metal corrosion but not protection by organic coating. The mechanism was shown to be film rupture / anodic dissolution by scanning electron microscope (SEM) analysis. The SEM work showed cracks were intergranular starting at corrosion pits. In addition to this cracks were also seen to originate from surface

micro-cracks developed during stressing, which corresponded to similar findings from the brass specimens.

In situations where general corrosion is prevented but localised corrosion mechanisms may be present potential noise monitoring can still provide sufficient information to indicate problems even though this is more qualitative than quantitative. Work done under pressurised water reactor conditions using stainless steel showed short duration potential spikes were correlated with crack initiation events (Eden *et al.* 1986). On average these spikes were around 0.25 mV but some as large as 1 mV were also recorded. Sudden increases in plastic deformation were associated with slower, higher amplitude potential transients as large as 15 mV. Once the material deformed plastically a marked reduction in potential noise level was observed.

2.4.1 ENM applied to pitting corrosion

The phenomena of pitting has attracted the use of ECN monitoring as a method. It has been used to assess the on-set and re-passivation of surface pits and some workers have extended the use of ENM by monitoring current noise in addition to potential noise (Kelly *et al.*, 1997). The use of simultaneously gathered potential and current data was used in an attempt to distinguish between pitting corrosion and stress corrosion cracking (Leban *et al.*, 1998). In order to separate local corrosion events from general corrosion of the specimens mathematical tools from chaos theory and spectral analysis were used. These were found to indicate localised corrosion in the presence of general corrosion which, it is claimed the data from the time domain could not discriminate.

Other workers (Cheng *et al.*, 1999) have used potential and current monitoring to study the effect of electrode capacitance on pitting and this is reflected in noise data from the time domain. The A516 carbon steel surface was passivated using 0.5M NaHCO₃. Initiation of pitting was found to occur when the solution was changed to 0.1M NaCl after incubation

period of around four hours. Observed during this time were potential fluctuations that appeared to be in phase with the current fluctuations. Initiation of pitting was characterised by sharp fluctuation peaks of potential and current. The recovery time for both potential and current was slower than the initial event the potential seen always to recover in excess of the re-passivation time. The re-passivation time is indicated by the recovery of the current and the slower rate is attributed to capacitance of the passive film. The capacitance was established as 80 mF using electrochemical impedance spectroscopy to give Nyquist data on the passive film in much the same way as the analysis of an organic coating on steel (Thompson and Campbell, 1994). It was therefore concluded that the electrode capacitance plays a major role in the fluctuations of corrosion potential. The potential fluctuations reflected the response of the electrode capacitance to the pit growth charge and the current signal giving indication of the breakdown and re-passivation of the passive film.

2.5 Current Noise Monitoring

As corrosion rate is a function of current density it was important, if ENM were to develop as a technique, that current data be obtained. Current noise is usually monitored in conjunction with potential noise. However, investigation of pitting corrosion has been carried out using current noise data in isolation, (Souto, and Burnstein, 1998) in this work the potential was held constant to initiate pitting and consequently the potential noise data was not investigated. Prior to and after the on-set of pitting transients in current noise were observed in the order of four to six nano amps on passive Titanium Ti_6Al_4V alloy, micro-electrodes ($5 \times 10^{-4} \text{ cm}^2$).

2.6 Current and Potential Monitoring

Electrochemical noise measurements of potential and current are usually made using a three electrode cell, and although there are different configurations (Murray, 1997a) they are electrically the same. Different configurations are discussed in the experimental sections. Comparisons with more established electrochemical techniques such as polarisation curves and electrochemical impedance spectroscopy (EIS) have also been made (Murray, 1997b).

Work has been undertaken in an attempt to standardise equipment, configuration, collection and treatment of noise data (Kearns *et al.*, 1996), with extensive reviews of the development of ENM as technique by Dawson (Dawson, 1994).

Two nominally identical specimens act as working electrodes and instantaneous current is measured between them using a Zero Resistance ammeter. A third electrode, usually a standard laboratory reference type, is used to monitor the potential fluctuations of the working electrode couple relative to the reference.

In most work on this area the importance of the working electrodes being identical is stressed. In a situation where only one electrode begins to corrode the resulting time domain data can be misleading as it tends to be dominated by the higher resistance in the system. Studies have been done that have confirmed this, but have also created a mathematical model that can take into account asymmetry in electrode impedance (Bautista and Huet, 1999). This model can be applied to coated and bare metal electrodes and in particular situations where pitting is occurring on only one electrode causing localised current transients. This is achieved by producing the power density spectra and determining separate impedance modulus for each working electrode.

Different configurations for noise monitoring are discussed, chapter 3.

Eden first monitored current and potential noise simultaneously in 1984 using analogue instrumentation (Eden *et al.* 1986). The quality of ENM was greatly improved in 1985 when

digital equipment replaced analogue equipment. Work was conducted using anti-corrosive coatings, with the coating being applied to the nominally identical working electrodes.

Skerry and Eden first used statistical analysis of noise data. They obtained the standard deviations of the potential and current plots and a relationship was found (Skerry and Eden, 1989) (Skerry and Eden, 1991), between the quality of the corrosion protection and the values obtained. It was found that good coatings gave relatively high values of potential standard deviation σ_v . By contrast poor coatings gave relatively high σ_i values. This result was indicating that a high coating resistance was not allowing dissipation of charge build-up on one working electrode to the other working electrode until higher potentials resulting in higher standard deviation values. Conversely, the poor coatings which were exhibiting high current standard deviations were following potential fluctuations more closely, allowing current to flow because of the low coating resistance. The work identified σ_v values for good coating such as the epoxy-polyamide tested around 2×10^{-3} V compared to 2×10^{-5} V for a poor coating which in this work was a porous alkyd. Conversely σ_i values were lower at 5×10^{-13} A/cm² for the epoxy-polyamide compared to the alkyd 5×10^{-9} A/cm².

An estimate of the extent of de-lamination of the coating from the substrate was also obtained from the data. This was established from the total charge passed between the working electrodes.

2.7 Characterisation of Noise

The type of noise signal being monitored can be characterised (Betts, 1990) and placed in a specific category. The character of the noise signal has been shown to be useful in establishing mechanistic information of corrosion processes. A mathematical model has been presented (Blank *et al.*, 1977) which successfully described the stochastic behaviour of two cases of non-equilibrium electrochemical interfaces. These were poisson white noise signals generated by

anodic dissolution of iron in acid medium and diffusion of reacting species in the bulk of the electrolyte.

2.7.1 White noise and coloured noise

White noise is found to approximate many types of noise that are encountered in all aspects of signal processing from various sources in nature and science. White noise is characterised by having a constant power spectral density at all frequencies. A power spectrum will therefore produce a horizontal line signifying equal power at each frequency.

If the power spectrum of the noise is not a horizontal line the noise is said to be coloured, that is the noise signal has higher power as frequencies decrease or increase. The most common method to specify frequency spectra slopes is in dB / decade where one decade represents an increase in frequency of a factor of ten (Cottis and Turgoose, 2000).

2.7.2 Measurement in the frequency domain

Analysis of data from EPN is typically transformed into the frequency domain. This gives power spectrum information indicating at what frequencies events are occurring and the power associated with the event (Cottis and Turgoose, 2000). By calculating the noise power of an event such as pit formation estimates of actual damage can be made. Analysis of the data was carried out using MEM (Maximum Entropy Method), this essentially has the same function as Fourier transform, in that it converts from time series to power spectra but produces a subtle difference in the final data which appear as a much smoother plot. This makes measure of any slope more precise. Uniform corrosion typically gives a flat frequency power spectra indicating random or white noise across the spectrum (Bissell, 1990).

2.7.3 Power spectra and corrosion mechanism

A relationships between corrosion mechanism and the slope of the power spectra have been reported (Legat and Dolecek, 1995). Uniform corrosion on stainless steel electrodes was induced using 5% H₂SO₄, data was compared to that from the same electrode material in 0.5% NaCl which produced mixed corrosion of pitting and uniform types. Previous work had shown slopes for localised corrosion to be 20 - 30 dB V / decade. The results presented for mixed corrosion produced slopes of 10 - 15 dB V / decade, whereas the general corrosion gave slopes of close to zero at -2 to 7 dB V / decade. This was confirmed, (Karrab, 1998) where it was claimed that the spectra slope was able to differentiate between localised and uniform corrosion.

The nature of the signals from the processes were obviously different in nature but both conformed to a spectrum characteristic of random and chaotic signals. Further work in the paper uses complex mathematical processes to produce a graph described as an attractor, which can represent completely a dynamic system.

Chaos analysis has been used in conjunction with spectral analysis and time domain analysis in the assessment of a low noise contact for rotating electrodes using a mercury pool instead of the more usual silver-carbon brush type of contact (Fei *et al.*, 1994). Distinct improvement could be seen between the mercury contact when compared to the silver-carbon brush when the data is shown in the time domain. On transforming the data into the frequency domain the difference between the two is still obvious but in this case the frequency values of the external noise is apparent. The attractors plotted from the same data show a cleaner more defined shape for the mercury contact. This indicates a less noisy signal in a pictorial image. Although the use of the attractor appears at this stage to be only a qualitative representation of the noise data, it can clearly be seen in this work that there is potential the use of chaos analysis in particular when it is used in conjunction with other analysis tools.

Mathematical analysis of data in this direction is beyond the scope of this work, but chaos analysis of data is producing interesting results for other workers involved in more mathematical approaches to the analysis of electrochemical noise signals. Other work has extended these techniques (Legat *et al.* 1998), to include the effect of metastable pitting and repassivation due to an adhesive organic layers.

2.7.4 Higher Order Measures for the Analysis of Electrochemical Noise

Analysis of the raw data in the time domain by higher order statistical measures has been used with some success and appear to have value in the detection of the type of corrosion (Bagley and Cottis, 1999). Skew and Kurtosis of the time domain data are used to give an indication of the nature of corrosion, but inherently large errors present in the parameters need to be considered when data is interpreted.

2.7.5 Fractal analysis of noise data

An interesting area of mathematics that has evolved with the increase in computing available is Fractal analysis. It has been shown that many patterns in nature which appear random on close inspection, have repeating patterns when the scale is increased or decreased. A good example of this is white noise; if audible frequency white noise is recorded and played back at various speeds the pitch and as such the “sound” of the noise will be the same. Only the volume level would require adjustment as the power would be altered. Fractal analysis has also been applied to electrochemical noise data (Moon and Skerry, 1995)

2.8 Noise from other sources

Electrochemical noise power spectra falls with increasing frequency (Cottis and Turgoose, 2000). Instrument noise at high sampling frequency becomes a more significant problem when using power spectrum as aliasing can occur between the two sources. It is desirable to sample at the highest frequency possible to include maximum information and as such the level of background noise of the instrumentation should be established.

Mains frequency can also be a problem, though filtering can successfully remove the majority of the signal or the use of battery power has been employed by some workers.

Thermal noise or shot noise is a problem associated with resistors both within the instrumentation and as part of the electrochemical process. Where long term monitoring of electrochemical cells is used problems are increased as effects of stability of the system with time need to be considered in the assessment of low frequency limits (Ansari and Cottis, 1997).

An overview of electrochemical noise analysis techniques is presented (Cottis *et al.* 1998), which examines the various techniques that can be used to analyse electrochemical noise data and explores the theoretical basis of the major methods. The methods reviewed include: Time domain analysis, Statistical methods, Frequency domain analysis methods and Discriminant analysis. The nature of noise signals are discussed in some detail along with concepts of the parameter of "noise resistance" (R_n). It is stated that although situations arising from differences in electrode behaviour have been examined in detail from a theoretical standpoint the concepts have not been subject to much practical examination. Despite this claim success has been achieved using the noise resistance parameter in numerous applications.

2.9 Electrochemical Noise Resistance (R_n)

From the work reviewed it can be seen that considerable effort has been made both in the characterisation and analysis of electrochemical noise from corrosion cells.

The work can be divided mainly into two distinct areas, interpretation of the raw data as collected in the time domain and secondly analysis of the data in the frequency domain. Although both approaches have been used with success for both general and localised corrosion mechanisms there are disadvantages.

Time domain data gives only limited information with transients and peaks being attributed to corrosion events but lacking quantitative information.

Frequency domain data gives more mechanistic information for localised corrosion mechanisms and can determine between different corrosion mechanisms. Unfortunately the mathematical processes involved make frequency domain analysis time consuming. Interpretation of the data requires a "trained eye". The same general information obtained from frequency spectra, in particular the slope can represent localised corrosion in one environment and general corrosion in another environment. Slopes are also different on different metals in the same environment. These facts make comparisons difficult and neither treatment has found much favour when applied to the assessment of anti-corrosive organic coatings. This was outlined (Bertocci *et al.* 1997), where the use of the parameter noise resistance (R_n) as simpler approach to characterise corrosion noise was proposed. In their work the parameter R_n was discussed and compared to other parameters extracted from noise data such as the power spectra. Attempts to employ noise resistance were initially empirical. It was found experimentally that under certain circumstances where anodic and cathodic reactions are totally activation controlled the parameter R_n can be equal to polarisation resistance.

More importantly for this area of work, it has been shown that there is a good correlation between R_n and the D.C. resistance value of many intact organic anti-corrosive coatings (Li *et al.*, 1998)(Bierwagen *et al.*, 1994).

2.9.1 Derivation of Noise Resistance (R_n)

If the standard deviation of the potential data series and the current data series are calculated to give parameters Voltage noise (V_n) and Current noise (I_n), further information can be obtained (Cottis and Turgoose, 1994). By using the V_n and I_n values in an Ohm's law relationship the parameter noise resistance (R_n) can be calculated. Empirically the value of R_n has been shown to correlate with the polarisation resistance (R_p) value. The relationship was seen to hold good in conditions of general corrosion that were proceeding at low to medium rate (Reichert, 1996).

Work has been done to establish a mathematical and theoretical basis for the assumptions made about resistance noise (Chen and Bogaerts, 1995). It is shown that where the anodic and cathodic reactions are totally activation controlled and can be described by the Butler-Volmer equation a mathematical derivation can be performed which leads to the following relationship (2.2).

$$\sigma_V / \sigma_I = R_n = R_p \quad 2.2$$

$$(R_p = R_n \text{ under activation controlled conditions})$$

For calculation of corrosion rate, corrosion current (I_{corr}) can be calculated as stated previously (2.1)

$$i_{\text{corr}} = B / R_n \quad 2.1$$

$$\text{where } R_n = R_p$$

and B = a proportionality constant (2.3) calculated from the anodic and cathodic Tafel numbers.

$$\text{Therefore, } B = B_a B_c / 2.3 (B_a + B_c) \quad 2.3$$

The Tafel numbers are the slopes of the anodic (B_a) and the cathodic (B_c) straight-line portion of the polarisation curves when plotted on a linear potential / log current graph. Tafel numbers are quoted in mV / decade. Where decade means a power of ten on the current axis.

Using the noise resistance parameter at the low frequency limit will give the resistance at the low frequency limit of impedance (Cottis and Turgoose, 1994). As stated this has been correlated to R_p which also includes the solution resistance (R_s). It therefore follows that because the R_n parameter includes solution resistance this may have to be taken into account where corrosion rates are being considered. With low conductivity solutions this is of particular relevance.

Chen and Bogarts derivation and others (Bertocci *et al.*, 1997) relate corrosion on bare metal electrodes to R_n . Derivations of R_n with relation to organic coating / metal substrate systems have also been done which has opened up investigation of organic coatings by ENM (Bierwagen, 1994) (Cottis and Turgoose, 2000). Further mathematical treatment of the derivation relates R_n to impedance data and R_{dc} (Bierwagen *et al.*, 1995). Further work by

Bierwagen's group correlates R_{dc} with R_n for anti-corrosive organic coatings and suggests practical extensions of the technique (NACE, 1993).

2.9.2 Applications of Noise Resistance

The use of current and voltage data transformed into the frequency domain has also been used to find the spectral noise impedance (R_{sn}) (Bertocci *et al.*, 1997); this work showed a correlation between R_{sn} and the impedance modulus of the electrodes. Analysis of Electrochemical Noise data from coated steel substrates using zinc-rich primer, epoxy polyamide mid-coat and top coats of polyurethane and latex was carried out which found a closer relationship between the R_{sn} value and impedance (bode) plots once coating degradation had commenced (Mansfeld *et al.*, 1996). The R_n values approached the R_{sn} values with increasing time but always remained lower. The difference between these two parameters was attributed to data collection. The data for R_n being collected at 2Hz whereas the R_{sn} was obtained from the dc limit of the spectral noise plots.

Further work in this area investigated the frequency dependence of noise resistance for coated metal samples exposed to sea water (Mansfeld and Lee, 1997). The noise spectra was compared to impedance data. The work found that there was agreement between the noise resistance parameter and R_p only if the bandwidth of the noise spectra falls within the dc limit of the impedance data. Protective coatings which exhibit capacitive behaviour between imposed ac voltages at frequencies of 1Hz and 1mHz are therefore assumed to have valid noise resistance values. Monitoring the breakdown of the protective alkyd coatings used in the work the following relationship was found; $R_n = R_{sn} = R_p$, where the impedance had reached the dc limit.

2.10 Relationship between Noise Resistance (R_n) and parameters derived from Electrochemical Impedance Spectroscopy (EIS)

Work on bare metal first established that the parameter R_n could be correlated to R_p where uniform corrosion was taking place under activation control. Mansfeld and Xiao investigated pure iron foils exposed to 0.5 N concentration sodium chloride solution de-aerated, aerated and containing sodium nitrite as an inhibitor. Using electrochemical impedance spectroscopy (EIS) to establish polarisation resistance (R_p), it was seen that in all three cases R_n and R_p correlated satisfactorily (Mansfeld and Xiao, 1996).

Using implanted segmented electrodes it was shown (Bierwagen *et al.*, 1993), that the ENM technique had potential as an in-situ corrosion monitoring tool for coatings in service. It was postulated that by analysing the data over the frequency range of the noise impedance information could be obtained and used as a function of time.

Laboratory investigation of epoxy and alkyd marine coatings were successfully conducted using ENM in conjunction with the more established electrochemical impedance spectroscopy method (Jeffcoate *et al.*, 1998). The work was done at elevated temperatures in an attempt to determine the effect of the glass transition temperature (T_g) on the R_n value. The results confirmed that R_n could be used to determine the T_g point of electrolyte swollen films and this was backed-up by EIS data. This is the first time thermal transition temperatures were noted by use of ENM and EIS methods. Direct current resistance (R_{dc}) was also used. For assessing T_g temperatures differential scanning calorimetry was employed. This work confirmed that not only can T_g of an immersed coating be measured by electrochemical means but results from EIS, ENM and R_{dc} correlated. Data from these experiments were plotted as log resistance against $1/T$, where T is absolute temperature. This produced Arrhenius plots where the point of the change in slope denotes T_g .

A study of the fundamental considerations of the use of electrochemical noise methods to investigate degradation and corrosion processes under organic coatings was presented (Bierwagen *et al.*, 1995), which established a good theoretical basis for the use of the noise resistance parameter R_n . Mathematical derivation of the theory was presented along with recommendations for improving experimental methodology. The work showed that from a time series electrochemical noise measurement of current and potential the relationship $R_n = \sigma_v / \sigma_i$ is valid. This situation is where the electrochemical noise data is acquired from a system which is stationary in a statistical sense over the period of data acquisition.

A basis for the derivation of R_n was published (Bierwagen, 1994), which calculates R_n from the low frequency limit of the spectral density functions for the potential and current noise and this was stated as being especially pertinent to the study of organic coatings / metal substrate systems. In light of the work by Mansfeld who compared R_{sn} to R_n for zinc-rich primer 3 coat systems, this cannot automatically hold good for all coating systems (Mansfeld and Xiao, 1996).

Attention is also drawn to the situation where two nominally identical specimens or working electrodes will produce lower R_n values if a coating defect is present in only one specimen (Bierwagen *et al.*, 1995). This is caused by the lower resistance of the defect dominating the resistance of the circuit in the same manner as a parallel resistance set-up in an electrical circuit. It is important therefore to ensure that the two working electrodes have not only the same impedance or resistance values but also that they do not contain defect areas which will produce premature low resistance of one electrode relative to the other. Resistance of the individual cells was measured using the D.C. resistance method and were found to be in agreement with the previously measured R_n values (Bierwagen *et al.*, 1995). The measurements were made at the end of the immersion period so not to interfere with the system. In the same work EIS measurements on the separate cells produced data used for Nyquist plots. Data from these plots, which show total system resistance including solution

resistance were used to obtain the parameter R_1 using an equivalent circuit model with constant phase element (cpe). The R_1 values were also in good agreement with the R_n values obtained. Coatings used for this work were not identified specifically but were of marine type ranging in the extreme from as low as 1.15×10^3 to 1.5×10^9 ohms.

Work using an alkyd system and an epoxy polyamide coating on cold rolled steel evaluated the coatings using electrochemical impedance spectroscopy (EIS) and Electrochemical noise analysis (Xiao and Mansfeld, 1994). Three parameters were obtained from the EIS data, the pore resistance of the coating R_{po} , the polarisation resistance R_p and the double layer capacitance C_{dl} . These parameters tracked the performance of the alkyd system with time with R_p and R_{po} decreasing and C_{dl} increasing with disbondment. The epoxy system showed excellent performance with no increase in capacitance. Noise data was obtained from statistical analysis and R_n derived. Frequency domain analysis was also carried out on the data to obtain another resistance parameter from the spectral noise plot; this is termed the spectral noise resistance (R_{sn}). Good correlation was established between the two parameters R_n and R_{sn} , but their numeric values were considerably lower. This was attributed to the sample interval chosen for the noise measurements that did not represent the low frequency end of the EIS spectra. More importantly the R_n and R_{sn} did show the same time dependence as both R_p and the pore resistance (R_{po}).

Further work was carried out on alkyd systems (Mills *et al.*, 1995). The electrochemical noise method was used to evaluate the performance of five alkyd primers which contained various inhibitive pigments and were applied to steel panels. The two nominally identical working electrodes were immersed in the same solution using a novel technique of blanking the majority of the specimen with a mix of bees wax and colophony resin and leaving an area exposed to the electrolyte solution as a working electrode. This has now been termed the beaker method as the electrolyte and three electrodes are contained in the same vessel (or beaker). This has the advantage the temperature and solution can be controlled more easily. Electrically the set-up

of the cell is identical to the bridge method where the two cells are isolated and the solution joined with a salt bridge.

2.11 Relationship between resistance noise R_n and D.C. Resistance measurement R_{dc} on coated substrates

It has long been established (Bacon *et al.*, 1948), that the D.C. resistance value of an organic coating gives a good indication of the level of corrosion protection that can be expected in service. D.C. resistance monitoring has also been used to assess suitability as a remote monitoring technique (Mills and Boden, 1993) and in attempts to monitor coating performance at scribes. This has been extended to investigation by ENM (Mills and Mabbutt, 1999).

Electrochemical noise characterised the performance of organic coatings on steel substrates by simultaneously monitoring current and potential of coupled electrode pairs via a low noise zero resistance ammeter (ZRA) with respect to time (Skerry and Eden, 1989). Simple statistics were used to calculate the standard deviation values for both the current and potential data and these were found to be indicative of the quality of coating protection. Good coatings were found to give relatively large σ_v values $> 10^{-4}$ V, where as poor coatings gave relatively large $\sigma_i > 10^{-7}$ Amp. The noise resistance parameter was not used in this work, but other useful information obtained was an estimate of the extent of de-lamination obtained from the total charge passed.

Work using only electrochemical potential noise looked at the evaluation of protective properties of organic coatings in marine atmosphere environments (Hukovic *et al.*, 1991). A two electrode multi-lamellar sensor was used to monitor phenol-formaldehyde based and coumarone-indene resin based coatings. Results were compared with those obtained from potentiodynamic polarisation measurements and optical microscopic photographs. The advantage of the results from the potential noise data was that it picked-up the very onset of

film rupture and pitting corrosion. An attempt was also made to distinguish between relative corrosion rates by converting the data from the time domain into the frequency domain using fourier transform. Relative corrosion rates being judged by the degree of slope of the spectral noise plots.

2.12 Area Effects of coated substrates on R_n

The question of area on current noise is addressed (Cottis and Turgoose, 1994), and it is shown that current noise can be expected to be dependent on the area of the working electrodes. Using the assumptions made in their work the currents generated from different areas of the electrode are independent from each other. The relationship between area and current noise in the paper is stated as current noise is proportional to (working area)^{1/2}. The reason for this is that noise circuit theory states that, when two un-correlated or independent noise currents are combined (as would be the case using the assumptions made in the paper) the resultant current is obtained by summing the mean current powers. A similar assumption is made about the relationship between potential noise and area. It is claimed that neither situation can be automatically assumed for all forms of electrochemical noise data (Eden *et al.*, 1986).

Work on carbon steel in 0.1M H₂SO₄ this system demonstrated noise resistance to be area dependent (Pistorius, 1997). Changes in current noise did track changes in corrosion rate but potential noise was seen to be approximately area independent. Polarisation resistance values for this system did not correlate well using this system. Noise resistance values were typically half to one order of magnitude higher than the measured polarisation resistance values. Two possible explanations for this are suggested (by this author); one is the evolution of hydrogen bubbles at the cathode which have been seen to effect noise values (Hladky and Dawson, 1981). The other cause of this discrepancy is the sample rates chosen for the tests, which was

50Hz and may have picked-up mains frequency. The choice of 1KHz for obtaining data in neutral solution could also be questioned as at this sample rate the 32,000 data points were only obtained over 32 seconds. In tests at our laboratory it can take this long for the experiment to become stable.

2.13 Standardisation of Electrochemical Noise Measurement

In 1996 the ASTM G1.11.04 Task Group was set up with the aim of addressing standardisation issues concerning electrochemical noise and from this produce a standard guide for electrochemical noise measurement (Kearnes *et al.*, 1996). The initial goal was to develop consensus on terminology, specifications and configurations for laboratory instrumentation, apparatus and data analysis methods. A round robin was organised to develop a body of information on different material and environment systems. This was done using different instrumentation configurations and data analysis techniques. The report which is mainly a review of the literature is published as a chapter of American Standards on Testing of Materials (ASTM), Special Technical Publication (STP 1277), (Kearnes *et al.*, 1996). The summary of the report concluded that it was important to have a body of data from a variety of systems and equipment that would eventually lead to the ability to compare data from various laboratories with confidence. This was to be achieved by the round-robin. The standard guide was to develop guidelines for three methods of gathering electrochemical noise data. a) electrochemical current noise at open circuit potential, b) electrochemical potential noise measurement at open circuit potential and c) potentiostatic noise measurement, whereby measurement of electrochemical noise is made at an applied potential.

The report suggested that the guide is to include extensive listing of terminology associated to ENM for all aspects including instrument specifications, configurations, calibration and validation of instruments and in addition to this data analysis methods. At the time of writing

reference data was being developed for four combinations of alloy and test environment to give standardised data values.

Further review of the literature comparing ENM with more established electrochemical methods such as D.C. resistance and Electrochemical Impedance measurement are given (Bertocci, 1996), also included is some supplementary data from NSWCCD studies (program on electrochemical methods for evaluating organic coatings - initiated by Dr. J. R. Scully).

The work underlines the importance of eliminating electrical input from sources other than the corrosion cell and shows an example showing noise of magnitude greater than 40 mV superimposed onto the monitored signal caused by background sources within the laboratory. In addition to this peaks of a magnitude in excess of 100 mV are also seen where human movement has caused electrical interference.

2.14 Experimental Investigation (NDSU Project): Characterisation of Corrosion Under Marine Coatings by Electrochemical Noise Methods

Aim of the project.

The main aim of the work at North Dakota was the study of marine coatings using electrochemical noise methods (ENM). Building on the work by Skerry et al who had used ENM to examine organic coatings on metal, (Skerry and Eden, 1991) (Chen and Skerry, 1991). This work had specific aims concerning the equipment used for the investigation. The areas of interest were purchase, installation, calibration of the apparatus along with implementation of the technique in situations of coated metal in salt water environments.

The work was to be done on coated metal systems using established standard coating test methods including elevated temperature testing, immersion and Prohesion testing. Other electrochemical techniques such as Electrochemical Impedance Spectroscopy (EIS) and D.C. resistance measurement were used to monitor coating performance.

The aim being to develop a protocol for interpreting results by comparison of ENM data with results from the parallel corrosion studies.

The accuracy of the ENM technique was to be improved by developing data treatment routines for noise resistance vs. time and analysis of frequency domain spectra of the noise data.

From this it was hoped that a mechanistic model could be developed for the corrosion prevention performance of the marine coatings.

The final aim of this work was the feasibility of the development of a sensor that could be implanted in coated metal systems and as such be used for continuous monitoring or intermediate monitoring of the coating over the service life span.

2.14.1 Overview of the NDSU Report

The report consists of five main parts excluding appendix and references:

Section 1 - Introduction, outlined above set-out the aims and objective of the work.

Section 2 - Experimental, covers experimental considerations and is subdivided into four areas covering: i) Materials and panel preparation, ii) Electrochemical Noise Method for immersion tests, iii) Accelerated tests and iv) Panel assessment methods.

Six coatings were investigated, four primers; an alkyd, zinc silicate and two types of epoxy.

These were used with an alkyd and an epoxy top coat applied to grit blasted steel in an attempt to re-create conditions encountered when applying the coating in service. Coating thickness was approximately 70 μm for each coat. Coatings were also applied to polished steel and glass panels for agitation studies and detached coating investigation. The panels were masked with beeswax and colophony resin to leave exposed test areas 50 cm^2 .

Electrochemical Noise Immersion tests were done by a different experimental technique since termed the beaker method to that used in previous work (Mills and Mabbutt 1998). The fact that both specimens are immersed in the same beaker and solution makes the effect of temperature and agitation easier to study. Some of the immersion tests were done using the

more traditional technique of two separate working electrodes (specimens) with cells attached and the solutions ionically connected using a salt bridge.

The equipment used was a CML data logger and zero resistance ammeter which was controlled by a standard PC. Monitoring twelve pairs of electrodes by use of a multiplexing device data points were recorded every 2 seconds typically over 8.5 minutes to give 256 data points. For some of the later work equipment manufactured by Gamry was used. For the high impedance systems it was noted that there was a difference in R_n value obtained between the two different measurement equipment.

Accelerated tests took the form of agitated solution where the electrolyte was stirred by electrically driven impeller to give a high speed vortex. To ensure reproducibility the base of the vortex relative to the specimen height was used, though no interface velocities are presented. The high temperature accelerated testing was carried out at 42, 55 and degrees centigrade using diluted Harrison's solution. Cyclic Salt spray which cycled between wet and dry every two hours was used with 3% NaCl, to give a more aggressive environment and finally a hot salt bath test was used containing sea water or 5% NaCl at 55 degrees centigrade.

Panels were assessed in each case by D.C. resistance, A.C. impedance and visual assessment in addition to the ENM measurements made during testing. An in-depth description of D.C. resistance measurement as an in-situ technique is given in appendix 1 of the report. Visual assessment was made using a scale of 1 to 10 to rate the appearance, with 10 indicating no blisters and 1 indicating several blisters. This was method was considered more suitable than the ASTM D610 or D714 standards. Results for specimens which had been scribed were rated on a similar scale.

Section 3 - Results on Coated Steel, also divided into four sections. i) and ii) Coat studies using ENM immersion tests and accelerated test results, iii) Effects of agitation / stirring and iv) High temperature experiments.

Results of the immersion tests on the 2 coat systems correlated well with the D.C. values. It is noted that the zinc based primer exhibited a lower R_n values due to higher current noise indicating a porous film which is itself corroding. It is postulated that the ENM R_n value is therefore a measure of the coating resistance itself. Accelerated testing on the primer systems using the hot salt bath and the 1000 hours spray ranked the same alkyd as the better coating. Specimens which had been scribed and exposed to the same tests showed the zinc haze to be the better coating at protecting at the scribe.

The three coat immersion tests using ENM was interesting in that four systems of the eight were identified as better performance but these could not be ranked further by electrical means alone. Also, from these tests it was stated that whether successful assessment of zinc rich systems by electrical means can be achieved is still open to question. Indeed, a moderate R_n and current value may be advantageous in that it assists in maintaining a low potential providing cathodic protection. The accelerated test results ranked the coating systems generally in the same order as that indicated by the ENM results.

Agitation of the solution to increase the rate of breakdown of the coating systems did not have an observable influence on the better coating systems, however there was an increased attack on the less protective systems. This was verified by ENM data which also showed increased attack in the agitated experiments. Considerable problems were encountered regarding extraneous noise from the stirring mechanisms which produced differences as great as two orders of magnitude between the stirrers being turned on or off. On further investigation of the effects of stirring using just the primer systems it was found that the measured R_n was in fact lower when the stirrer was operational. Inspection of the data led to this being attributed to the fact the agitation was having a greater effect on current noise than potential noise.

High temperature experiments also caused problems with extraneous data being generated by the heater thermostat cutting in and out. In this instance the 55 °C tests did not give a clear definition between the results from the 42 °C. This was attributed to the interference of the

heater on the 55 °C data. D.C. resistance values recorded at the end of the test did show considerably lower values for the higher temperature samples, but because of the amount of scatter on the samples it was not possible to rate the four better systems.

Section 4 - Fundamental Studies, covers i) work on detached films using D.C. resistance, Electrochemical Noise Measurements (ENM) and inhibition tests and ii) Fundamental studies on Noise Resistance (R_n), investigating derivation and meaning, factors affecting ENM and data treatment and ways of improving accuracy.

Work on detached films is detailed for both D.C. and ENM. D.C. resistance measurement of detached films is described in detail in appendix 2 of the report. Electrically the set-up for these experimental procedures is the same as when the coating is attached to the substrate. However, there is considerable scope with these experiments to study the effect of different substrates by using different working electrodes (Mills and Mabbutt, 1998). At resistance below 1×10^8 there is quite good agreement between the D.C. resistance, and ENM R_n values measured by both sets of noise equipment. Differences at higher resistance values was attributed to equipment limitations. There was also a difference in R_n values between those obtained when copper working electrodes were used in place of the steel. It was suggested that this may have been caused by an increased tendency for drift on the copper electrodes. (NB. Subsequent work with alkyd coatings on different substrate materials has also shown a difference in R_n values, all other things being equal.

Description of leaching experiments is given, which were used to establish the effectiveness of inhibitors contained in the primer coatings. Further details on this procedure can also be found (Mills, 1973).

Derivation and meaning of Noise Resistance is outlined briefly. It is stated that both current and potential noise should be Gaussian in distribution. This is certainly the case if the maths is to hold good for giving R_n values equivalent to R_p . Further, the two main sources of noise

considered being Thermal noise and Shot noise conform to this criteria. Detail derivation was produced from this work (Bierwagen, 1994). Although some criticism has been levelled (Mills and Mayne, 1981) the general conclusions are in agreement and these have been stated previously in the literature review. The most important finding was that for a particular area on a given specimen the R_n value relates strongly to the measured D.C. resistance value.

Factors effecting the data obtained from ENM techniques were generalised as environmental disturbance and equipment considerations. In the first instance disturbances by external interference such as a passing person is discussed regarding the influence on potential and current noise values. In the second instance the equipment is discussed and the conclusions drawn are that at the high impedance end of the range the electronics of equipment will influence the final value. Also of consideration in general terms is the susceptibility of the instrument to extraneous interference generated by external sources.

Improved accuracy of ENM is recommended by use of increased software sophistication. A program which allows spectral as well as ordinary analysis to be done on the data is suggested. The advantage of this program is that it can correct for the largest two influences on ENM data, that of D.C. drift which can give errors of up to and occasionally greater than an order of magnitude for R_n . The second problem which can be countered is that of data spikes caused by sudden external interference such as switching operations on a mains circuit or a passing person. Spikes are termed wild points in this work and the definition of how a wild data point is identified and accounted for in the final data set are given in the appendix 3. It is also mentioned that improved accuracy can be obtained by the use of a Faraday cage to house the experiment, however it is still felt that the main limitation of the technique regarding accuracy is the equipment itself.

Section 5 - Conclusions and Future Work.

Conclusions are divided into three main areas of; 2 and 3 Coat Investigations, Fundamental Work and Mechanism Investigation.

The main conclusions to come out of the 2 and 3 coat work are that all noise parameters R_n , I_n and V_n are of use. In general terms the R_n parameter is most useful because of the correlation with D.C. resistance values for individual specimens which has relevance to the original Bacon, Smith and Rugg criteria.

In the ambient temperature static immersion tests ENM correlated with both D.C. resistance values taken at the end of the test and visual observations. The results were sufficiently consistent to be able to divide the coating systems into four groups ranging from good to poor protection. However, it was found difficult to separate different good systems because of lack of reproducibility and it is suggested that more samples should be used in future.

Correlation was also good between scribed coated specimens when examined using ENM when compared to cabinet and hot bath test results.

Agitation of the solution accelerated breakdown of less protective coating systems but the noise response was not consistent. This appears to be because of problems of the stirring mechanism causing interference on the data.

Increased temperature of the test solution reduced the R_n value but lack of reproducibility prevented ranking of the good coating systems.

Conclusions of the fundamental work found strong relations between the R_n parameter and the D.C. resistance value of the individual specimen. It is stated that where the D.C. resistance values of the two specimens are different the best estimate for R_n is to take the geometric mean of the two D.C. values.

The importance of the data set being stationary around the mean during the test duration is emphasised if R_n values are to be accurate. It was also found that the data approximated a

Gaussian distribution regardless of whether the noise was from shot or thermal noise processes.

The limiting factor on accuracy found for this work was the equipment itself with R_n values above $5 \times 10^9 \text{ ohm-cm}^2$ unable to be measured accurately.

Mechanistic Investigations were not carried out in depth with the project but some findings were presented in the conclusions.

Namely the results implied that the ionic resistance of the coating is the main controlling factor and that of the coating tested only the alkyd showed any significant chemical inhibition during the first thirty days of testing.

This information implies that with epoxy systems which provide barrier protection attack at breaks in the coating would not be prevented.

The detached resistance values demonstrated that at least three coats would be necessary to give adequate barrier properties for protection against ions.

The zinc coatings although protecting had low R_n values that indicated the coatings were porous and caution is advised when interpreting results from electrochemical methods.

It is suggested that further information could be obtained on mechanisms by spectral analysis of the noise data.

Future work recommends analysis of current and voltage data in the frequency domain. It is also suggested that segmented electrodes be developed that can be placed beneath common organic coatings which can be used as in-situ monitoring techniques. Further work on detached coatings and aqueous extract by electrochemical means is detailed along with characterisation of homogeneity of films that exhibit local heterogeneity.

A variation on the EIS technique is suggested for better comparison with ENM data. Also the idea of obtaining ENM data under the presence of an imposed voltage is put forward. This would simulate the conditions where the coated structure is under cathodic protection.

The three appendices cover background information on:

- i) D.C. resistance measurements on coated substrates,
- ii) D.C. resistance measurements on detached coatings and
- iii) The method used for data compression using FORTRAN programming.

2.14.2 Continuation of ENM research

On completion of this report the Senior Investigator continued research relating to electrochemical noise at University College Northampton (UCN), UK. Work at UCN has built on the work done at NDSU and this project is a continuation of this work.

2.14.3 Publications from the North Dakota research project

The NDSU report produced publications including two accepted for publication at the time of writing the original report. (Mills *et al.*, 1993), (Bierwagen *et al.*, 1993), (Bierwagen, 1994), (Bierwagen *et al.*, 1994), (Bierwagen *et al.*, 1995), (Mills *et al.*, 1995).

2.15 Publications from Early Work at University College Northampton (UCN)

Prior to PhD registration some preliminary work was carried out at UCN on water-borne anti-corrosive primers using solvent based alkyd for comparison where appropriate. A journal paper gave a more general description of the techniques for electrochemical noise monitoring contrasting ENM with more established test techniques (Mabbutt and Mills, 1997). A full list of publications is given in Appendix 5.

2.16 Preliminary Published Work Presented at Conference

Work presented at international conference covered both in-tact and preliminary findings on scribed coating, also the effect of coated aluminium substrates on R_p were investigated and

compared to data from coated steel substrates. This work was published as publications in conference proceedings.

2.16.1 EuroCorr 96

Work prior to registration, presented at EuroCorr 96, and published work gave a good correlation between six pairs of specimens coated with water-borne acrylic coating using the D.C. resistance method (Mabbutt and Mills, 1997). This was repeated with a water-borne black vinylidene which showed similar reproducibility though values of resistance are consistently lower.

Further analysis of the experimental results demonstrated a generally close correlation between R_{dc} and R_n for these systems across a range of resistance values from 1×10^5 ohm-cm² to 1×10^9 ohms-cm². R_n values at the lower end of the scale $10^5 - 10^6$ were slightly higher than the D.C. resistance values (R_{dc}). At the higher end of the resistance range the R_{dc} values were higher than the R_n values. The closest correlation between R_n and R_{DC} was at around resistance values 10^8 ohms. The difference between R_n and R_{dc} values at the high end of the spectrum is attributed to instrumentation limitations. The difference at the lower end of the spectrum is discussed in depth subsequently but is a characteristic of the low resistance vinylidene coating under test.

The agreement between R_n and R_{dc} was seen on both the Al and the Fe coated substrates. When the coatings were investigated as detached film using a glass cell and the D.C. resistance technique with time a close correlation was seen between the values obtained for the attached coatings. The exception to this was the vinylidene coating which had a much higher resistance initially but dropped to the attached level of resistance then below after 24 hours. This is now thought to be because the coating is very porous and although a good corrosion inhibitor it relies on chemical inhibition. However, when the D.C. values are compared to the R_n values for this coating a difference between R_n and D.C. resistance values is apparent. At this stage

the coating had dis-bonded from the substrate and it is stated in the conclusions that the D.C. method has picked this up. Conversely it seems likely that the Noise has in fact shown that there is no corrosion occurring demonstrated by the higher R_n values for the same specimens. The importance of assessing scratched organic coatings is suggested as future work and had just been embarked upon at the time of this work. Overall the paper concludes that the technique has been demonstrated beyond reasonable doubt its usefulness as a tool for monitoring corrosion protection by organic anti-corrosive coatings.

2.16.2 EuroCorr 97

The work presented at EuroCorr 97 (Mills and Mabbutt, 1997) used the same two water-borne coatings described in the previous section. For comparison and to establish the correlation between R_n from ENM and D.C. resistance values both were investigated again as a function of time. Again, good correlation between R_n and R_{dc} was seen for both coatings. The work on the scribed coatings appeared to demonstrate that R_n was indicating protection at the scribe as the R_n value was higher than that observed using the D.C. method. Inhibitor experiments were used to successfully protect steel electrodes from corrosion and gave R_n values comparable to those observed for the inhibiting scribes. There was greater than an order of magnitude difference between inhibiting and corrosive environments when molar concentration and solution conduction remained equal. This was seen in another experiment where the concentration of NaCl was increased to a point where inhibition broke down. R_n values dropped to within half an order of magnitude of the value for steel in 0.2 M NaCl which were corroding freely and corrosion was observed using potassium ferricyanide indicator to indicate the production of Fe ions at the anodic sites. The work showed a promising beginning to the investigation of corrosion protection at scribes or holidays in anti-corrosive coatings. Unfortunately the nature of the inhibitors did not offer a high enough degree of protection in more aggressive media for mechanistic study or investigation of the electrochemical noise data.

2.17 Justification of Present Work

It was from this work that the decision was made to investigate established successful coating systems. It was hoped to show with higher performance coating systems that ENM could successfully show the ability of a coating to protect at scribes or holidays. As suggested in the NDSU report more detailed data analysis procedures and investigation of the potential and current data was thought to contain information that would give mechanistic detail of the processes.

Data analysis has subsequently been used for work included in this thesis. Also more advanced methods of producing scribes and holidays have been developed and this has been shown to increase reproducibility of results. The coating systems are established alkyd and epoxy resins and some work has been done on red lead where total inhibition was required for data analysis purposes.

CHAPTER 3.

Experimental Methodology for General Electrochemical Experiments

3.1 Instrumentation

Specialist instrumentation used in this work is available from ACM Instruments and consists of the zero resistance ammeter and data logger along with dedicated software. Other laboratory equipment is standard equipment and instrumentation commonly available. Exceptions to this are the glass U-tubes used for the detached coating work, that were manufactured by Abinghurst Laboratory Equipment, Northampton. to the Author's drawing. The mechanical coating removal tool used and explained in Chapter 4 was designed and manufactured by the Author.

3.2 Computer

The computer used throughout this work consisted of a standard IBM compatible Pentium II PC and printer.

All files are contained in a sub-directory C:\WinSeqV3\. The names of the files for each experiment correspond with those recorded in the lab book and given in relevant chapters of this work.

Each test automatically generates four files within the relevant experiment file. The files containing the current and potential data including calculated parameters have the post script **.cvd. The original data in binary form is contained in the file post scripted **.seq. The two remaining files, post script **.cvh and **.set contain the information for the screen headers and the software settings for the test respectively.

In addition to these files is a fifth with the postscript **.xls. This file contains the information from the cvd file in a format that can be read into standard Excel software. This operation is performed as a manual step using the software during inspection of the data.

3.3 Zero Resistance Ammeter (ZRA)

Other hardware consists of a zero resistance ammeter manufactured by ACM. This equipment has a very high input impedance which is selected automatically on commencement of each test run. Counter resistors to achieve this can be selected up-to $10\text{M}\Omega$ resistance. The ammeter has three electrode connections with shielded leads - two for the working electrodes and one for a reference electrode to measure potential relative to the working electrodes. If potential measurement is not required the reference electrode can be grounded to the instrument earth by connection to working electrode WE2.

The ZRA circuitry is built around an operational amplifier and counter resistor, Figure 3.1.

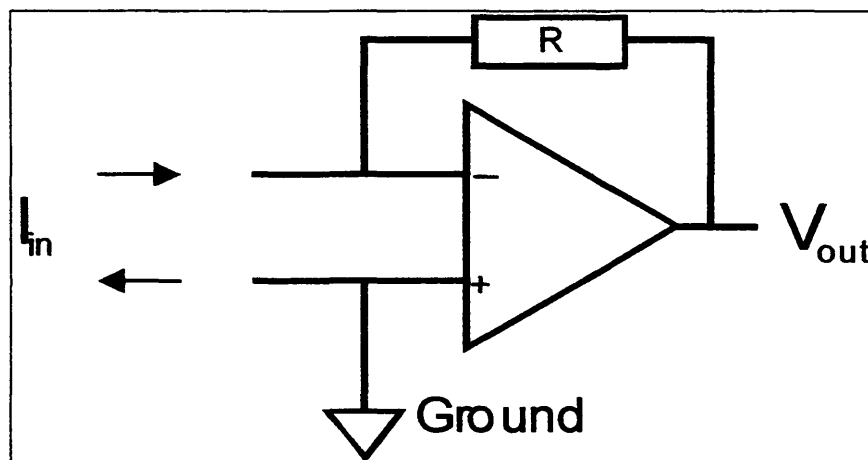


Figure 3.1 Schematic representation of an operational amplifier -the basis for the zero resistance ammeter (ZRA) (Taken from Cottis and Turgoose, 2000)

The working electrode, WE2 (+), is connected to instrument ground. The negative input is connected to working electrode, WE1. Connected across the input (-)WE1, of the operational amplifier and V_{out} is a counter resistor. The function of the operational amplifier is to polarise WE1 to the same potential as WE2. This creates a situation where the two electrodes act as if coupled together by wire and is achieved by the application of a current over the counter resistor. The voltage produced at the output of the operational amplifier is measured relative

to instrument ground and using Ohm's Law the magnitude of the instantaneous current calculated.

The potential of the coupled working electrodes is measured against the external reference electrode.

3.3.1 Software

Dedicated software supplied by ACM controls the zero resistance ammeter (ZRA) and data logging function, allowing instantaneous sampling of potential and current. The software interface uses Windows 95 operating system or Windows NT. The software is divided into separate programs; data logging and analysis that can be run concurrently or individually.

The data logger program enables the user to choose from a range of test parameters as well as giving a choice of file name and directory where data records will reside.

Options that can be specified include:

Cell settle time - from 0 seconds, this option connects the electrical circuit incorporating the working electrodes to enable potential differences to dissipate before data logging begins. This helps considerably in reducing D.C. drift in the early part of the first test run.

Pause - from 0 seconds, this provides a period of time between multiple test runs of the same test.

Number of tests - from one, though only a maximum of six can be held in the analysis field and only four in the analysis buffer at any time.

Electrode area - can be set so parameters such as resistance or current density do not need to be calculated.

Measure - an on / off function which can provide the facility to monitor only current or potential or both.

Read rate - is the sample interval or frequency of data acquisition, minimum sample interval being 0.02 seconds or 50Hz.

Points per test - the amount of data points recorded at the assigned read rate before the test ends.

The data analysis software can be accessed through the data logger software by a button or pull down menu.

3.4 Electrodes

A three electrode set-up has been used for all of the ENM experiments. In normal electrochemical noise monitoring configurations the two working electrodes consist of two separate specimens of the substrate metal. Potential is measured in all tests using a reference electrode relative to the coupled working electrodes. Because monitoring of potential fluctuations (noise) are the aim of this activity it is important that the reference electrode be as noiseless as possible. Of the standard range of laboratory reference electrodes available the Saturated Calomel Electrode (SCE) is reputed to be one of the least noisy. Reference electrodes produce noise across different frequencies and the profile of this varies with reference electrode type (Cottis and Turgoose, 2000). Power spectra of noise in the frequency range 0.001 Hz to 0.1 Hz show a good SCE to be generally less noisy at lower frequencies by about 20% compared to silver-silver chloride (Ag / AgCl). As such SCE's were used for potential measurement throughout all general noise monitoring experiments. AgCl are better suited to elevated temperatures and are stable up to 105 degrees Centigrade (supplier information), however Ag/AgCl are sensitive to light which can increase electrode noise this can be induced by florescent lighting. The Ag / AgCl electrodes used in this investigation were shielded against external light sources.

3.4.1 Evaluation of electrode noise

It was considered important that the contribution made to the noise data by the reference electrode was established. This was done by immersing three SCE's in 3% NaCl solution. Two were connected to the working electrodes (WE1 and WE2), the third to the reference electrode connection. The noise resistance (R_n) produced from this arrangement averaged at 8×10^3 ohms. The potential noise (V_n) contribution to this value was around 8×10^{-6} Volts. The current noise (I_n) was calculated at 2.0×10^{-9} Amps. For the coating systems and corrosion cells investigated in this work these values were sufficiently low as to be neglected in subsequent evaluation of the resistance noise parameter (R_n). Preliminary work on bare steel using 1M H_2SO_4 as electrolyte gave significantly lower values of R_n due to high corrosion current density. Values in the low 1×10^3 ohms region were seen which indicates a significant proportion of the R_n value derived in NaCl is attributable to solution resistance.

3.5 Evaluation of instrument noise

Instrumentation noise can be established by running a test with the electrode leads disconnected from any electrodes. The reference electrode connection requires grounding for this operation and this is achieved by connection directly to working electrode 2. The potential noise was 5.8×10^{-6} Volts, around 75 % of the V_n value found in the SCE noise test above. This demonstrated that the SCE in this application can be regarded as noiseless. The current noise value calculated from the instrument was 5.5×10^{-13} amps or 5/10ths of a picoamp. These values complied to option 1 for calibration with respect to intrinsic instrumentation noise, ASTM STP 1277 (Kearns *et al.*, 1996) and confirmed that instrument noise could be regarded as negligible for the work investigated here.

3.6 System Noise

Noise from the corrosion cell has been successfully modelled, (Cottis, 2000) using electronic components of the same resistance and impedance values as the system under test in the particular conditions of the test. The dummy cell can be used to determine the noise of the system under investigation. In the situation of coating investigation this step is unnecessary because it is the changes and dynamics of the system that are under investigation and not the nature of the noise signals. Tests of instrumentation noise have been extended to include reference electrodes in solution. These tests demonstrated low background noise in the same region seen for the grounded reference electrode tests. The results of these preliminary tests therefore eliminate all components of the system regarding background noise leaving only the substrate / coating and coating / solution interfaces as additional noise sources. A different approach was used in this work with the noise of the instrumentation being measured directly.

3.7 Specimen Materials and Preparation

The specimens for all experiments were prepared in the same manner as set out in section 3.7.

3.7.1 Substrate

Q-panel test panels were used as substrate material throughout this work. The panels were mild steel, unless otherwise stated. The substrate material was cold rolled to 0.8 mm thickness and 150 mm long by 100 mm wide.

Before use the panels were degreased using isopropane-1-ol. The surface finish used was as supplied - rolled. Where bare Fe was used as working electrodes the surface was cleaned with 1200 grit paper and degreased in the same manner. This additional step was included to restore the surface to original after handling during preparation of the electrodes.

3.7.2 Coatings

Coatings used for this work included solvent or water-borne alkyds and 2-pack epoxies, one solvent based (CM) and two with a water based amine (Ind. Co-polymer 152 and 148), water-borne acrylic (Neocryl) and water-borne vinylidene (Haloflex). In addition to this red lead primer was also used with and without a commercial alkyd top coat as a control in inhibition work. Coatings and specifications used for each experiment will be given in relevant areas of the work. The coatings were chosen for this work because they represent a range of industrial grade materials. Thermosetting high-build epoxy systems to emulsion based water-borne systems were used to give a broad cross section along with the traditional long proven coating, red lead in linseed oil, used as a control in the inhibitor experiments. These coating systems not only give a varied range of protection against corrosion to the substrate but also offered a full range of electrical resistance values essential for the investigation of ENM.

3.7.3 Coating application

Coating application was by spreader bar. A method used in previous work (Mills and Mabbutt, 1998), as it gives consistent coating thickness with minimal defects. The spreader bar has a stepped central section machined to give a required thickness. Actual thickness of the final coating however, depends on the build characteristics of the coating, pigment volume concentration (PVC) of the liquid coating and the amount of solvent. As a rule of thumb; wet film thickness is approximately half of the spreader bar gap. The dry film thickness being equal to approximately half of the wet film thickness.

3.7.4 Blanking

Some testing in this work involved submerging the two working electrodes in the same vessel, (see beaker method 3.9). In order to test only a controlled area of coating and insulate corners and edges where the coating is inherently weak a blanking agent of very high electrical / ionic

resistance was used. This consisted of a mixture of beeswax, 75% and colophony resin, 25%. The melting temperature of this mixture is around 60 °C, it is applied by paint brush with the area to be tested protected by a cylindrical steel blank of a predetermined area. The thickness of the beeswax / resin compound is normally in excess of 0.5 mm thick.

3.7.5 Detached coating

The same coatings investigated on the substrate were also electrochemically examined when removed from the substrate. This investigation and further specific experimental details are included in chapter 4. This approach has been adopted in view of the experimental set-up being different to that used for general noise measurements.

3.7.6 Preparation and removal of detached coatings

The process of producing a detached coating involves casting the coating on to a glass plate to the required thickness. Preparation of coated panels involved the glass being degreased in the same way as the metal Q-Panels and dried. A spreader bar was used for the application of the coating. Several coats can be applied in this way to give the required thickness.

Once dried removal of the coating from the glass can be a difficult operation, particularly if large areas are required. The best method of removal has been established as soaking the coated glass specimens in a hot water bath. Prior to this the coating is scribed through to the glass with a razor blade or scalpel. In the bath the coating is heated to above its glass transition temperature. The scribes allow water to penetrate to the glass / coating interface. When the coating had softened sufficiently it was then be parted from the glass surface using a conventional razor blade. The areas required were only in the region of 3 cm² and this was quite easily attained with most of the coating systems used. Preliminary experiments and past work (Bierwagen *et al*, 1994a) has shown that with care this procedure does not have a

detrimental effect on the coating and that Tg is reversible with regards to the properties of the coating.

3.8 Experimental set-up

Two established experimental set-ups were used throughout this work where general electrochemical noise monitoring was conducted.

3.8.1 Three electrode system

The need to obtain values of R_n requires both current and potential noise values. Hence all experiments used a three electrode set-up. This is necessary if the resistance noise parameter R_n is to be derived as this relies on both current and potential noise values being obtained.

3.8.2 Working electrodes

The working electrodes, with the exception of work in chapter 7 and detached coating investigations, consisted of the steel or aluminium Q-panel substrate. These were regarded as nominally identical for experimental purposes.

3.8.3 Reference electrodes

Reference electrodes were saturated calomel electrodes. These were used for measurement of potential relative to the two working electrodes (WE1 and WE2). They were chosen as stated (3.4.1), because they are the least noisy of the commonly available laboratory reference electrodes.

3.9 Experimental arrangements

Experimental arrangements used for ENM consisted of either the beaker method or the bridge method. Each method has specific advantages but as stated both are electrically identical.

3.9.1 The beaker method

The beaker method, Figure 3.2, has been used in previous work as a reliable method of obtaining ENM data (Bierwagen *et al.*, 1994a).

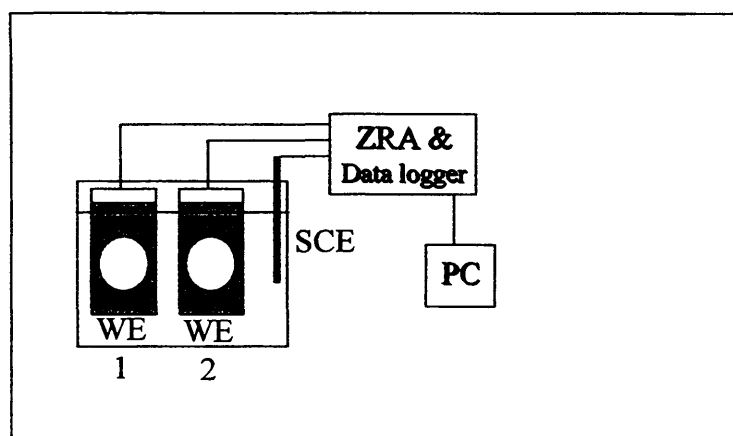


Figure 3.2 Beaker Method of Electrochemical Noise Measurement

It is effectively the same set-up suggested in ASTM STP 1277 (Kearnes *et al.*, 1996) and has the advantage over other methods that both working electrodes and the reference electrode are contained in the same solution and vessel. This makes experimental procedures more simple when the effects of such parameters as solution temperature or flow rate on electrochemical noise are being investigated. It also allows solution concentrations or flow rate to be adjusted more easily as only one volume of solution has to be considered. This method has been found to be more suitable for the investigation of low resistance systems such as bare metal or

C

experiments where noise from bare metal areas such as scribed coated substrates dominate the data. Solution resistance is minimal with the three electrodes in such close proximity and can be relatively easily measured if needed.

3.9.2 Bridge method

The bridge method is also a well established set-up for ENM experiments and has been used widely (Bierwagen *et al.* 1994a). It involves creating two separate but nominally identical working electrodes from the coating system / substrate under investigation, Figure 3.3.

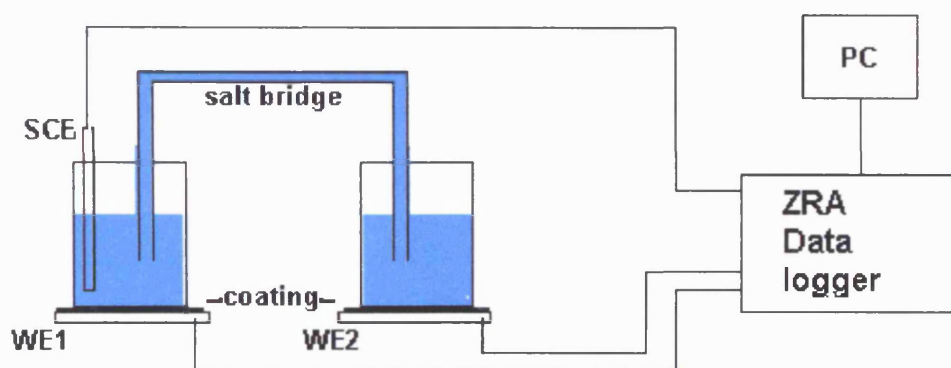


Figure 3.3 Bridge Method for Electrochemical Noise Measurement

The bridge method is used for experiments where the coating systems or cells are of relatively high resistance ($> 1 \times 10^3 \text{ ohm-cm}^2$). The bridge method involves the attachment of polyvinylchloride (PVC) cells to the two separate working electrodes. The PVC cells are attached to the coated working electrodes by silicone sealer. This was chosen for its chemical resistance and inert properties in relation to electrolytes used. The cells contain the electrolyte, the two cell solutions are connected by a salt bridge that is filled with the same solution. The salt bridge provides a path of ionic conduction that is necessary for completion of the electrochemical cell and current monitoring. One of the cells contains the reference electrode to monitor the instantaneous potential of the working electrodes. Although the set-up looks

different physically to the beaker method, electrically they are identical. Solution resistance will obviously have a greater effect with this set-up because of the greater distances between the electrodes and the cross sectional area of the salt bridge.

3.9.3 Salt bridge preparation

The salt bridges for the bridge set-up were prepared using clear 3mm diameter flexible plastic tubing. A ribbon of filter paper ran the length of the tube held in place by a porous plug of filter paper at each end of the tube. Before the second porous plug was inserted the tube was filled with the appropriate electrolyte solution and all air bubbles expelled. Storage of the salt bridge between tests involved the plugged ends being submerged in the same electrolyte fluid to prevent drying out and the formation of air bubbles. The whole beaker was then sealed to prevent evaporation and consequent increase of solution concentration.

3.9.4 Effects of salt bridge diameter on ionic conduction

Early tests on low resistance systems using bare metal in 0.1 Molar H_2SO_4 acid and 0.1 Molar NaCl solutions indicated a discrepancy between the derived R_n values obtained using the bridge method when compared to those obtained using the beaker method. All other experimental parameters were constant and as such the discrepancy was attributed to the difference in experimental set-up. The resistance values from the bridge experiments were consistently higher than those obtained from the beaker method and the salt bridge appeared to be the most probable cause of this. This was investigated by conducting a series of tests where the cross sectional area of the bridge was gradually increased.

A set-up, Figure 3.4 was developed whereby the bridge could be effectively the same cross sectional area (C.S.A) or larger than the cells.

Working electrode area for these tests were 1cm^2 bare Fe in 0.1M H_2SO_4 , the bridge area was

A-11.2 cm², B-1.2 cm² and C-0.14 cm².

Time hours	“A” R _n ohms-cm ²	“B” R _n ohms-cm ²	“C” R _n ohms-cm ²
0.5	3.2E2	3.92E2	1.65E3
1.0	3.85E2	1.89E2	2.39E3
5.0	2.07E2	5.21E2	2.84E3
21	6.55E2	1.22E3	2.84E3

Table 3.1 Results from 1cm² working electrode tests using different bridge cross sections.

It was found that the trend in R_n value had an inverse relationship to that of the cross sectional area of the bridge. Further tests were done with working electrode areas of 11.2 cm².

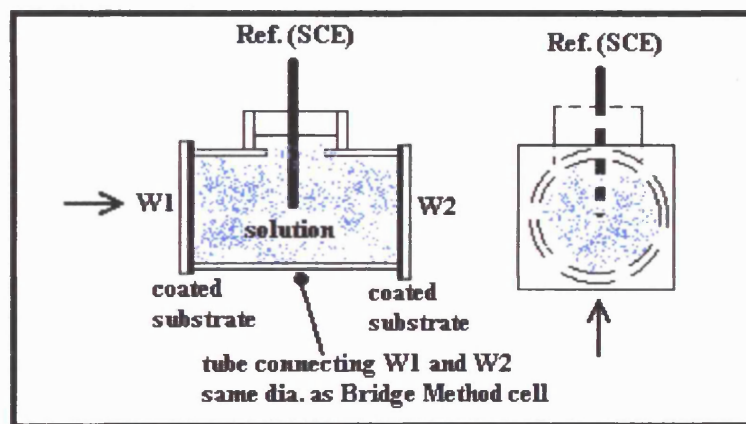


Figure 3.4 Novel test cell for evaluating lowest salt bridge solution resistance for a given cell area.

Using bare Fe electrodes the relationship in table 3.2 was observed after 5 hours of general uniform corrosion.

Bridge Area cm ²	R _n ohms (not area corrected)
11.2	207
1.12	521
0.14	2840

Table 3.2 Data from 11.2 cm² working electrodes in 0.1M H₂SO₄ using different bridge cross sections.

The trend indicated was due to the solution resistance cross sectional area. This finding led to the use of the beaker method for low resistance systems throughout the work.

3.10 Solutions

Solutions for the experiments were prepared as molar solutions or as full strength solutions where the ratios of different components were given in the literature. Because of the small volumes of electrolyte required for the tests, less concentrated solutions were obtained by the system of series dilution to reduce error.

3.10.1 Testing Solutions

With the exception of some early experiments conducted on bare metals in dilute acids and inhibitors (these are described in the relative sections), two different salt solutions were used for the coatings investigations.

The most aggressive of the two was sodium chloride (NaCl). Used at various concentrations from 3% to 0.03%.

The other solution was Harrison's solution. Harrison's was originally developed following investigations of atmospheric pollution and contamination found in atmosphere close to railway operations (Harrison, 1970). Samples taken from the environment showed that the coatings were encountering much higher levels of ammonium sulphate than sodium chloride.

The final test solution formulated for testing coatings destined for this sort environment was recommended as 3.5 % Ammonium Sulphate and 0.5 % Sodium Chloride. This was said to be more representative of service conditions.

Harrison's solution was used through out this work as a full strength solution and again at various dilutions down to 1%. Further reference to Harrison's solution in this work will infer full strength unless the dilution is given. Where the dilution is given it will be as a percentage of full strength, ie 10% Harrison's is 0.1 times the full strength salt masses in water. The same approach will be adopted for other mixed salt solutions. Where acids and bases are used molarity will be given.

3.10.2 Ionic Conduction

The ionic conduction between the two working electrodes and the reference electrode will have an effect on the resistance noise value. R_n inherently includes the solution resistance R_s in the same way as polarisation resistance R_p measurements include solution resistance. The important factor is whether the solution resistance is high enough to have detrimental effect on the data. Typical values for solution resistance using R_n between 1cm^2 electrodes at 1cm spacing in 3 % NaCl were found to be in the region of 175 - 200 ohms. When compared to a D.C. reference electrode resistance of around 7.0×10^3 ohms and coating resistance typically greater than 5.0×10^4 ohms, and this was considered negligible. Noise resistance values quoted throughout this work therefore include the solution resistance unless otherwise stated.

3.11 Experimental parameters

For general ENM experiments the software setting parameters were kept constant. Preliminary work on bare Fe and coated samples established the parameters for convenient and accurate results. This was considered important if ENM and in particular R_n is to be established as a tool that can quickly assess the nature of a coating system.

3.12 Data gathering

Data gathering can be done as a series of test runs, up to a maximum of six. One of the major problems concerning data acquisition and a criticism often levelled at ENM as a technique is the problem of D.C. shift or drift of potential / current data plots over the period of the test run. The effect of drift on the data set can mask the fluctuations or noise of the system and give an artificially high standard deviation value or skewed data sets. Data sets tend to drift in one of two ways: either a linear drift or a power law drift. Both can be corrected mathematically but this is time consuming and recommendations in ASTM STP 1277 (Kearnes *et al.* 1996), suggest that optimisation of the experimental conditions is preferable to correction of data at a later stage.

3.13 Test protocol

Considering the recommendations of ASTM STP 1277 a protocol was developed for obtaining the “best data set” for a particular system. Software settings were adjusted to give ten seconds for the cell to settle. (This time period involves the electronics of the circuit being connected to the corrosion cell, but no data is gathered). Also the ten second delay allows the operator to clear the area of the experiment so as to not induce operator (Bierwagen *et al.*, 1994a) interference. It also reduces to a minimum an initial drift that was observed during the first few seconds of each test, probably caused by disparity of potential between WE1 and WE2. The second part of the protocol adopted was a two run system. The software enables a series of test runs to be performed with a pause between. By separating the first and second run by ten seconds a more stable set of data is produced by the second run. In a stable system there is usually very little to distinguish between the two. But by inspection if a problem does occur it is easily seen in the analysis mode of the software.

Using this protocol repeatable values were obtained. These compared favourably with data sets that had been mathematically corrected. The values from tests having virtually no drift were confidently used to calculate R_n values comparable to R_p .

Data drift was corrected in some circumstances during the early work and preliminary experiments to establish the magnitude of error produced by such drift in data sets. It was found that on average the error was less than half an order of magnitude around the corrected value of R_n . Chapter 4 shows the effects of drifting data sets on R_n where the total current and potential data was corrected before calculating R_n .

3.13.1 Test length

It is considered that the shorter the test length the more attractive the ENM method will be to potential users in industrial situations. Previous work on coated systems has used 264 data points. In this work we are mainly interested in time domain data and what information can be extracted from it. However where data is required in the frequency domain Fourier analysis is often used to transform data into the frequency domain, and using software running Fourier transforms requires data sets that are a power of two. The length of data sets for this work were usually 300 data points. These were compared to results from tests running up to 3000 data points and 500 data points over 5000 seconds and were seen to give representative R_n values. Typical R_n values for intact alkyd after 145 hours in 10 % Harrison's solution were 3.17×10^8 ohms for the usual 300 data points at 2 Hz reading frequency compared to 1.45×10^8 ohms for 500 readings over 5000 seconds at 0.1Hz reading frequency.

Using 300 allowed removal of any early drift if necessary. Preliminary experiments on bare Fe and coated systems found that 300 data points were sufficient to give a good representation of potential noise and current noise on stable systems.

3.13.2 Sample interval

Useful data from corrosion cells can be determined between the 0 to 10 Hz bandwidth (Kearns *et al.*, 1996). The type of data analysis to be performed will determine which frequency is chosen as the sample interval. Most corrosion monitoring work to date has used between 0.5 and 2 Hz. The data analysis for this work has been primarily in the time domain and with the constraints on test time previously discussed a sample interval of 2 Hz was used throughout unless otherwise

stated. Again, preliminary experiments were carried out on the effect of sample interval on final R_n value. It was found that the instrumentation was capable of sampling at higher than 10 Hz and still give good correlation with values from data sets obtained at more conventional sample rates. The ZRA contains low pass filters which give anti-aliasing to high frequency elements of the noise signal preventing mains noise from being included in the data recorded. In corrosion cells with very high corrosion rates - Fe in 1M H_2SO_4 , the effect of sample interval was more pronounced and gave a bath tub distribution of R_n values when R_n was plotted against sample interval, Figure 3.5. For higher resistance coated systems this was not seen, Figure 3.6 where a sample interval of 2 Hz was still used as the cause of the effects was beyond the scope of this work.

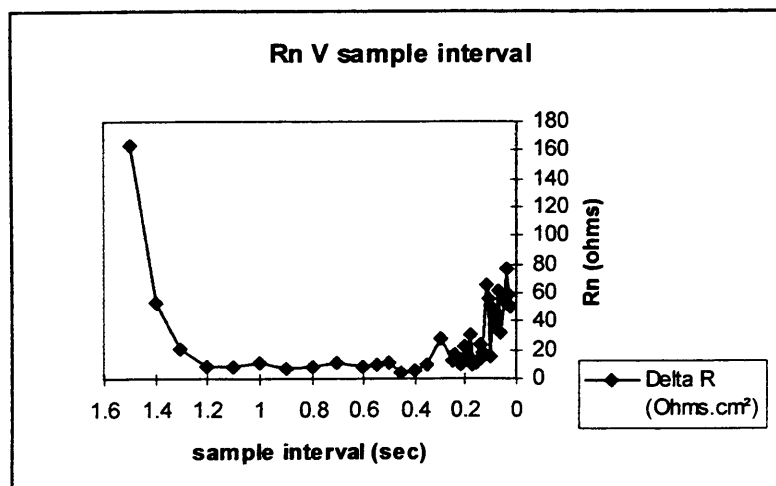


Figure 3.5

Bath Tub type Distribution of High Corrosion Rate R_n V Sample Interval

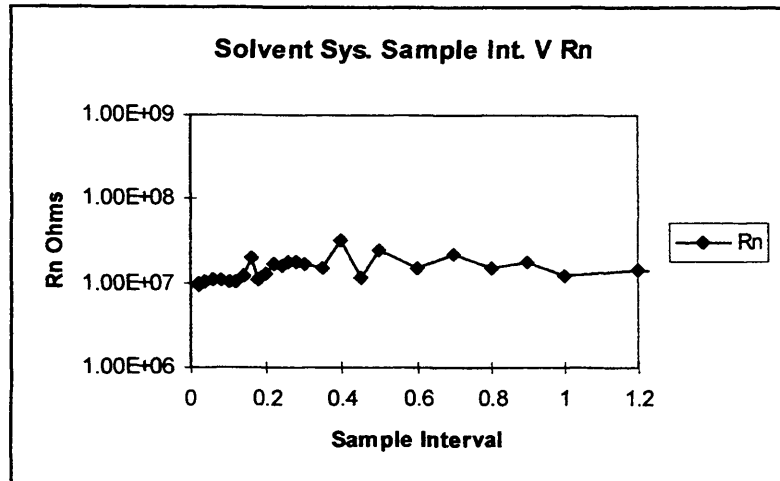


Figure 3.6 Effect of Sample Interval V R_n for a Coated System (Solvent based alkyd anti-corrosive primer) Exhibiting Good Corrosion Resistance

3.14 Shielding

Investigation of the effects of shielding on data sets was undertaken in light of information from the NDSU report on organic Naval coatings (Bierwagen *et al.* 1994a). In that work data clearly showed interference caused by human activity in the area of the experiment. The other area of concern was interference from mains induced sources.

The first issue was easily resolved, as the location of the instrumentation (a laboratory with no windows and 20cm thick brick walls, within another laboratory) shielded any passing human interference. Where very high resistance systems were examined $> 1 \times 10^9$ ohm-cm² the operator vacated the laboratory during the settle period of the first test.

The issue of mains interference was also quite easily solved. The instrument has very effective filtering (low pass filtering) which removes mains effects and the possibility of aliasing. The success of the electronic solution to this problem was verified by the adaption of the instrument to battery power which gave equally comparable results across the resistance ranges investigated. Results of low resistance tests are given in Table 3.3.

R_n Mains Power	R_n Battery Power
3.09e6	3.87e6
1.94e6	1.50e6
6.15e6	8.06e6

Table 3.3 Comparison of R_n obtained from waterborne alkyd using mains power and battery power for instrumentation.

The use of a noise reduction probe made no difference to current or potential noise plots which was another indication that the noise being measured was emanating from the corrosion cell and not external sources.

One problem which had to be resolved early on was large spikes on the potential and current plots (potential spikes were several mV). This was traced to thermostatically controlled heaters which were causing slight potential and current fluctuations on the mains input when they cut in or out. Because of the very low frequency of this interference the filtering of the instrument did not remove it. The problem was solved by simply turning off the heaters in the adjacent laboratory during tests.

3.15 Calculated parameters

Calculated parameters for general electrochemical noise measurement in the time domain involve statistical analysis of the distribution or scatter of values for potential and current noise plots. The population standard deviation for each data set is calculated automatically using the ACM Instruments software to give a potential Standard deviation value (noise value) σ_V and a current Standard deviation value (noise value) σ_I . The Noise Resistance Parameter R_n is also calculated automatically by the software by the division of the potential noise value by the

current noise value in an Ohms Law relationship. The values given for R_n across the range of coating resistance 1×10^6 ohms to 1×10^8 ohms from ACM software calculations have been confirmed by taking the raw data values into Excel and calculating them using spreadsheet software.

$$R_n = \sigma_v / \sigma_I \quad 3.1$$

Derivations leading to the validity of equation 3.1 to find R_n and its correlation with R_p are published in the literature and a good theoretical and mathematical basis has been shown (Cottis and Turgoose, 1994)(Chen and Bogaerts, 1995). This is discussed in Chapter 2.

3.16 Repeatability of Experiments

Experiments conducted for this work typically consisted of triplicate tests. In the case of coatings on metal substrate material this took the form of three cells per Q-Panel using two panels to give three pairs of cells for the bridge method. Where the beaker method was used the specimens were limited to one pair per beaker to avoid any electrical interference between pairs. Duplication was achieved in these experiments by multiple beakers.

Where experiments were not run concurrently repeat experiments were performed under the same conditions to ensure repeatability of the work. Any work which could not be performed as multiple experiments was subject to parallel testing using well established and defined techniques both electrochemical and chemical which are described fully in the relevant areas of the work.

3.17 Other techniques - D.C. resistance tests on systems

The most established of the two electrochemical techniques for parallel measurements was the D.C. resistance method. This is well proven for coating systems on metal substrates (Bacon *et al.*, 1948). The equipment used for these measurements was a Keithley Electrometer. The electrometer has a very high in-put impedance $> 1 \times 10^{13}$ ohms, which allows measurements of very high resistance systems up to $\sim 1 \times 10^{11}$ ohm-cm².

A main disadvantage of the D.C. resistance technique is that to obtain a resistance value a current must pass through the coating. This can involve the impression of a high voltage on the coating system in making a measurement. It is postulated that this can induce paths of weakness in the coating structure which then act as conduction paths for aggressive ions, accelerating degradation of the coating. Using D.C. resistance monitoring as a continuous process is therefore not possible. The technique also does not give mechanistic data of any corrosion processes only a point-in-time value, however this has proved very useful as a fast check of coating resistance when using more sophisticated measurement methods.

3.18 Other Techniques - Electrochemical Impedance Spectroscopy (EIS).

Electrochemical Impedance Spectroscopy (EIS) was also used to characterise some scribed coating systems, Chapter 6. Where it has been used for parallel experiments, specifications and experimental details are given. The technique is very useful as a parallel measuring method. It allows the total resistance to be easily determined and normally solution resistance can also be resolved separately from the resistance of the coating system. Under certain circumstances other resistance can be separated and the controlling process may be determinable (Gabrielli, 1990)(Jones, 1996). The disadvantage is that it is time consuming, complicated to treat data and interpret results. It also applies an external perturbing voltage which can interfere with the system under test. See Chapter 6.

Electrochemical Impedance Spectroscopy has developed over the past twenty years as a useful laboratory technique in the analysis of corrosion mechanisms and corrosion protection. Under conditions of an alternating current an organic coatings behave as a capacitor (Michael, 1980)(Turgoose and Cottis, 1991). This also applies to the interface between coating and substrate and corrosion product.

Ohm's law under A.C. conditions becomes $E = I.Z$, where Z is the resistance caused by all elements that impede flow.

$$\text{ie: } E = E_{\text{real}} + E_{\text{imag}} = E' + jE''$$

$$I = I_{\text{real}} + I_{\text{imag}} = I' + jI''$$

$$Z = Z' + jZ'' = E' + jE'' / I' + jI''$$

The resistance value comprised of inductors and capacitors is dependent on the frequency of the alternating current. Resistance values causing a voltage drop across resistors or elements acting as resistors are independent of frequency. Therefore resistors cause a change in amplitude of the applied A.C. current but no change in time of the signal (phase shift). Circuits consisting of capacitors and / or inductors cause a change in amplitude of the A.C. current and a phase shift.

The Electrochemical Impedance Spectroscopy technique uses vector analysis of an impressed ac signal from the corrosion circuit to calculate the impedance value. Impedance values can thus be represented by complex numbers. The real component of the complex number representing the value of resistors in the circuit, and the imaginary component representing the value of the capacitance of the circuit.

The aim of EIS is to model the corrosion process in terms of circuit elements and then to draw conclusions of the corrosion process. Measurements can be taken at the corrosion potential, therefore the characteristics are obtainable at the alloy state found in practice. By recording data at different frequencies a profile of the corrosion cell can be produced.

3.18.1 The Nyquist Plot

Data can be interpreted by the use of a Nyquist plot (Figure 7), where the imaginary impedance values are plotted against real component of impedance as a function of frequency.

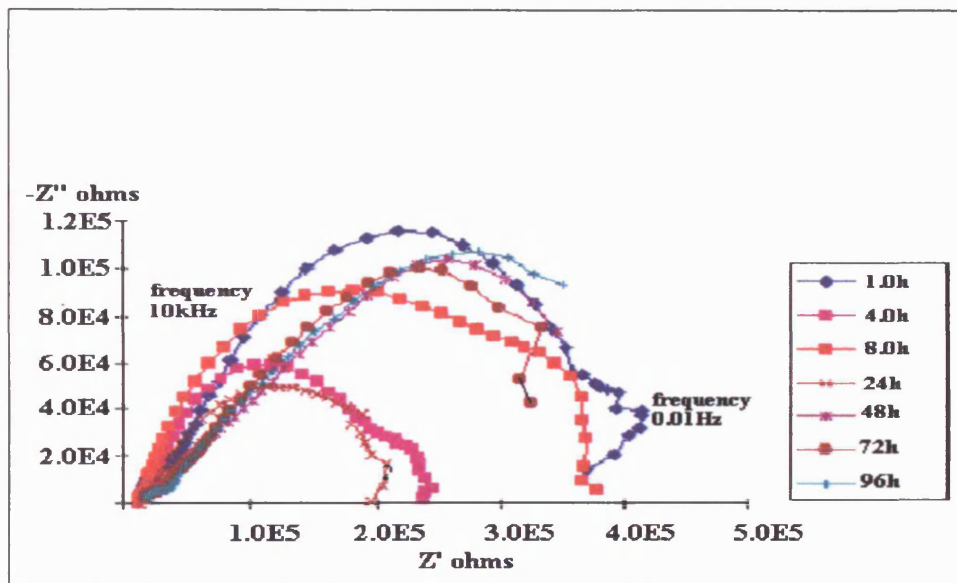


Figure 3.7 Typical Nyquist plots of Z'' against Z' with time for corroding system

For a corrosion cell under charge transfer control the resulting Nyquist plot will be a semi-circle. Work investigating polarisation resistance when applied to coated substrates (Scantlebury and Ho, 1979), used EIS and the changes in both resistance and capacitance with time were clearly shown using the Nyquist plot (Walter, 1981).

Resistance values however, which can be read directly from the X axis of the plot, continued to fall over seven days corresponding with the formation of rust spots.

It is stated that; Theoretically, the Nyquist plot for a defective coating undergoing active corrosion should contain two semicircular responses, a high frequency response due to the coating and a low frequency response due to the corrosion cell formed at the defect (Thompson and Campbell, 1994). The diffusion process will give a different response in the form of a Warburg impedance (Bierwagen, *et al.*, 1994a). This appears as a 45° line as opposed to a semi-circle form. Experience has shown however, that a number of situations can lead to the production of a single semicircle the origin of which is often difficult to establish and software has been developed which will deconvolute a single semi-circle. Thompson and Campbell's work investigated factors which influence impedance plots such as electrolyte conductivity, coating thickness and in particular the effect of variables such as defect size. Experience has shown, however, that a number of situations can lead to the resolution of a single semicircle the origin of which is often difficult to establish.

They also developed a protocol which it is claimed can distinguish between a coating response and a corrosion response in situations where only a single Nyquist semi-circle occurs. Circuit information can be computer modelled from this information to give an equivalent circuit. Electronic components (capacitors and resistors) with known values can be substituted for elements of the corrosion cell or coating system to simulate changes in the system.

CHAPTER 4

Novel Developments of the Electrochemical Noise Method

4.1 Introduction - Questions and Problems of ENM

The work in this chapter looks at questions about characterisation of data obtained by the noise method. The developments of the electrochemical noise method contained in this chapter are aimed at increasing the accuracy of the data and increasing confidence in the method. The feasibility of ENM as a field application is also a considerable step nearer using a new experimental technique. Most the methods and techniques in this chapter have not been investigated before and the purpose of this chapter is to explain the reason for the developments and give their technical detail. Data obtained using these techniques are contained in chapter 7. The developments fall into three areas; Investigation of detached coating, assessment of data distribution and a description of the new experimental set-up. The order these investigations followed was a logical development of the laboratory experiments.

Assessment of a coating for anti-corrosive applications is typically done by testing the coating on a substrate in a corrosive environment. This part of the work addresses the question of whether the electrochemical noise method has applicability to the testing of the coating in a detached state. Much useful information was obtained in Mayne's laboratory in Cambridge between 1960 and 1990 by examination of detached coatings using D.C. measurements (Mills, 1974) (Mayne, 1990).

The mathematical treatment of ENM data to obtain the parameter R_n assumes a normal distribution of the data sets. However, in the situation of a limited population, eg. 300 data points, although the data may be generally normally distributed it will only comply to a Gaussian distribution to some degree.

Investigation of normality can be done mathematically by kurtosis analysis and the departure from a Gaussian distribution quantified (equation 4.1). In this chapter the process of obtaining a kurtosis value is detailed along with examples of extremes of data distributions and limitations of the technique. Skewness is also described, which indicates numerically the position of the peak of the distribution above or below the arithmetic mean.

The third area of work in this chapter investigates a novel technique for obtaining potential and current data for ENM using a single substrate element instead of two. Application of the classic set-up for ENM in the field has been hindered so far by the problem that two electrically isolated substrate elements are required (Mabbutt and Mills, 1998). This method is a new experimental set up and is named the Single Substrate Technique reasons for which will be explained in section 4.4.

4.2 Detached Coatings

Previous work (reviewed Chapter 2) regarding the source of electrochemical noise would suggest that the investigation of coatings by ENM has applicability to detached coatings also and work on detached coatings is presented in Chapter 7. By using the detached coating apparatus (Chapter 7.2) the bridge method is modelled using the same coatings that were investigated on the substrate for comparison. Details of the development of the detached coating set up are given in section 4.4.

Detached coatings were produced by casting the coating onto glass plate, once removed from the glass plate (details Chapter 3.1) it was then mounted and sealed between the halves of a glass u-tube using silicone rubber seals. A schematic of two of the "cells" is shown in figure 4.1 with the arrangement for ENM measurement. The cells are filled with electrolyte which can be varied with ease and the two cells connected by a salt bridge.

The main advantage of this set-up is that a coating intact and on the substrate but locally detached can be modelled by using solution in the inner halves of the U tubes that represents that found under a blister in practice (Bierwagen *et al*, 1994b). The inner cells (connected by salt bridge) then

represent the test solution in what would normally be an attached cell on the surface. The two outer cells containing WE1 and WE2 can be filled with the solution expected to be present at the coating / substrate interface. The solution in this area can be considerably different to the test solution in concentration and composition as it may well contain leached inhibitor from the coating. Electrode material can be altered with equal ease to represent the effect of different substrate material or surface treatment.

Noise measurements are made in the usual way with WE1 and WE2 normally being metal strips of the substrate material.

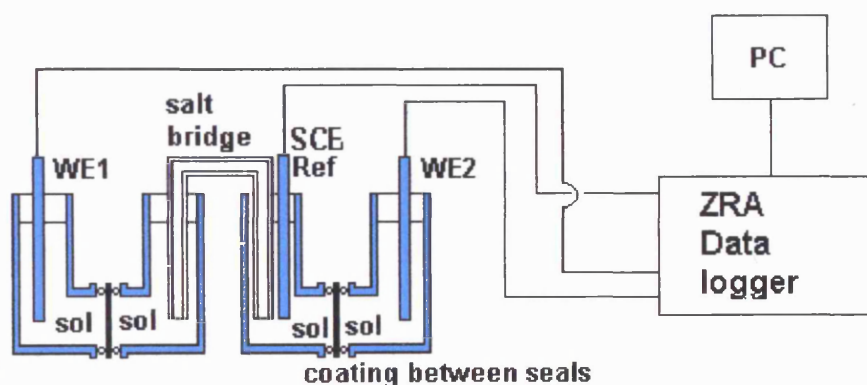


Figure 4.1 Standard set-up for investigating detached coating by ENM

The dominant noise from the cell is presumed to originate at the coating solution interfaces in the situation where the working electrodes are not corroding. In preliminary tests to establish electrode contribution to noise resistance values were typically lower than 8×10^3 ohms including solution resistance (3% NaCl solution) and this data was given in Chapter 3.2. The data below is from detached alkyd primer (RH) in Harrison's solution with de-ionised water in the outer cell halves. The data was gathered at 50 hours in full strength Harrison's solution and where no deterioration in the coating was seen.

Electrode WE1 and WE2	R_n Value (set1)	R_n Value (set 2)
Steel	2.82×10^8	5.62×10^8
D. C. Resistance. Sat. Calomel	7.5×10^8	7.9×10^8

These results indicate that it is the coating impedance which dictates the R_n value obtained from the detached coating set up. The D.C. resistance values are included as further evidence of this. Effects of temperature on coating performance can also be studied easily and used to facilitate degradation by storing in a laboratory oven.

4.3 Data Analysis of Potential and Current for Frequency Distribution

Frequency domain data can be interpreted to indicate localised corrosion “events” such as stress corrosion crack initiation and propagation to pitting and inter-granular corrosion. Work reviewed in chapter 1 covered this in some detail (Cottis and Lotto, 1986)(Lotto and Cottis, 1987). It has also been claimed that it can be used to distinguish between uniform and localised events occurring on the same substrate by a change in the slope of the power spectrum (Karrab, 1998).

Data from uniform corrosion or from intact coating have frequency spectra that are flat. This is because each frequency component of the transformed data contains essentially equal powers and is what would be expected for a random signal of normal distribution eg. shot or thermal noise (Cottis and Turgoose, 2000). Hence, no useful information about corrosion rates can be derived from transformation of general corrosion data into the frequency domain.

A new approach adopted in this work is an extension of preliminary work by C. Schultz, North Dakota State University (Bierwagen *et al*, 1994a). Schultz used frequency distribution with limits set at 1, 2 and 3 standard deviations from the mean. In the time domain, examination of potential and current distributions appeared to show promise for indicating mechanistic information. This is investigated in Chapter 7 where a departure from single Gaussian

distribution has been observed with scribed coated specimens. With time domain analysis the magnitude of the fluctuations and their frequency in the data is observed. The following looks at novel ways of analysing the time domain data.

4.3.1 Kurtosis (4th order moment)

Data that conforms to, or approximates to, a normal distribution can be assigned a numeric value to indicate the degree of normality. Kurtosis characterises the relative peakedness or flatness of a distribution compared to the normal distribution mathematically by application of the formula 4.1. The formula calculates a numeric value of kurtosis. A positive kurtosis number indicates a relatively peaked distribution. A negative kurtosis number indicates a relatively flat distribution. This assumes an approximation of data to a normal distribution, and as such, data sets that are not of a normal distribution but quantified using this expression produce numeric values that are meaningless.

$$\text{Kurtosis} = \left\{ \frac{n(n+1)}{(n-1)(n-2)(n-3)} \sum \left(\frac{x_j - \bar{x}}{S} \right)^4 \right\} - \frac{3(n-1)^2}{(n-2)(n-3)} \quad 4.1$$

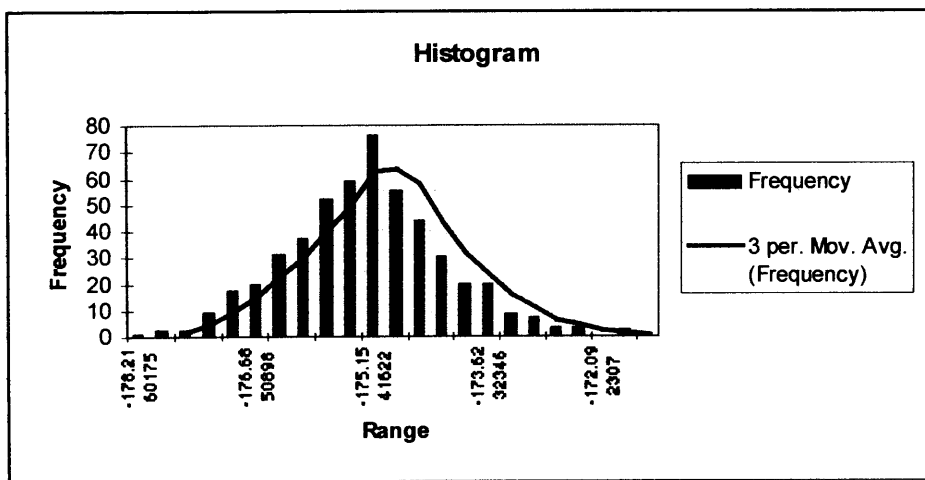


Figure 4.2 Histogram of generated random data of normal or Gaussian distribution.

Using a random number generator an artificial set of potential data was created that conforms to a Gaussian distribution. The histogram of the data set is shown in Figure 4.2. Artificial data was used for this example as the data set can be guaranteed to be Gaussian and conform closely to a perfect distribution. There is also no chance of D.C. drift on the data set which ensures no skew. The moving average technique of predicting the best fitting curve has a damping effect on the shape of any curve which in this case is demonstrated by the shift to the right and lower maxima.

Analysis of the data used for this distribution returned the following values when used in equation 4.1.

$$\text{Kurtosis} = -0.03826$$

The closer a distribution is to being perfectly normal the closer the kurtosis numeric value is to zero. It can be seen from figure 4.3 that the fitted curve is indicating a close to perfect normal distribution reflected in the low value returned of less than -0.04.

By contrast the following two figures show the extremes of kurtosis using much simplified generated data sets to emphasise the point.

Figure 4.3 shows a histogram of very peaked data. As positive kurtosis (also known as a leptokurtic distribution) the numeric value returned using equation 4.1 is + 2.037.

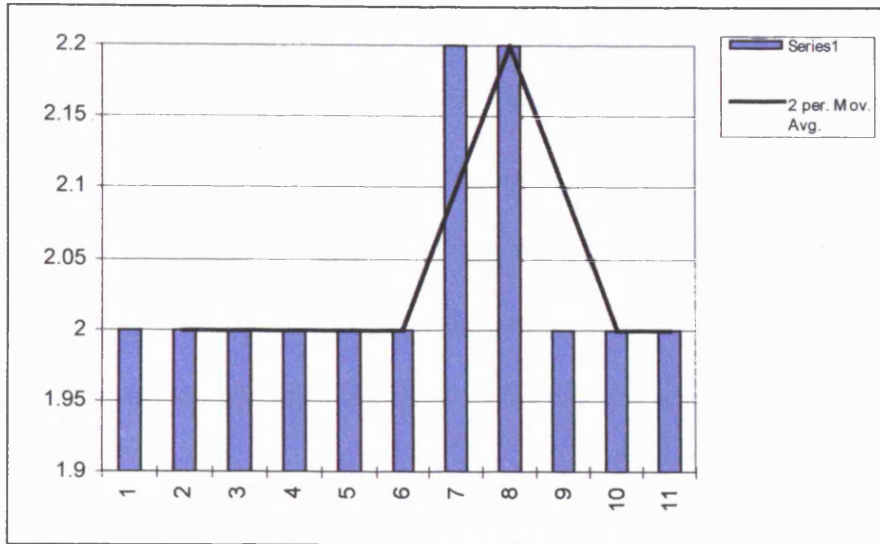


Figure 4.3 Positive Kurtosis

Figure 4.4 shows a normal distribution again artificially generated which is flatter than a perfect normal distribution (platikurtic) giving a negative kurtosis value. When the data contained in table 4.1 Appendix 1 was used in equation 4.1 a value of - 1.857 was returned.

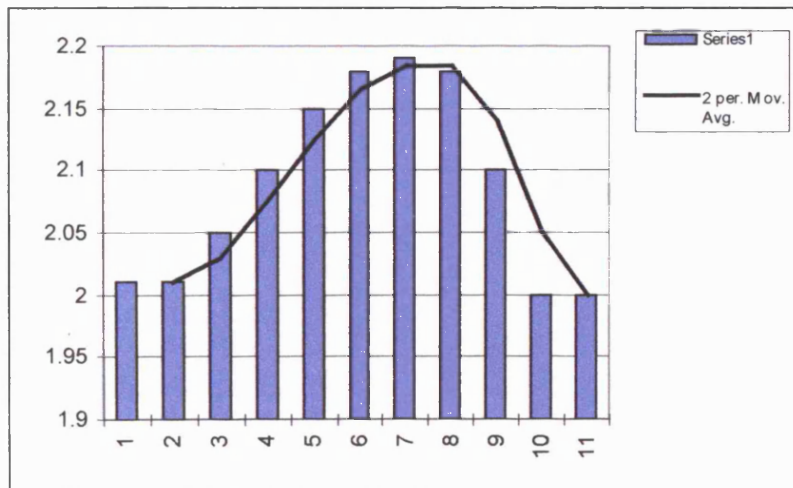


Figure 4.4 Negative Kurtosis

The data for the distributions in figures 4.3 and 4.4 are contained in table 4.1 Appendix 1.

4.3.2 Application of Kurtosis to real data

From the investigation of the data sets used for figures 4.3 and 4.4 a kurtosis number within the limit ± 1.8 give a reasonably normal appearance when plotted as a bell curve. As such the mathematics should hold good for comparison with R_p for uniform corrosion. The effect of kurtosis values away from these limits on values of R_n and how these compare to R_p require further experimentation on bare metal systems. This work is considered outside the remit of this project.

Figure 4.5 shows a histogram of data frequency obtained from an electrochemical potential noise data set from an intact alkyd coating after approximately 8 hours immersion in 10 % Harrison's solution. The kurtosis number returned is -1.391 indicating a flatter than perfectly normal distribution whilst still conforming to a Gaussian distribution. It can be seen by comparison of the shape and kurtosis number that the data is closer to Gaussian than the examples in figure 4.4, but does not conform so closely as the generated artificial data set in figure 4.2.

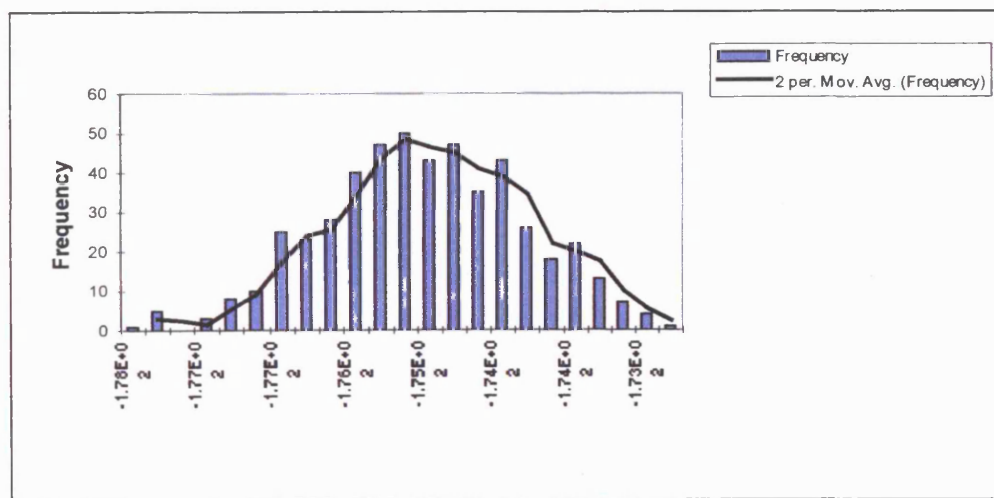


Figure 4.5 Frequency distribution of potential data set from an alkyd coating at approx. 8h

The data used for the frequency distribution in figure 4.5 could be used in confidence should the R_n value be required for determination of kinetics of the process. This is presuming the

current noise is also normally distributed which can be checked easily by the same means. In this instance the R_n value should correlate with R_p and give a good indication of protection afforded by the coating when compared to other electrochemical methods such as D.C. resistance.

4.3.3 Skewtosis (3rd Order moment)

Skewtosis can be linked to kurtosis analysis by virtue of being a mathematical expression for investigating the nature of data sets with a Gaussian distribution. Skewtosis is a positive or negative number derived from equation 4.2, which indicates the degree of symmetry of the distribution around the arithmetic mean of the data set.

$$\text{Skewness} = \frac{n}{(n-1)(n-2)} \sum \left(\frac{x_j - \bar{x}}{S} \right)^3 \quad 4.2$$

As with the case of kurtosis the expression works on the assumption of a normal or tending towards normal data distribution.

A skewtosis value of zero implies that the mean value of the data set corresponds with the greatest frequency value or top of the curve. Visually the gaussian distribution is therefore central on the histogram and symmetrical.

A negative value of skewtosis indicates that the maximum frequency is positioned, or skewed towards the positive side of the mean value and the longer of the two tails extends towards lesser data values. Conversely a positive skewtosis number indicates the maximum frequency peak is situated or skewed towards the lesser values, with the longer of the two tails extending towards the larger data values. A value of $+ / - 3$ indicates a maximum frequency peak at the extremes of a histogram over $+ / - 3$ standard deviations.

The major cause of skew in the applications used for this work is D.C. drift of the data sets. As advised in ASTM STP 1277 (Kearns *et al*, 1996), it is preferable to avoid this phenomena in the original experiment and in the collection of the data than eliminating the drift mathematically at a later stage. Investigation of D.C. drift was carried out at an early stage in the project to establish the effect of drifting data sets on final R_n value.

Linear drift was corrected by a procedure of curve fitting of the original data using a spreadsheet.

An equation (4.3) of the form; $Y = AX + B$ 4.3

was used, where Y = corrected data value,

A = original value,

X = the slope, (taken from the fitted curve)

and B = mean value of the data set.

Analysis of numerous data sets showed corrected values of R_n were within half an order of magnitude of the uncorrected data (see appendix 1) when applied to coated specimens. In many instances the difference was much less.

When coatings are being investigated the absolute value of R_n is not so important for rating, whereas the relative order of magnitude is of the R_n value is. Data contained in appendix 1 from four pairs of scribed alkyd on Fe substrate specimens are presented in both the uncorrected and corrected form. It can be seen in Figure 4.7 that the correction for drift has had the effect of bringing the R_n value closer to the R_p value.

Data for table 4.3 Appendix 1, was corrected using one iteration of the formula 4.3. The values from table 4.3 Appendix 1 were then averaged using arithmetic mean to give values for Figure 4.6.

For comparison R_p values are shown for parallel experiments. These were averaged from a set of four specimens. The R_p value was obtained from Electrochemical Impedance Spectroscopy (EIS) and R_p was taken from the Nyquist plots of the data. R_p values from EIS do not incorporate the solution resistance whereas ENM does. This was not considered significant as solution resistance was in the region of 5×10^3 ohms.

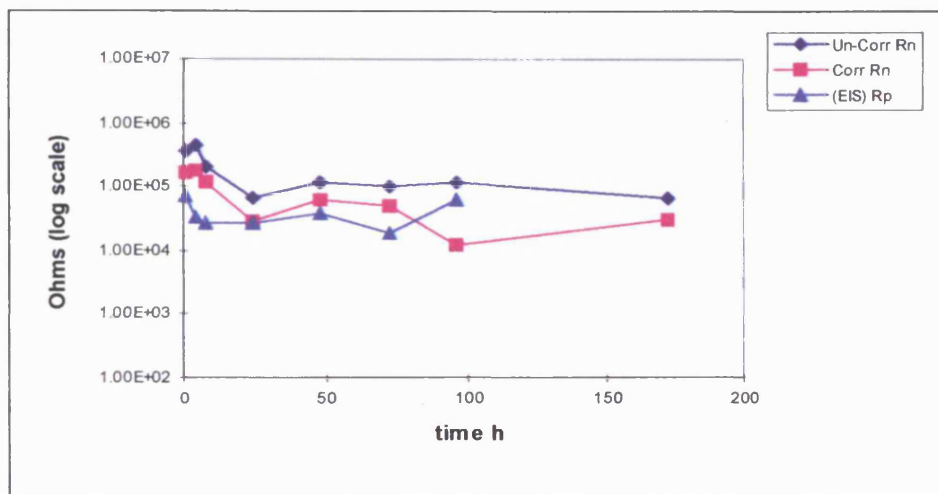


Figure 4.6 Averaged uncorrected and corrected R_n values compared to averaged values of R_p from Nyquist plots

The most important information from the data is the value of the order of magnitude for R_n . Therefore for comparison of relative values or changes, uncorrected values can be as useful and less time consuming than correcting the data.

By adopting a new protocol of using two runs per test, data sets of negligible drift have been consistently obtained and unless otherwise stated the values presented in this work have been taken from the better of the data sets. This negates the requirement for de-trending when investigating coated specimens. The use of at least two test runs enables overlaid plots for current and potential giving a very clear indication of extraneous data points or severe drift.

4.3.4 Bi-modal or non-normal distribution

In the investigation of scribed coating systems, analysis of potential and current data sets showed a distinct shift from a normal distribution. The data sets for the current in particular contained a bi-modal distribution under certain conditions where inhibition mechanisms are in progress (Chapter 7).

Analysis of the data by kurtosis is used in chapter 6 in an attempt to identify the effects of inhibitor containing coatings. Frequency distributions are used in the first instance as a quick visual indication of a process operating other than general corrosion.

In Chapter 6 the nature of the distribution has been seen to deviate from Gaussian where corrosion is being inhibited at a scribe in organic coating. It is believed that this could provide useful mechanistic information without transformation of the data into the frequency domain. Specific examples are shown and discussed in Chapter 7 which demonstrates frequency distribution can be of use when used in conjunction R_n value to give a good indication of a change in the system dynamics.

4.4 Alternative Configuration - The Single Substrate Technique

This area of work investigates the Single Substrate technique for obtaining potential and current data for ENM using a single substrate element instead of two. Application of the classic set-up for ENM in the field has been hindered by the problem that two electrically isolated substrate elements are required. The Single Substrate (SS) technique addresses this problem. Theoretically enabling measurements to be made on any structure with a metallic substrate using just one electrical connection.

Working from a schematic circuit diagram it was decided to try and re-configure the experimental set-up to eliminate the need for two separate substrate elements. This was accomplished by replacing the two working electrodes (the substrates), with Saturated

Calomel Electrodes (SCE). The reference electrode connection was then made to the substrate onto which the coating and both cells are attached (Figure 4.7).

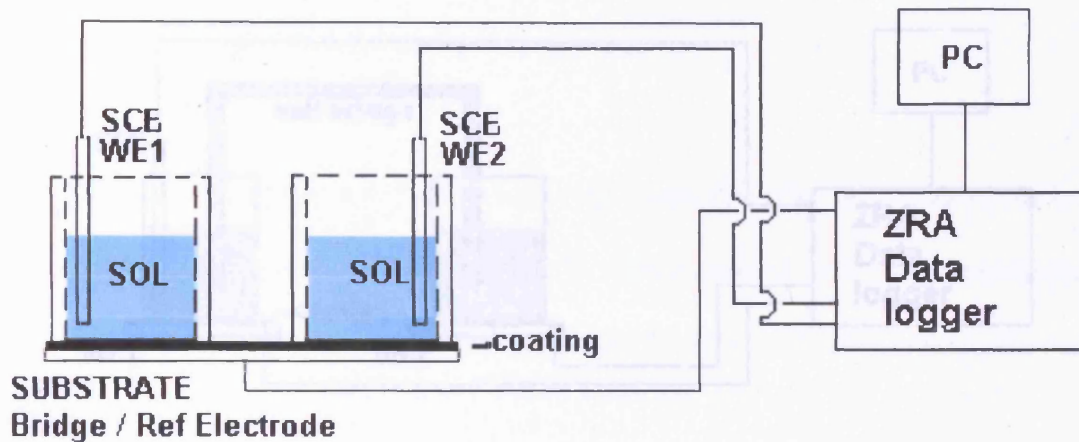


Figure 4.7 Single Substrate (SS) Technique

The cells are secured by silicone sealer and filled usually with 3% NaCl for solvent systems or 10% Harrison's Solution for the water-borne coatings. The substrate then essentially replaces the solution or the salt bridge (see Figure 4.8) to complete the circuit and is connected to the reference electrode terminal. The potential of the two SCE electrodes (WE1 & WE2 connections) are measured relative to the substrate (Ref. electrode connection), through the coatings of both cells which are electrically in parallel, as they are with the normal method. This gives a positive instead of negative value for potential because the connections of the experiment are reversed. However, the formula for calculating the standard deviation makes this irrelevant because the values are squared cancelling the negatives. The voltage fluctuations that give rise to the noise value are the same as in the normal arrangement. Note that in the usual set-up WE1 and WE2 are assumed to be nominally identical. Using SCEs this

assumption is closer to reality because of the greater stability of the electrode potentials compared to metal substrate.

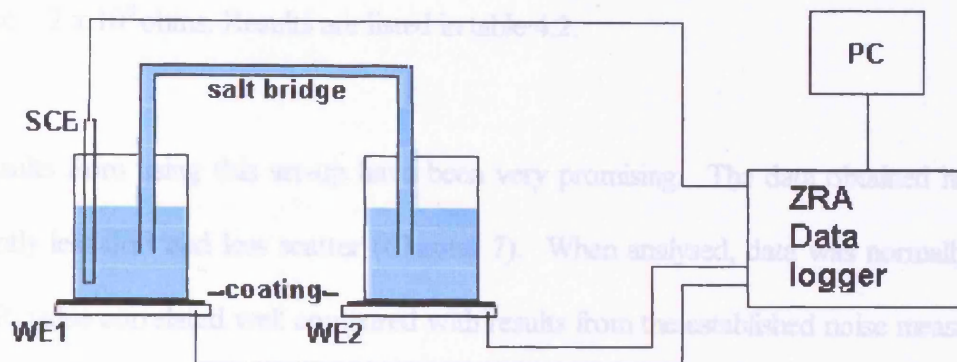


Figure 4.8 Schematic diagram for the traditional bridge method set-up

The current noise is measured between WE1 and WE2 as with the original set-up, using the ZRA. These signals are unlikely to arise in the calomel electrodes, which are generally considered to be low in noise. More likely is that they originate from ionic activity in the coating or at the coating substrate interface (thermal or shot noise). It is important to note that the circuit diagram for the new arrangement is electrically equivalent to the normal one even though the current must pass through the SCE electrode. This is not considered a problem in this application because the impedance of the electrodes are low at 2 - 3000 ohms compared to that of the coating.

Preliminary experiments were done on bare Fe in 0.1 M sulphuric acid. Three systems (147, 148 and 152), water-based (WB) epoxy were tested in 10% Harrison's solution and a 3 coat solvent based (SB) alkyd system was tested in 3% NaCl. R_n using the standard method, R_n by the new

configuration (SS method) and DC resistance were compared table 4.1. Data is not corrected for area which was 11.8 cm² in all cases.

In addition several single data set experiments were done on bare Al $\sim 3 \times 10^3$ ohms, a solvent (SB) system with a resistance (single coat) of $\sim 4 \times 10^8$ ohms and a waterborne (WB) system with resistance $\sim 2 \times 10^8$ ohms. Results are listed in table 4.2.

Initial results from using this set-up have been very promising. The data obtained has contained significantly less drift and less scatter (Chapter 7). When analysed, data was normally distributed and the R_n value correlated well compared with results from the established noise measurement set-up and dc resistance data.

System	Time h	Rn	Rn (New Config.)	D.C. res (ave)
bare Fe	18	3.94E+02	6.05E+02	n/a
bare Fe	46	3.11E+02	5.18E+02	n/a
WB epoxy (147)	1.5	1.89E+04	2.49E+04	7.88E+04
WB epoxy (148)	1.5	1.49E+05	2.26E+05	2.75E+05
WB epoxy (152)	1.5	2.12E+04	2.11E+04	6.25E+04
SB 3 coat a	1	1.34E+09	1.15E+09	(ave) 4.75E+09
SB 3 coat b	1	3.84E+09	2.31E+09	(ave) 5.75E+09
SB 3 coat a	6	5.70E+07	9.42E+07	(ave) 1.05E+09
SB 3 coat b	6	6.90E+07	1.61E+07	(ave) 8.90E+08
SB 3 coat a	24	1.39E+07	2.68E+07	(ave) 3.90E+08
SB 3 coat b	24	1.29E+07	3.30E+07	(ave) 3.55E+08

Table 4.1 Experimental data from tests comparing traditional R_n , new configuration R_n and D.C. resistance measurements

System	Rn		Rn (New Config.)
SB system	2.73E+08		4.37E+08
SB system	3.00E+08		2.70E+08
WB Neocryl	2.17E+08		3.09E+08
WB Neocryl	4.01E+08		4.12E+08
WB Neocryl	1.18E+08		2.66E+08
bare Al (52 hours)	5.37E+03		(sample interval (S.I) 0.5 sec) 1.92E3
bare Al (52 hours)	2.66E+03		1.87E3 (SI. 0.05 sec)
bare Al (6 hours)	3.51E3 (ave)		2.81E3 (SI. 0.5 sec)

Table 4.2 Single data set experiments comparing traditional bridge method and single substrate technique

CHAPTER 5

Intact Anti-corrosive Coating.

5.1 Introduction and Aims

The mechanisms by which organic anti-corrosive coatings prevent corrosion have been described previously in Chapter 1. The aim of accelerated testing is to enhance the time mechanism greatly to cause break-down of the coating naturally, without causing mechanisms to operate that are not present during real-time degradation of the coating (Whittman and Taylor, 1995). Hence there is a need to understand mechanisms to create effective accelerated tests. There is also a need to decide on, and to measure a parameter which will relate to, the ability of a coating to protect against corrosion. Because corrosion is an electrochemical process it is likely that an electrochemical parameter will give the information required.

Electrochemical tests aim to establish the ability of anti-corrosive coating to protect the substrate using electrical values. These may be obtained from relatively short term monitoring with the coating immersed in an electrolyte. This is shown to be possible using D.C. resistance measurement of organic coatings in artificial sea water (Bacon , *et al*, 1948) The coatings used for their work were traditional oil based anti-corrosive coatings.

The literature has shown that from modern electrochemical techniques values can be derived that correlate with D.C resistance values and give good indication of the ability of solvent and oil based coatings to prevent corrosion. This has included work using electrochemical noise measurement (ENM) to establish R_p . Electrochemical methods can be used to assess coating performance during (at intervals) or after exposure to accelerated tests such as salt spray or Prohesion tests. This approach has not been used for this work.

The bulk of testing in the experiments here were done as immersion tests in different concentrations of saline solution at room temperature. Actual concentrations and compositions are given for each experiment but range from 0.6 Molar to 0.06 Molar in general.

Immersion testing is not necessarily an accelerated test but is used here because it provides a reduction in the electrochemical measurement parameter which precedes the onset of visible rusting. It also provides a numerical value which is more easily correlated with other systems. However, immersion at raised temperature can provide an acceleration in degradation. This is because at temperatures above the coating's glass transition temperature (T_g) ion transfer mechanisms that contribute to degradation processes are accelerated. It is used on occasion, where a "good" coating is required to breakdown quickly for a particular experimental purpose, for example where detached coatings are examined.

The aim of the first section of this work was to establish whether electrochemical noise measurement, and in particular the parameter R_n , can be used as an indicator of the quality of waterborne anti-corrosive organic coating in a similar way to results from solvent based coatings.

This work investigates:

- 1) Two waterborne coatings using electrochemical noise measurement to derive R_n .
- 2) An epoxy resin using a waterborne amine was tested with and without pigmentation. It was intended to differentiate between the two regarding anti-corrosive performance using ENM and visual observation.
- 3) For comparison, and to characterise coatings for Chapter 6, three solvent-based coatings were also investigated.

5.2 Coatings and Electrolyte

COATING	TYPE	No. COATS	THICKNESS μm +/- 10
Neocryl	Water-borne alkyd	3	120
Haloflex	Water-borne chlorinated vinylide	2	120
Ind.Co-polymers Two-pack water-borne amine / epoxy resin	Un-pigmented 152	2	120
Ind.Co-polymers Two-pack water-borne amine / epoxy resin	Un-pigmented 148	2	120
CARRS PRIMER	Solvent based alkyd	1	50
SIGMAFERRO RUSTHOLD	Solvent based alkyd	1	80
SIGMACOVER PRIMER	Two-pack epoxy primer	1	90
Red lead	Linseed oil based	1	100
Hammerite TM	Solvent based	2	70

Table 5.1 Coatings for intact experiments

The coatings were immersed in an electrolyte of NaCl at 0.8 M or 0.6M and 3.5% ammonium chloride + 0.5% NaCl (Harrison's solution) diluted to 10% full strength. The coatings were applied to standard mild steel and Al substrates, (Q panelsTM) by spreader bar following degreasing as described in chapter 3. The surface finish was as received in all cases for specimens used in the experimental work.

5.3 Testing Procedure

The coatings were monitored against time using Electrochemical Noise Measurement. The bridge method was employed using a sample frequency of 2Hz for 300 data points, i.e. 150 seconds, (see section 5.4). Initial experiments were done at various sample intervals to validate the 2Hz frequency on solvent based and water-borne coatings. The area of coating exposed to the test solution was generally 11.8 cm²(L). Some testing was done using smaller

areas of 7.5 cm² (S) which are detailed with the relevant test. Results were correlated by the established electrochemical method of D.C. resistance and in the case of the transparent 2 - pack epoxy by visual observation.

5.4 Preliminary experiment using solvent based alkyd (Carrs) on steel and aluminium substrate

Tests were run at 1Hz sample frequency. This experiment was started prior to establishing 2Hz frequency chosen for subsequent experiments. Bold italics (Table 2 - Appendix ii) were taken at 5Hz following the sample interval experiment and are shown as an indication of consistency with the 1Hz sample frequency values. The solution was 4% by weight artificial sea salt solution.

The R_n values of the six pairs of cells were averaged to produce the graph in figure 5.1 which compares the values of R_n on Fe compared to those on Al.

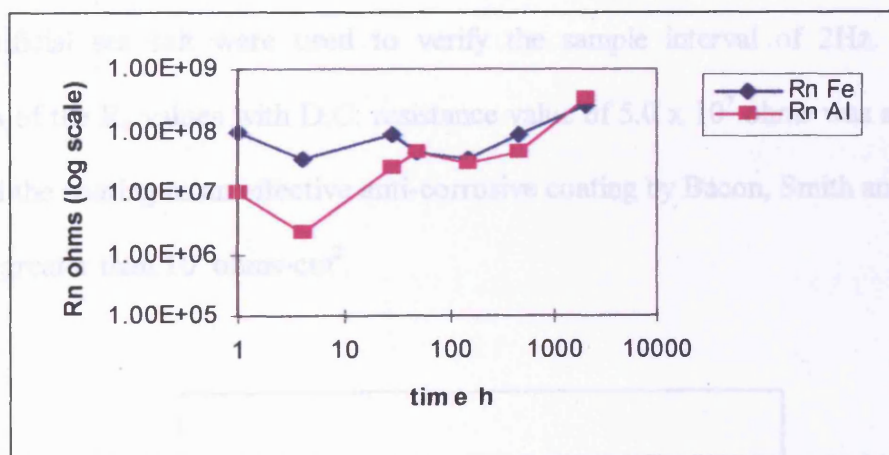


Figure 5.1 R_n values V time for solvent based alkyd on Fe and Al

Initial values for R_n were an order of magnitude lower for Al. As water uptake increases the R_n values become very close. This difference in R_n between the two substrates is attributed to the Al potential being more variable leading to drifting plots. The Fe potential was more stable and this has the effect of giving lower potential noise values and hence higher R_n values. This

appears to be an indication that ENM can be used to investigate the nature of attached coatings independent of the substrate. The investigation of free or detached coating is investigated in other areas of this work and compared to coated substrate values. An interesting observation with this experiment was the fact that the resistance values actually increased slightly with time and no breakdown of the coatings was observed. This coating was established as an excellent performer up to 2000 hours when there was no apparent breakdown. Since, in order to do the experiments successfully, coatings needed to “break down” reasonably rapidly, other coating types were used subsequently.

5.4.1 Preliminary experiments on solvent based alkyd to establish parameters for tests

These results are not corrected for area because like sized specimens were used.

5.4.2 Sample interval experiment using solvent based alkyd

A pair of cells using the solvent based alkyd (area 11.8 cm²) on steel substrate and a solution of 4% artificial sea salt were used to verify the sample interval of 2Hz. An excellent correlation of the R_n values with D.C. resistance value of 5.0 x 10⁷ ohms was seen. This also established the coating as an effective anti-corrosive coating by Bacon, Smith and Rugg criteria of a value greater than 10⁸ ohms-cm².

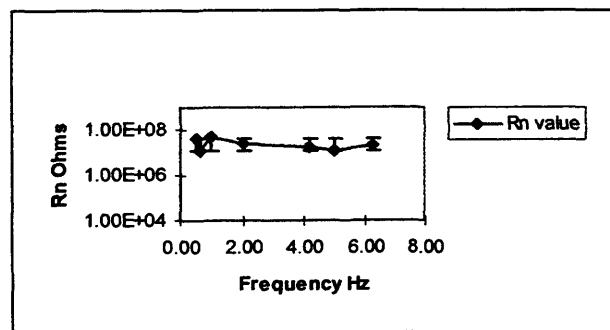


Figure 5.2 Sample interval V R_n for solvent based alkyd

The D.C. resistance values of $5.0E7$ ohms for the cells were measured immediately after the noise measurements to avoid disturbing the system before or during the test. Error bars indicate one standard deviation. The R_n values for 2Hz came within one standard deviation compared to other sample frequencies. This was deemed sufficient correlation to D.C measurements for 2 Hz to be used for other work.

5.4.3 Sample Interval Experiment using Waterborne Alkyd

The experiment in 5.4.1 was repeated using a waterborne alkyd to establish the suitability of the 2 Hz sampling frequency on waterborne organic coating.

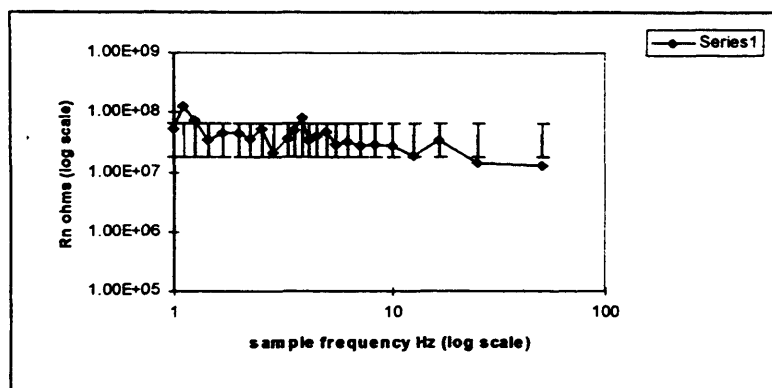


Figure 5.3 Sample interval $V R_n$ for waterborne alkyd. Error bars indicate 1 Standard Deviation.

A greater deviation in R_n values was seen on the waterborne coating compared to the solvent based alkyd. However, greater than 80% of the values are within one standard deviation across the frequency range investigated. At 2Hz, as with the solvent based alkyd, the R_n values are within the standard deviation error bars. This was thus considered to be a valid sample rate. D.C values were on average within half an order of magnitude of the R_n value. Note that D.C. values were again measured after the ENM measurements were complete. This was because a previous test on a waterborne coating had shown a tendency for the substrate - coating interface to be polarised by the D.C. resistance measurements, this caused drift on data sets and errors in subsequent ENM data treatment.

5.5 Intact water-borne coatings on Fe

In previous work on solvent based systems a close correlation was seen between D.C. resistance value taken as geometric mean of the two individual cells and the R_n parameters (Mills and Boden, 1993). This has been confirmed with the solvent based experiments in this chapter and means the Bacon, Smith and Rugg criteria can therefore be applied with confidence to solvent based systems.

This part of the investigation was aimed to establish whether the R_n parameter could be used to quantify a waterborne organic coating with respect to corrosion protection in the same way that has been seen in the investigation of solvent based systems. The question being asked is: "Can the same criteria can be applied to water-borne coatings as solvent based coatings in relation to ionic resistance values and corrosion protection?"

5.5.1 Neocryl Results.

The water-borne coating Neocryl was applied to a steel substrate to 130 μm dry-film thickness. The coating was then were monitored using ENM and D.C. resistance for 1200 hours under immersion conditions in an electrolyte of Harrisons solution (section 5.1), diluted to 10%, cell area was 11.8 cm^2 . The D.C resistance experiment was repeated with four cells which gave very repeatable results. This indicated that the coating was consistent on all four specimens which were used as two pairs of nominally identical electrodes for ENM. Original data is in table 5.3 - (Appendix ii), which is compared to the haloflex performance in section 5.5.3.

5.5.2 Haloflex Results

The water-borne coating, Haloflex, was applied to a steel substrate to 130 μm thickness, and monitored using ENM and D.C. resistance for 1200 hours under immersion conditions in an electrolyte of 10 % Harrison's solution, with a cell area of 11.8 cm^2 . The D.C. resistance experiment was repeated with four cells which also gave very repeatable results to within a factor of two. These were used as two pairs of nominally identical electrodes for ENM. The original data is contained in table 4 - (Appendix ii), these were used in section 5.4.3 below in comparison to the Neocryl results.

5.5.3 Comparison of Results from Neocryl and Haloflex.

The Neocryl and Haloflex D.C. resistance values from the experiment replicates were sufficiently close (usually within 0.1 of an order of magnitude between the pair of cells).

Hence the arithmetic mean was used to calculate the average D.C. resistance data for graph

5.4.

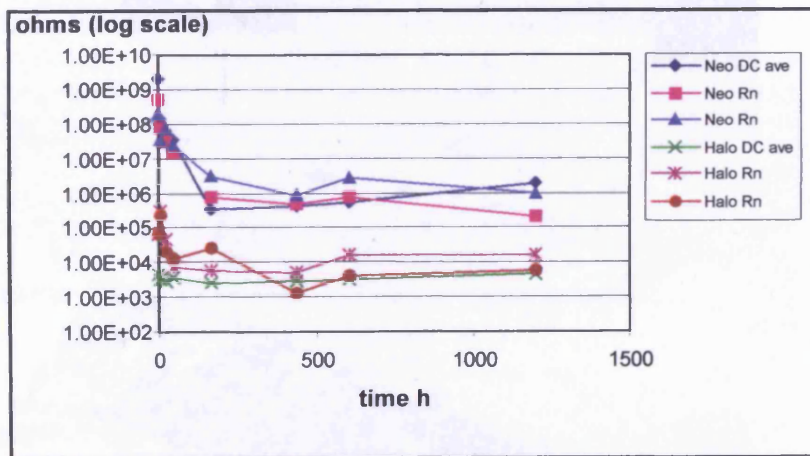


Figure 5.4 Graph showing R_n values compared to R_{dc} values for Haloflex and Neocryl waterborne coatings.

5.5.4 Observations on water-borne Haloflex and Neocryl experiments.

Close inspection did reveal small blisters in the Neocryl cells after 430 hours and this corresponds to the fall off in R_n value and R_{dc} value to 10^6 ohms indicated on the graph. This implied coating failure, although at the time no obvious corrosion product was visible. By 610h rust spots were appearing. In this instance ENM has effectively indicated coating failure at only 60% of the time required for a visual confirmation in an observation test by the fall off in R_n value before any visual signs of failure. It is thought that Neocryl uses ionic barrier properties to prevent the migration of ions to the substrate. The lamella structure appears to support this hypothesis and is indicated in Figure 5.5 (SEM micrograph). D.C. Resistance has identified this mechanism and the graph shows a good correlation between D.C. resistance values and R_n values from early in the test, continuing to track the break down of the coating.



Figure 5.5 SEM micrograph of section through Neocryl on steel. The course band running left to bottom right shows the course plate-like structure through the coating thought to constitute the barrier protection mechanism.

The Haloflex results produced a different scenario. At the end of the test micro-blistering of the Haloflex was visible. Coating was removed to expose the under-side of the blisters and substrate area. There was no red rust, but the plate-like formations on the underside of the Haloflex coating shown in Figure 5.6 (SEM micrograph), appear to be a black ferrous oxide and compared closely to a known structure (Reid and Weidmann, 1990). It is possible that the crystalline structure seen may be a compound formed by the inhibitor in the coating, but in the absence of further analysis this cannot be substantiated. The Haloflex coating was inhibiting initially, this was indicated by the R_n values around 1×10^5 ohm-cm² and was substantially reducing corrosion even though the coating had failed by disbondment. This was not shown by the D.C. resistance method. The inhibitor contained in the Haloflex was not identified by the supplier but leaching experiments in Chapter 6 demonstrate the effectiveness of the inhibitor in protecting bare steel electrodes.

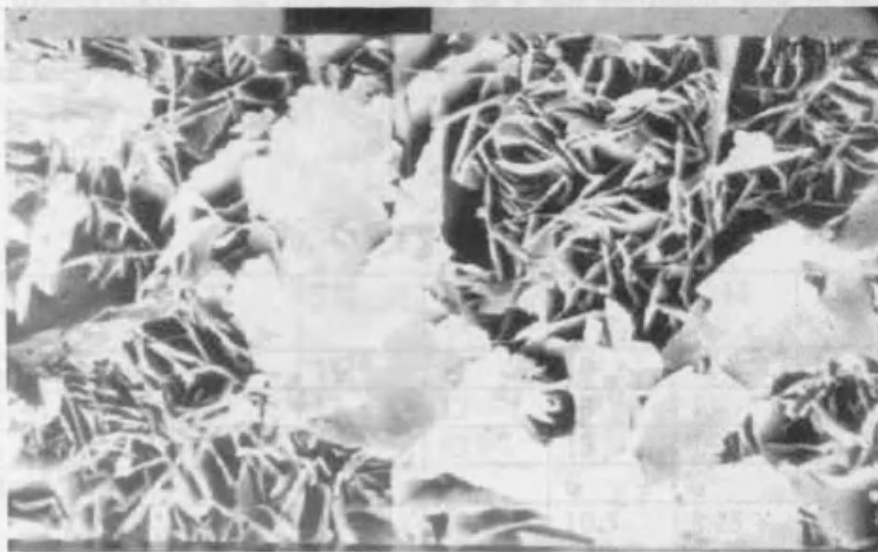


Figure 5.6 SEM micrograph of the underside of Haloflex showing top right and bottom left what appears to be a ferrous oxide or possibly a crystalline product of the inhibitor.

This was not indicated by R_{dc} which demonstrates the limitation of the D.C. instrument where a coating has low ionic resistance but good inhibitive properties. The graph shows that the R_{dc} values were low from the start of the experiment. The fact that a significant current flows when the instrument applies a voltage across the coating substrate interface implies that the Haloflex relies on chemical inhibition rather than ionic barrier properties.

5.6 Waterborne amine - 2 pack epoxy. Unpigmented 148 and 152

This data was obtained in conjunction with an under-graduate project by (K. P. Chettri) Nene University College Northampton, April 1998. The number of corrosion spots for 148 and 152 in 0.6M NaCl, cell area 11.8 cm², were recorded against time. The waterborne amine - 2 pack epoxy on Fe was tested over 3050 hours and performed very well.

Table 5.6 shows the results of the visual observation of corrosion spots in cells of 148 and 152 2-pack epoxy. When compared to the data in table 5.5 (Appendix ii) and the graph in Figure 5.7 it can be seen that there is good correlation with the ranking of the coatings by visual and ENM measurement. The 152 generally gave less corrosion spots at approximately half the amount seen for the 148 coating. By 1560 hours this had increased to greater than a factor of three.

	Hours	672	912	1132	1176	1248	1320	1560
152 a	11	11	11	11	10	11	11	18
152 b	6	8	12	12	13	13	14	19
152 c	11	13	13	13	13	15	15	21
152 d	3	5	5	5	6	6	5	41
152 ave	7.5	9.25	10.25	10.25	10.5	8.25	11.25	24.75
148 f	10	12	14	14	16	18	20	28
148 g	10	12	14	14	15	15	16	34
148 h	18	17	21	21	23	25	26	115
148 I	21	21	23	23	30	25	28	160
148 ave	14.75	15.5	18	18	21	20.75	22.5	84.25

Table 5.6 Results of counted corrosion spots in 148 and 152, water-borne amine 2-pack epoxy cells.

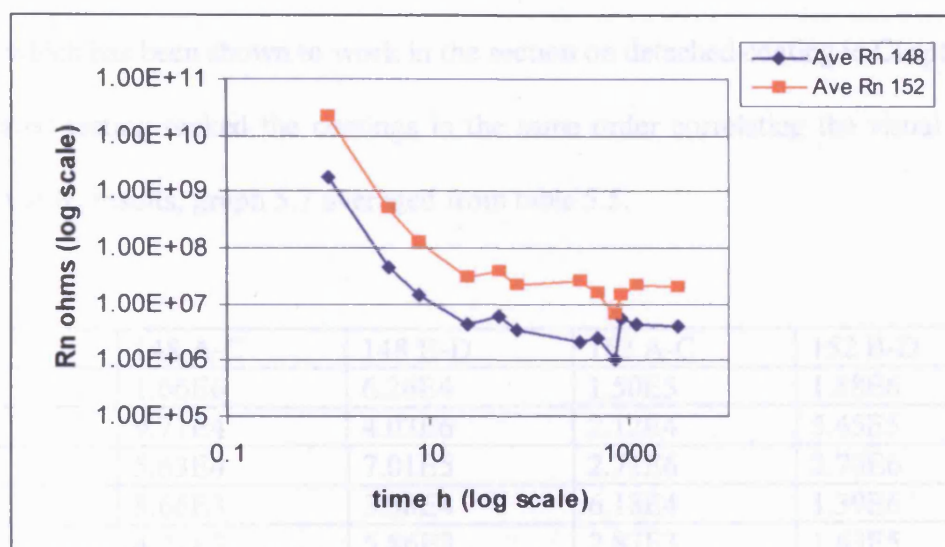


Figure 5.7 Graph of averaged R_n values for 148 and 152 epoxy.

The graph ranks the 152 epoxy as giving better corrosion resistant properties than the 148 epoxy verifying the visual test results.

5.6.1 Elevated temperature testing of 148 and 152 epoxy

The 148 and 152 epoxy on Fe were also subjected to accelerated testing and the results compared to those from the ambient temperature tests. The tests were done in 0.6M NaCl solution, the area was 11.8 cm².

The mechanism of corrosion protection by these coatings is controlled by ionic resistance as neither contained any pigmentation. The reduction of ionic resistance of the coating can be accelerated by exposure to elevated temperature and this has two measurable effects. An immediate drop in coating resistance can be measured when the coating temperature reaches then exceeds the glass transition temperature (T_g). This change is reversible on reduction of temperature.

The second change is a slow change over several hours, caused by ion exchange on the polymer chains which reduces the ionic resistance by the same mechanism as room temperature

testing but at a higher rate. This can be a reversible change if the degradation process has not gone too far. It can only be achieved by introduction of different ions (hydrogen) to the system, which has been shown to work in the section on detached coating in Chapter 7.

Accelerated testing ranked the coatings in the same order correlating the visual results table 5.6 and the R_n results, graph 5.7 averaged from table 5.5.

Time h	148 A-C	148 B-D	152 A-C	152 B-D
1	1.66E6	6.26E4	1.50E5	1.88E6
4	9.71E4	4.03E6	2.12E4	5.45E5
8	5.63E4	7.01E5	2.71E6	2.70E6
24	8.66E3	3.38E4	6.18E4	1.39E6
48	4.27E3	5.86E3	2.87E3	1.63E5

Table 5.7 High temperature testing of 148 and 152 water-borne amine, 2-pack epoxy.

Note: the accelerated testing was conducted at 60 °C, while the ENM measurements were carried out at 35 °C. The lower temperature was used for the measurements because it was sustainable throughout the measurement period which gave more stable data plots.

5.7 Main Experiments on solvent systems

This section of work investigates solvent based systems that are used in the following chapters where they are investigated in scribed and detached states.

5.7.1 Intact 2-pack epoxy system (CM) and Intact solvent based alkyd (RH)

These tests were carried out using 11.8 cm² cells or 7.5 cm² cells attached to each coating by silicon sealer. Sample interval was 2Hz over 150 seconds. The solution was Harrison's solution (section 5.2) diluted to 10%. Values (Table 5.8 - Appendix ii) of R_n are corrected for area to give ohms / cm² plotted on the graph in figure 5.8. D.C. Resistance data was obtained at 100h.

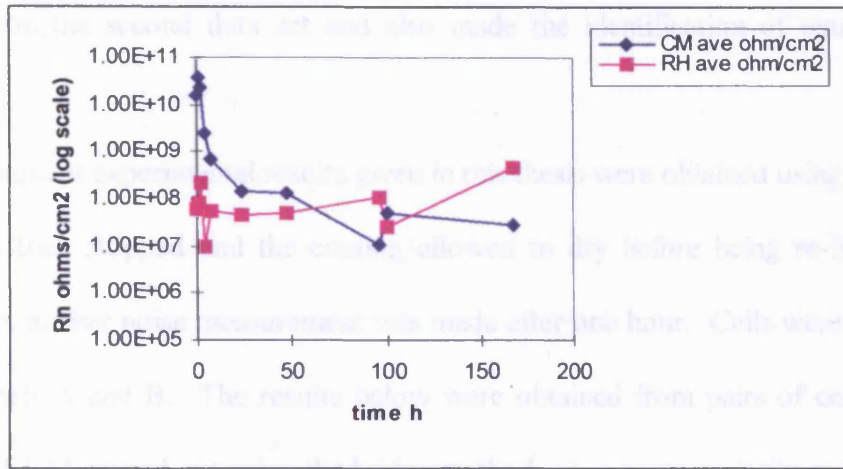


Figure 5.8 Rn V time for CM and RH coating

CM = epoxy, RH = alkyd, L = Large area, S = Small area

Coating / Cell	R _n Value	D.C. Resistance A	D.C. Resistance B
CML	2.01E6	5.0E7	1.15E7
CMS	1.02E7	4.0E7	7.0E7
RHL	9.70E6	2.0E8	2.0E6
RHS	1.31E7	2.0E7	3.0E7

Table 5.9 Comparison with D.C. Resistance values at 100 hours for CM and RH coating

5.7.2 Additional testing of intact 2-pack Epoxy (CM).

The desirable characteristics of the CM 2-pack epoxy of high adhesion and good corrosion protection led to the decision to use it for further development of the noise technique. Further testing was therefore carried out using a new set of samples. The preparation of the specimens was identical to the previous experiment using two coats to obtain the coating thickness. Solution was Harrison's diluted to 10% and sample frequency 2Hz. The test area of the cells were 11.8 cm².

A new convention was adopted at this time that uses at least two runs of data collection in succession for each test as explained in section 4.7. This was found to reduce drift

considerably on the second data set and also made the identification of extraneous results possible.

Note all subsequent experimental results given in this thesis were obtained using this method.

The test was then stopped and the coating allowed to dry before being re-filled with fresh electrolyte. A further noise measurement was made after one hour. Cells were numbered 1, 2 and 3 on panels A and B. The results below were obtained from pairs of cells of matching number with ENM carried out using the bridge method.

D.C. Resistance data was obtained on these samples at eight and forty eight hours for each cell 1 to 3 on specimens A and B, table 5.11.

Time h	Cell 1A	Cell 2A	Cell 3A	Cell 1B	Cell 2B	Cell 3B
	R_{dc} ohms					
8.0	4.1E7	3.8E7	4.2E7	3.4E7	3.3E7	2.8E7
48	4.4E7	4.6E7	4.4E7	3.4E7	3.7E7	3.8E7

Table 5.11 D.C. Resistance values for CM coating at 8 and 48 hours

These data were averaged to produce the figure 5.8 comparing R_n to R_{dc} at the time intervals shown.

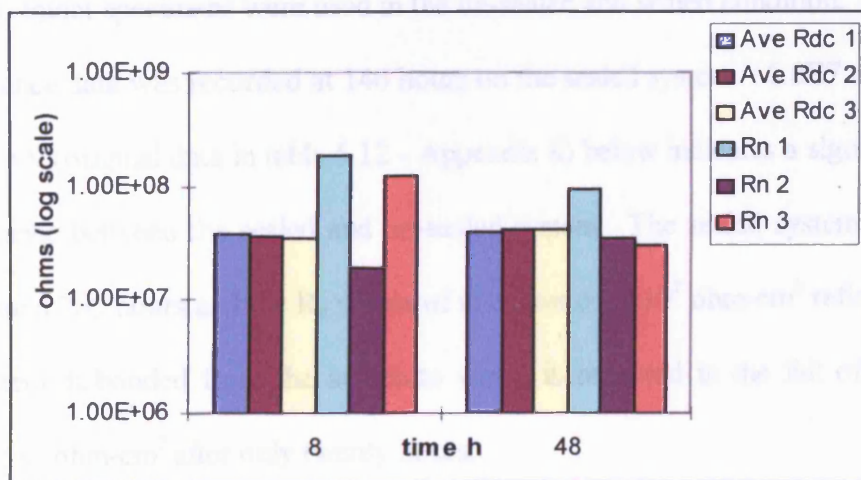


Figure 5.8 Histogram comparing averaged R_{dc} pairs and R_n values for 2-pack Epoxy CM coating at 8 hours and 48 hours.

5.8 Intact sealed red lead.

Although not commercially available for on-shore use in the UK red lead primer was used in Chapter 6 to investigate protection at scribes by inhibitive pigments. Red lead was chosen as a control because of the excellent corrosion protection afforded to the substrate at breaks in the coating.

It was important that coating systems used for the scribed coating investigation be characterised in the intact condition. As such results for intact red lead and sealed intact red lead are given here. The red lead was applied as one coat using a spreader bar which gave 100 μm dry film thickness. The sealed red lead system was coated with Hammerite™ in two coats of 70 μm giving a total thickness of 240 μm dry film thickness. The reasons for this are discussed in the scribed coating chapter, 6.

The bridge method was used on the samples which had an exposed coating area of 7.5 cm^2 . The tests were carried out in Harrison's solution diluted to 10%. The main aim of the scribed coatings experiments was to investigate R_n values produced at scribes. These were expected to be several orders of magnitude lower than the intact values as essentially the resistance of the scribe is being measured in parallel with the coating resistance. To characterise the intact coating two intact specimens were used in the un-sealed and sealed condition.

D.C. resistance data was recorded at 146 hours on the sealed system = 6.0E7 $\text{ohm}\cdot\text{cm}^2$.

The graph 5.9 (original data in table 5.12 - Appendix ii) below indicates a significant difference in performance between the sealed and un-sealed system. The sealed system was performing well at around 700 hours and the R_n values of in excess of 1×10^7 $\text{ohm}\cdot\text{cm}^2$ reflect this. The un-sealed system disbonded from the substrate which is reflected in the fall off in R_n value to below 1×10^6 $\text{ohm}\cdot\text{cm}^2$ after only twenty hours.

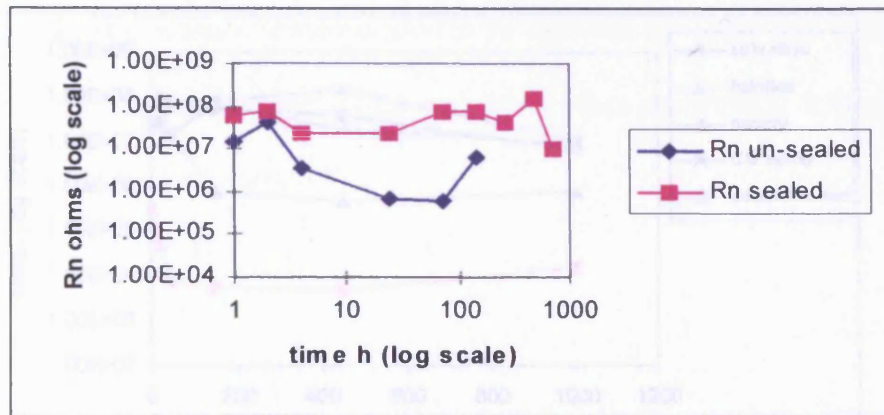


Figure 5.8 Intact unsealed and sealed red lead on Fe.

The recovery in R_n value observed in the case of the unsealed coating is attributed to inhibition of the Fe surface after initial disbonding of the coating. This was confirmed by the total absence of corrosion under disbonded areas of coating when later investigated.

5.9 Interim conclusions - justification for work in Chapter 6.

The experiments on the water-borne coatings gave initial findings that R_n indicates protection afforded by water-borne coatings in much the same way as D.C. resistance. The R_n parameter successfully ranked the water-borne amine, 2-pack epoxy and this correlated with visual and accelerated high temperature tests to degradation.

Figure 5.10 shows the range of coatings tested in experiments from this chapter on the same graph. Although solutions differed conduction values were close and the difference in values of R_n are attributed to the resistance of the coating under investigation. The graph shows that the parameter noise resistance (R_n) can be used in confidence to rank coating systems.

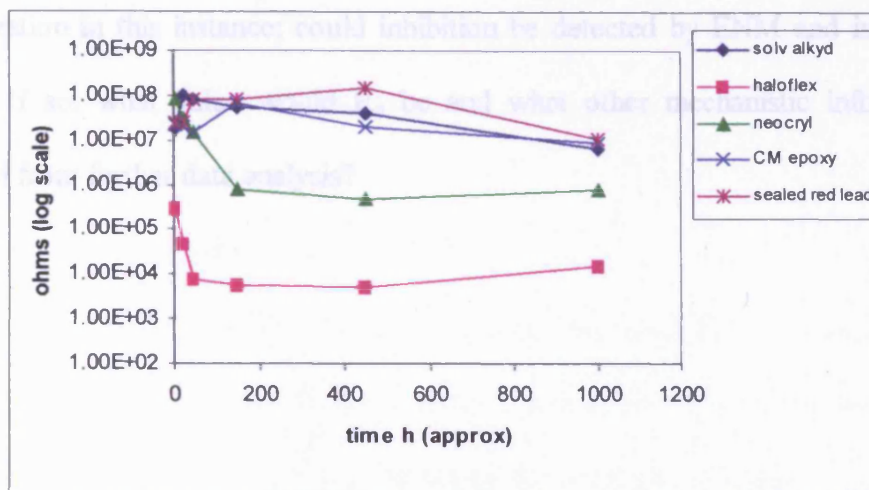


Figure 5.10 Ranking by R_n value of coatings tested in Chapter 5.

The Neocryl and Haloflex coatings were below the Bacon, Smith and Rugg criteria for a borderline coating and both failed early in testing. The R_n parameter showed better mechanistic information, indicating the on-set of blistering with Neocryl and the fact that the Haloflex was inhibiting despite the very low D.C. resistance values.

The fact that R_n appeared to be indicating inhibition, or at least very low corrosion rates in the absence of ionic barrier pigments suggested that R_n was measuring the polarisation resistance at the coating / substrate interface. This has been observed in previous work (Mabbutt and Mills, 1997) when good coating systems have eventually failed.

These conclusions led to further investigation of anti-corrosive organic coating by ENM where a break or holiday in the coating is present. The protection of the substrate is provided by the coating adjacent to the exposed area. The mechanism operates by leaching of chemical inhibitors from the coating as water permeates the coating and fills the defect, see Chapter 1. Inhibitive compounds are formed at the break that complex with Fe to form stable oxides, preventing or significantly reducing further corrosion.

The question in this instance; could inhibition be detected by ENM and indicated by the R_n value. If so, what value would R_n be and what other mechanistic information could be obtained from further data analysis?

CHAPTER 6

Investigation of Scribed Organic Coating

6.1 Introduction

An important property of anti-corrosive organic coatings is the ability of the coating to protect exposed substrate material from damage by corrosion. This work investigates non-metal containing organic coating which protect by the presence of inhibitive pigments contained in the paint. Inhibitive pigments were discussed in Chapter 1 and the coatings used in this work were investigated intact in Chapter 5. The extent to which this reduces corrosion will depend on the immediate environment. High levels of chloride lead to a soluble product which have minimal effect on corrosion protection. However, phosphorous can form insoluble product in conditions where ammonia is present which can significantly reduce corrosion.

Investigation in the previous chapter of intact waterborne Haloflex showed that despite the low R_n ($\sim 3 \times 10^5$ ohm-cm² after just 2 hours in Harrison's solution - (3.5% (NH₄)₂SO₄ + 0.5% NaCl) diluted to 10%), there was no corrosion beneath the coating.

It appears that the Haloflex contained inhibitors which were leaching into the water as it diffused through the coating and these were preventing corrosion. Although the coating had clearly failed due to formation of blisters the R_n value was an order of magnitude higher than R_{dc} . If R_n were giving an indication of inhibition beneath a coating then it seemed a good possibility that ENM could be used to investigate the performance of inhibitors at breaks in an organic coating with exposed substrate.

6.2 Aims

The aim of this section of work is to establish the effectiveness of ENM and in particular R_n to indicate the degree of protection by inhibitors of exposed substrate at artificially produced scribes. An R_n value that indicates inhibition of corrosion at a scribe was considered to be an important outcome of this work along with a method of obtaining mechanistic data by data analysis in the time domain.

6.3 Experimental

The preparation of specimens for this work followed the procedures set out in Chapter 3 up to the stage of scribe production.

The coatings used for this work are:

Waterborne: Haloflex and Neocryl

Solvent based: CARRS alkyd and CM 2-pack epoxy

Linseed oil based: Red lead primer (control) with and without alkyd barrier top coat.

These coatings have all been characterised in the intact coating work described in Chapter 5.

The ENM measurements were made either using the beaker method or bridge method and areas of coating and exposed substrate not required for testing were blanked off using beeswax / colophony resin. The exposed coating areas were recorded for each experiment, the noise data from these experiments is dominated by that from the scribes whose area was carefully controlled. Most scribes are 0.2 mm x 10mm but some earlier work on waterborne Neocryl and Haloflex used scribes of 25mm x 0.2mm.

The solutions were Harrison's solution - (3.5% $(\text{NH}_4)_2\text{SO}_4$ + 0.5% NaCl) diluted to 10%.

6.3.1 Scribe Production (Mechanical coating removal)

The scribes were produced by two methods: A novel mechanical removal technique and by laser ablation. The mechanical technique involved the production of a special tool. This was designed to remove the area of coating rather than displace it by plastic / elastic deformation, found to be the case when using a conventional blade. The cutting edge of the tool resembles a small lathe (part-off tool) when viewed under magnification, Figure 6.1a. The tool lifts the coating and shears the edges to give a square section scribe, Figure 6.1b, with an easily calculable area. Close control of area should make more reproducible results possible.

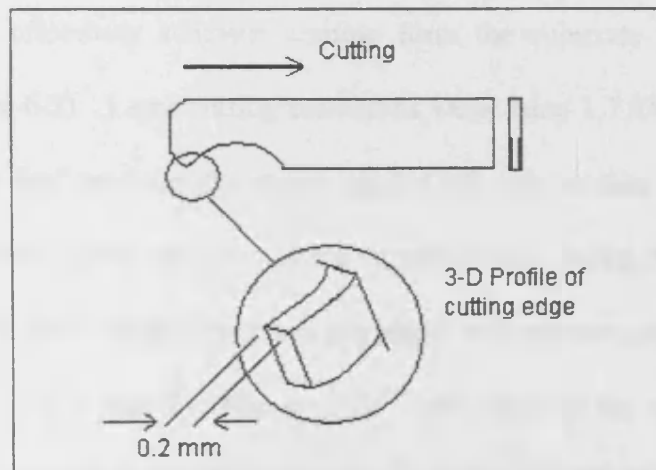


Figure 6.1a Geometry of mechanical-scribing tool

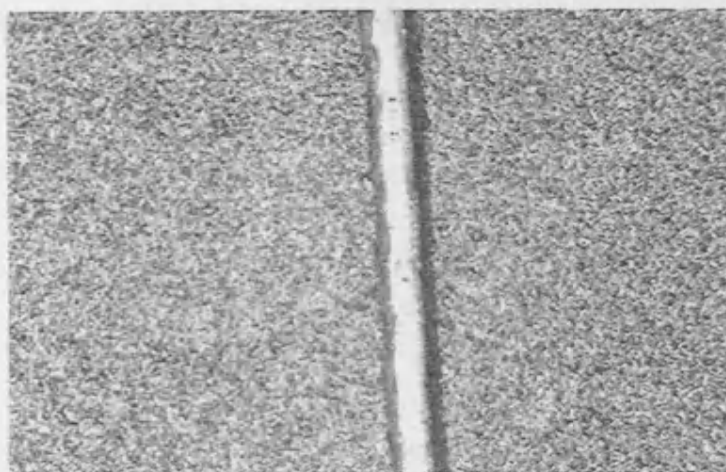


Figure 6.1b Mechanically produced scribe

Note that blade produced scribes led to some closure of the scribe when the coating began to absorb solution. It can be argued that the mechanism of closure contributes to the overall corrosion protection ability of the coating, which is true in practice. Blade produced scribes also tend to vary on width depending on the blade angle and damage to the substrate usually occurs because of the geometry of the blade. To investigate inhibitor performance at scribes it was considered important to remove this variable from the experiments.

6.3.2 Scribe Production (LASER Ablation of coating)

Laser ablation effectively removes coating from the substrate with little or no substrate damage, (Figure 6.2). Laser cutting conditions were: lamp 1.7 kW, pulse width 0.5 mS, rate 200 Hz and the feed rate was 70mm per min to 1100 mm per min. The quality of the ablation was very sensitive to feed rate and was the variable for producing the correct depth of ablation. All ablation was done under a nitrogen gas shield at a pressure of 5.5 bar. The width of the ablated area was 0.2 mm by 10mm ($1/50^{\text{th}}$ cm²) thus giving a direct comparison to the mechanically produced scribes. Comparison of results from laser and mechanically produced scribes will be presented. The comparative tests were undertaken to establish if the laser process would have detrimental effect on inhibitor performance. It was thought that the laser process may vaporise inhibitor material at the coating / substrate / scribe interface or that it may seal the edge of the coating preventing leaching of the inhibitor. Neither of the two scenarios was seen in the results that correlated well with the mechanically cut scribes.



Figure 6.2 Laser produced scribe

Laser production was only used for a limited production run for some of the earlier work on Haloflex and solvent based alkyd. Later work was restricted to mechanical scribe production because of limited access to the laser. The findings that a laser could be used without detrimental effects on the coating were considered important for future work as the laser has several advantages. Firstly the speed of operation, once optimum settings are established scribes can be produced at extremely high rates (60 per minute would be realistic on a standard 100 x 150 mm Q panel). A scribe using the mechanical production tool takes about 30 seconds. Secondly is repeatability of the laser. Even though the mechanical tool has greatly improved consistency there is still some operator variables such as over run on length which the laser does not have.

6.3.3 Data collection

The adopted protocol of using at least two test runs where necessary to obtain good data was used. Explained in Chapter 4, this is considered a better alternative to post correction of data (Kearns *et al*, 1996). Further investigation of data from the scribed experiments is discussed in Chapter 7, Results from Novel Techniques of ENM.

6.4 Results

The results presented here look first at the effects of proven inhibitors with bare Fe on ENM and then extends this to the use of inhibitor leached from coating prepared in the laboratory.

The second part of the experiment investigates water-borne coating and the third part of the work investigates solvent based coating using red lead primer as a control.

6.4.1 Effect on ENM of potassium dichromate inhibitor with Fe in sulphuric acid

Experiments using bare Fe in solutions of acid, acid plus inhibitor and inhibitor without acid were done.

Blanking with beeswax / colophony resin to gave areas of 15cm².

The surface was abraded using 1200 grit paper and degreased with isopropanol.

The inhibitor was potassium dichromate. The solutions were made using de-ionised water and G.P.R sulphuric or G.P.R citric acid to give the following solution:

- a) 0.05M Potassium dichromate with 0.05M sulphuric acid,
- b) 0.1M sulphuric acid,
- c) 0.1M Potassium dichromate,
- d) 0.1M citric acid.

The tests were done at laboratory temperature between 21 C - 24 C. The data in table 6.1 was taken after 19 hours when the systems had stabilised. Numbers in the tables are presented in scientific format $E2 = 1 \times 10^2 \text{ohm-cm}^2$

Solution	Solution A	Solution B	Solution C	Solution D
pot. Noise mV	8.16 E-2	1.67 E0	1.9 E-2	2.38 E-2
curr. Noise mA	3.91 E-4	8.95 E-3	3.37 E-6	1.86 E-4
Noise res. R_n	2.09 E2	1.87 E2	5.63 E3	1.28 E2
R_n ohm / cm ²	3.14E3	2.81E3	8.45E4	1.92E2
pot. Noise mV	1.63 E-1	5.36 E -1	2.04 E-2	6.38 E-2
curr. Noise mA	5.91 E-4	1.92 E-3	3.19 E-6	9.34 E-4
Noise res. R_n	2.75 E2	2.79 E2	6.39 E3	1.76 E2
R_n ohm-cm ²	4.13E3	2.09E3	9.59E4	2.64E3

Table 6.1 data from bare Fe in solutions of acid, inhibitor and acid + inhibitor

The two R_n values for each solution that were corrected for area to give ohms-cm² were averaged to provide data for figure 6.3. The effect of inhibitor in the solution on R_n value is to cause an increase in excess of an order of magnitude when compared to values of R_n for freely corroding Fe in acid. The value of approximately 1E5 ohm-cm² corresponds with total inhibition where no corrosion occurred.

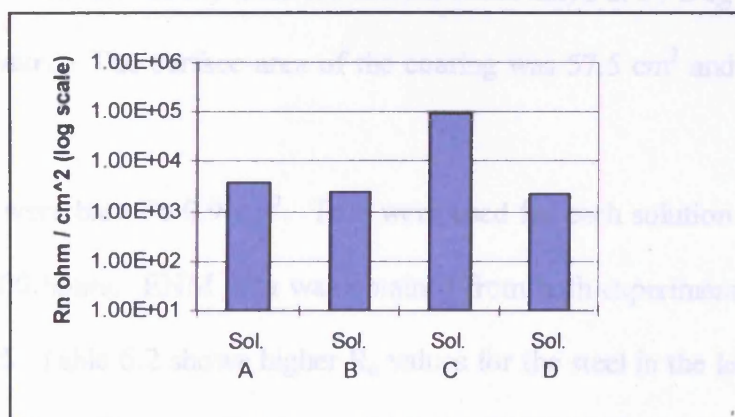


Figure 6.3 Averaged R_n values for bare Fe in solutions of inhibitor, acid and inhibitor + acid

The situation of solution A, which contained equi-molar acid and inhibitor, consisted of corrosion spots evenly distributed on the sample surface. The R_n value reflects the fact that total inhibition is not being provided. A considerable area of the specimen surface is not corroding and as such the R_n value remains higher than those for the freely corroding specimens in solutions C and D. The acid solutions produce rapid corrosion of the bare Fe which have R_n values approximately half that of the border line case in Solution A.

The increase in corrosion rate / decrease in R_n values can be seen to correspond with larger current noise values contained in table 6.1. By inspection the current noise value gives a better indication than the potential noise to the presence of inhibition of the Fe.

6.4.2 Effects of leached inhibitor in Harrison's solution - (3.5% $(\text{NH}_4)_2\text{SO}_4$ + 0.5% NaCl) diluted to 0.5%

In the previous experiment it was seen that ENM is capable of indicating inhibition in a corrosive environment using an established inhibitor. This experiment used leached inhibitive components from a good performance alkyd based on phosphate. The inhibitor was not expected to be as effective as the chromate used in the previous experiment so the solution was diluted to 0.5% salt with a control solution of 0.5 % containing no inhibitor.

The inhibitor was leached slowly from the solvent based alkyd at 50 Deg over 500 hours in 27 ml de-ionised water. The surface area of the coating was 57.5 cm^2 and it had a dry mass of 840 mg.

The electrodes were bare Fe 0.9 cm^2 . Two were used for each solution and photographed in solution after 500 hours. ENM data was obtained from both experiments in four tests over a two hour period. Table 6.2 shows higher R_n values for the steel in the leached solution which are generally around 10^4 ohm-cm^2 compared to $5 \times 10^3 \text{ ohms-cm}^2$ for the uninhibited solution.

	Time hours	Leached sol. R_n	Uninhibited sol. R_n
Test 1	0.1	4.22E4	8.84E3
Test 2	0.5	7.28E3	5.22E3
Test 3	1.0	1.28E4	5.67E3
Test 4	2.0	8.89E3	4.3E3

Table 6.2 Bare Fe in leached and uninhibited solution.

There is approximately a factor of two difference between the inhibited and non-inhibited samples which is not great if taken in isolation but the fact that the four tests repeat this trend indicates that there is a consistent trend with the data.

The experiment was continued on a visual basis for 500 hours and the photograph, Figure 6.4 shows that although the steel electrodes in the uninhibited solution continued to corrode freely the ones in the leached solution remained bright.

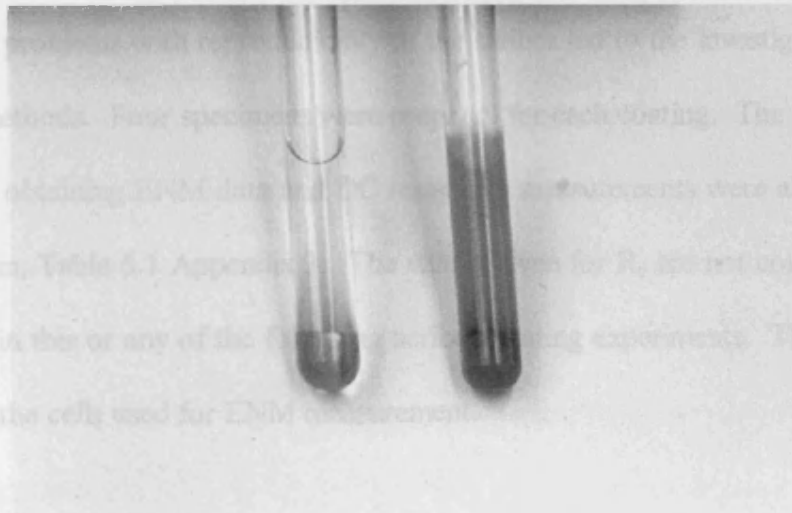


Figure 6.4 Bare Fe in leached and non-inhibited solution after 500 hours

It was observed in these first two experiments that ENM was capable of distinguishing between identical inhibited and non-inhibited specimens. In addition the difference was more noticeable very early on in the experiment which makes the technique an attractive method of assessing the effectiveness of inhibitors.

6.4.3 Scribed Waterborne Haloflex and Neocryl in Harrison's solution

The following experiments were devised to see if the effects noticed previously could be observed in the situation where the coating is attached to the substrate but scribed through. In this situation inhibitive organic coating relies on inhibitive components of the coating leaching into solution that will come into contact with the scribed area. The mechanism should be the same as that observed in the beaker. The following experiment was conducted using scribed waterborne coating in Harrison's solution - (3.5% $(\text{NH}_4)_2\text{SO}_4$ + 0.5% NaCl) diluted to 10%. The total coating thickness was 80 μm applied by spreader bar in two coats. After five days scribes 25 mm long were made through to the substrate and a cell attached over each (area 11.8 cm^2). The scribes in these first experiments were produced using an ordinary scalpel blade. Initial problems with reproducibility of the scribes led to the investigation of alternative production methods. Four specimens were prepared for each coating. The bridge method was then used for obtaining ENM data and DC resistance measurements were also taken following each ENM run, Table 6.1 Appendix 3. The values given for R_n are not corrected for the area of the scribe in this or any of the following scribed coating experiments. The DC values were averaged for the cells used for ENM measurement.

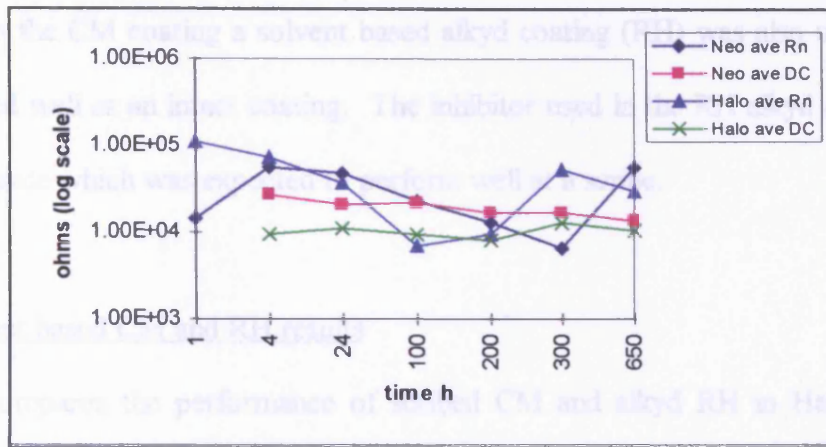


Figure 6.5 R_n and DC resistance over time for scribed Haloflex and Neocryl in 10% Harrison's solution

Corrosion product was visible in all scribes on both coatings within four hours indicating that in this environment Haloflex and Neocryl would not protect a scribed area. The low R_n value and D.C. resistance value appeared to reflect this fact but at this point there was no other data for comparison.

6.4.4 Scribed solvent based organic coating in Harrison's solution (3.5% $(NH_4)_2SO_4$ + 0.5% NaCl) diluted to 10%

It was decided after the previous experiment that a better characterised coating should be investigated. In the previous work little information was provided by the manufacturer concerning inhibitors or pigmentation of the waterborne coating as the product was in the market place and relatively new.

The coating chosen for the next experiments was a solvent based two pack epoxy (CM). This is an industrial grade organic coating which is well proven and performed well in the intact experiments in Chapter 5. Also information on pigmentation was provided which gave useful indicators as to the environments in which the coating would provide protection to a scribe.

The inhibitor used in the CM coating is zinc phosphate.

In addition to the CM coating a solvent based alkyd coating (RH) was also used which again had performed well as an intact coating. The inhibitor used in the RH alkyd coating was zinc tetroxy chromate which was expected to perform well at a scribe.

6.4.5 Solvent based CM and RH results

Figure 6.6 compares the performance of scribed CM and alkyd RH in Harrison's solution (3.5% $(\text{NH}_4)_2\text{SO}_4$ + 0.5% NaCl) diluted to 10%.

For this work it was decided to standardise the scribe area as much as possible. This was done by producing the scribes with the newly devised mechanical tool and a laser beam as described previously. The area produced by both methods was therefore easily calculable at 0.02 cm^2 .

The coating thickness was $85 \pm 5 \mu\text{m}$ for each coating, applied by spreader bar as described in Chapter 4. The total exposed coated area was 15 cm^2 provided by blanking explained in Chapter 4. The beaker method of obtaining ENM data was used for the tests and two runs of data collection produced excellent data sets with the drift on the current being less than

$1 \times 10^{-8} \text{ mA / s}$ and drift on potential of less than $1 \times 10^{-5} \text{ mV / s}$. Eight cells were used for each coating of which four had scribes produced by laser and four by the mechanical tool.

Data from the individual pairs are given in table 6.2, Appendix 3.

CM = Two pack epoxy, RH = Rust hold alkyd, L = laser ablated scribe, M = Mechanically.

The values were averaged to produce the graph in Figure 6.6 which compares the two coatings. Values are not corrected for the area of the scribe.

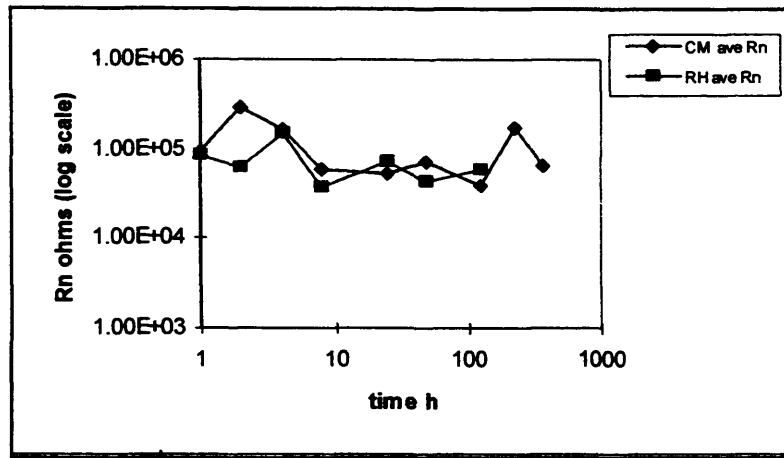


Figure 6.6 Scribed CM and RH in 10% Harrison's

6.4.6 Observations on CM two pack epoxy and RH alkyd in 10% Harrison's solution

The R_n values for the two coatings were very close but overall the RH alkyd was generally below CM epoxy. There was no red rust visible in either the laser or mechanically produced scribes on the CM with the exception of two small areas on one of the samples. Closer inspection showed this to be metallic shavings embedded in the ends of the scribe from the cutting process and not the substrate itself. The scribes however did not remain bright and a very dark dense corrosion product was seen in the scribe. Electrochemical measurements were discontinued at 360h but the samples were left in solution for a total 1000h without further visible corrosion. The photograph in Figure 6.7 shows two of the eight samples of CM coating from the experiment compared with two identical samples from the following experiment which were corroding freely.

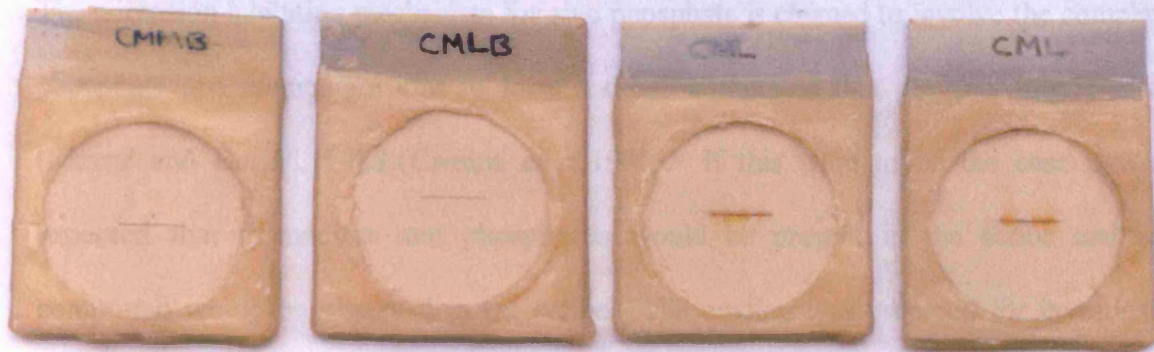


Figure 6.7 Inhibited and corroding scribes

It was this corrosion product which had prevented or considerably slowed continued corrosion and it was considered that this warranted further investigation.

The RH alkyd scribes showed no red rust but the coating failed by blistering after 120h and it was decided to continue the investigation into corrosion prevention at scribes using the CM two pack epoxy. An interesting observation on the alkyd was that although the coating blistered considerably and effectively failed, the R_n values remained reasonably high returning values of between 2 and 9×10^4 ohm. On removing the blistered coating it was seen that there was no corrosion beneath the blisters. This phenomena corresponds with the behaviour of the Haloflex in the previous experiments indicating that R_n appears to register inhibition.

6.5 Scanning electron microscopy investigation of corrosion product at CM scribes from immersion in Harrison's solution (3.5% (NH₄)₂SO₄ + 0.5% NaCl) diluted to 10%

The corrosion inhibition mechanism for zinc phosphate is claimed to involve the complexing of phosphate and ammonium ions to form a dense compound that prevents migration of ions (Mayne and Burkill, 1988)(Camina *et al*,1990). If this were to be the case it would be expected that ammonium and phosphorus would be present in the scribe and a dense compound would be observed in the scribe. The coating was prepared for investigation by scanning electron microscopy (SEM). After being allowed to dry thoroughly for a week the samples were gold sputtered and stored in a desiccator jar until required.

Figure 6.8 shows an SEM micrograph of a section of scribe in the CM epoxy coating that had been exposed to 10% Harrison's solution for 1000 hours. Magnification is x400 and it can be clearly seen that the scribed substrate area is completely filled with a dense product which has obviously acted as a barrier to further corrosion. The main lateral fracture and adjoining longitudinal fracture along with the series of smaller ones to the right are believed to have formed on dehydration of the coating in preparation for SEM examination. The micrograph in Figure 6.9 at x3600 and shows one of the extreme regions of product growth. It demonstrates that the fractures have formed after the coating has been removed from the solution as the outer extremities of the product have been cleaved, no further film growth could be observed in or around the fracture areas.

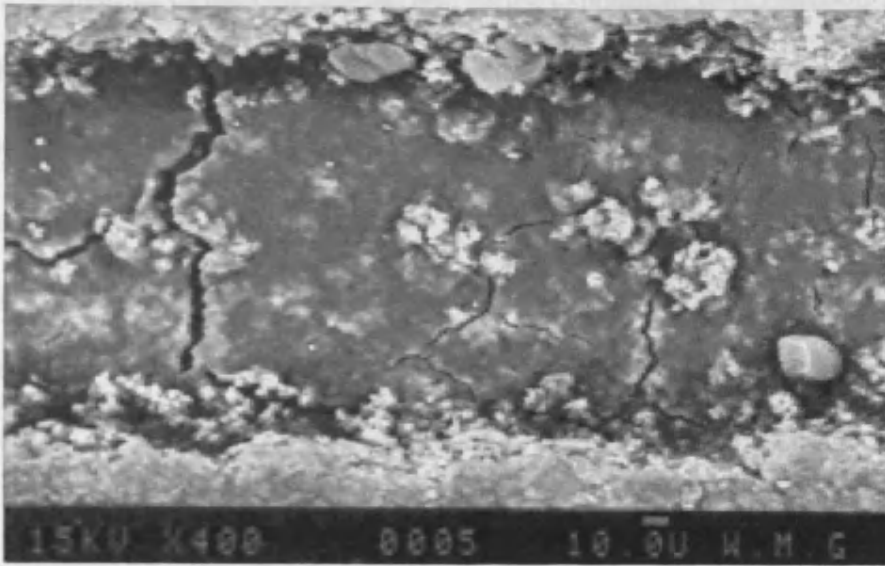


Figure 6.8 SEM micrograph x400 of a section of scribe area of the CM epoxy after 1000h immersion in 10% Harrison's solution

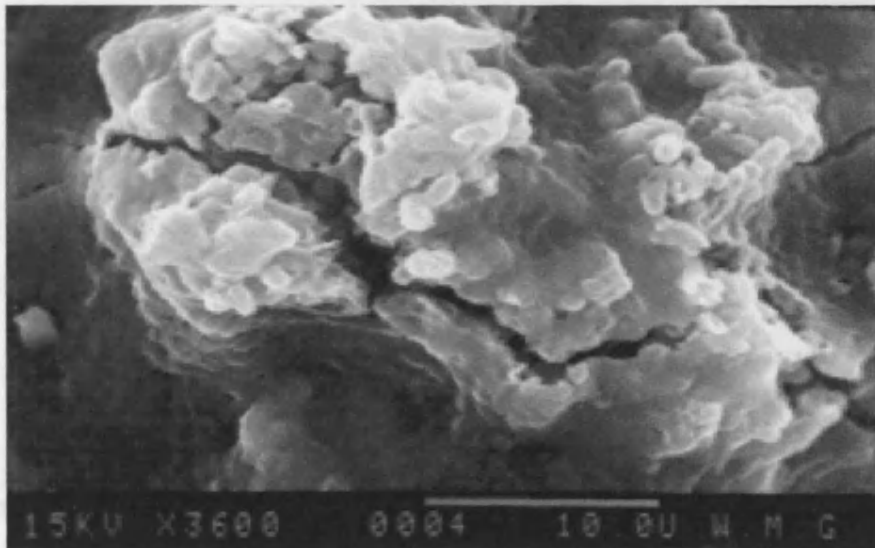


Figure 6.9 SEM micrograph x3600 of extreme area of product growth on the corrosion product in the scribe of the CM epoxy after 1000h immersion in 10% Harrison's solution.

deposit occurs to indicate that the combination of phosphate with ammonia from the solution

6.5.1 EDX analysis of the CM coating and scribe exposed to 10% Harrison's solution

The method of analysis does not allow the accurate calculation of amounts of one element for two reasons. Firstly, there is a non-linear distribution of background counts which cannot be separated from the peaks of the elements. Secondly, the counts only indicate the presence of the element and cannot distinguish between X_n and X_{n+1} . It is however a very useful technique for identify the presence of a particular metallic element and an approximate ratio of the element to others can be established easily. The coating was analysed away from the scribed area and Figure 6.10 shows the main metallic elements present in the coating.

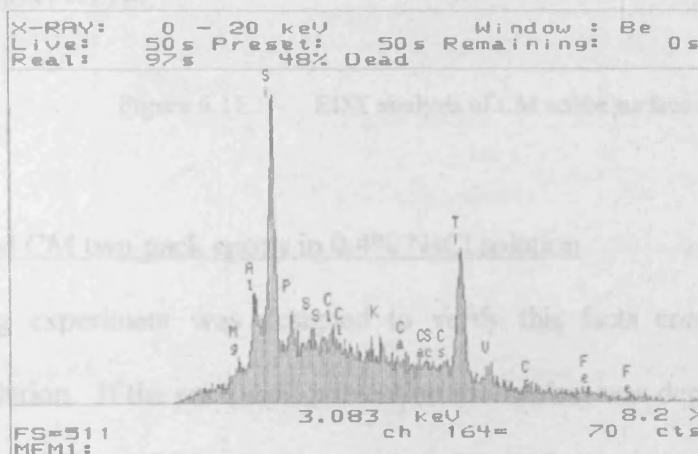


Figure 6.10 EDX analysis of CM coating surface

There are peaks of silicon, titanium and aluminium. The phosphor peak can be seen on the right hand side of the silicon peak. Figure 6.11 by contrast shows the EDX analysis taken from the centre of the scribed area. As expected there are large peaks for iron and small peaks for zinc which were not within the range of the data presented in Figure 6.10. There are also large peaks of phosphorus, silicon and to a lesser extent chloride which represents the small quantity of 0.05% used in diluted Harrison's. The presence of quantities of phosphorus in the scribe

deposit appear to indicate that the combination of phosphate with ammonia from the solution was the mechanism involved.

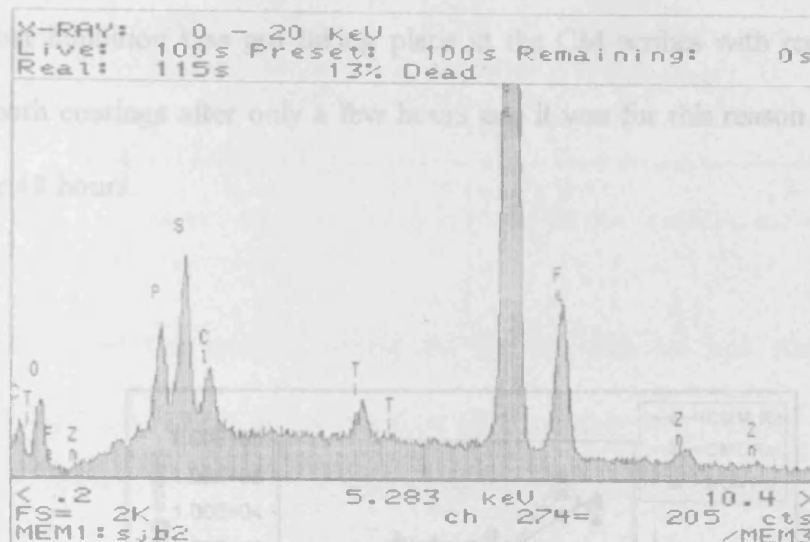


Figure 6.11 EDX analysis of CM scribe surface area

6.6 Scribed CM two pack epoxy in 0.4% NaCl solution

The following experiment was designed to verify this facts concluded from the tests in Harrison's solution. If the corrosion prevention mechanism was dependent on the ammonia in the environment, then if the CM coating was tested in an NaCl solution of the same concentration there should be no formation of the dense product and corrosion would proceed. The difference in performance of the CM coatings dependent on solution environment was shown in the photograph in Figure 6.7. The R_p values also reflect this difference with those from the NaCl environment falling to low 10^{-10} R_p values compared to and to high 10^{-7} R_p values from the original Harrison's solution (Figure 6.13). The aim was to see if this was the case and if so could the difference in mechanisms be distinguished by ENM. The previous experiment was repeated using four new samples from the original set of panels. Two samples were mechanically scribed and two were laser ablated. Conditions for the experiment were kept the same except for the test solution which was changed to 0.4 NaCl.

In addition to the CM coating two samples were prepared from Incorez 152, two pack epoxy using the same techniques as those applied to the CM coating. The 152 is a totally un-

pigmented epoxy and these were scribed using the mechanical tool to give a control coating with no corrosion inhibitive properties at a scribe. Data for the graph in Figure 6.12 is contained in table 6.3, appendix 3. It can be seen that there is good correlation between the values of R_n obtained from the CM coating and those from the 152 control coating. This indicated that inhibition was not taking place at the CM scribes with red rust visible in the scribes of both coatings after only a few hours and it was for this reason the experiment was only run for 48 hours.

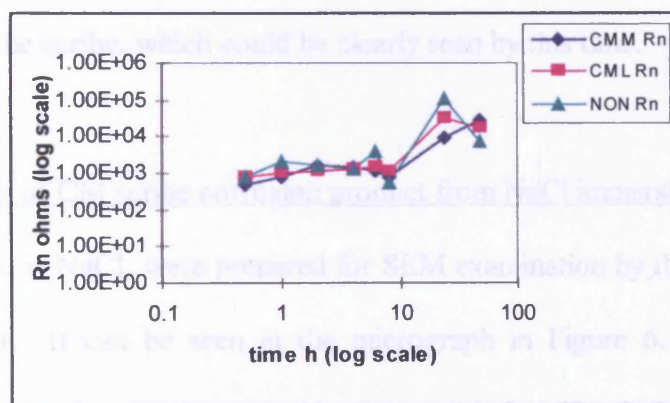


Figure 6.12 R_n over time for CM and 152 (control) coating in 0.4% NaCl

The difference in performance of the CM coating dependent on solution environment was shown in the photograph in Figure 6.7. The R_n values also reflect this difference with those from the NaCl environment falling to low 10^3 R_n values compared to mid to high 10^4 R_n values from those in the diluted Harrison's solution (Figure 6.13).

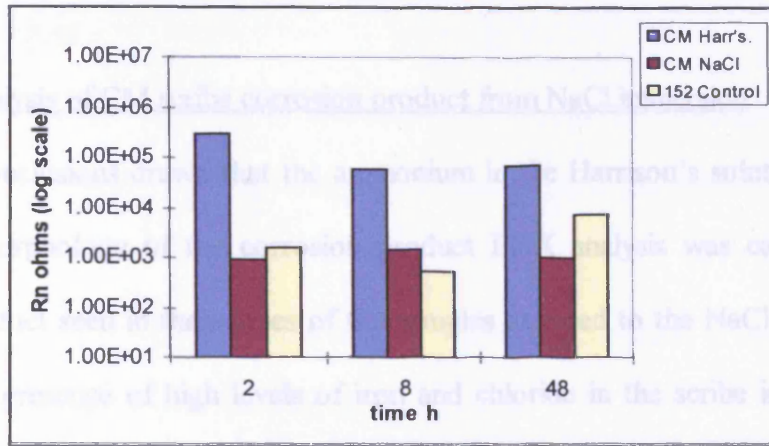


Figure 6.13 Comparison of CM coating in diluted Harrison's solution and NaCl with control

The higher value of the control coating for the 48h data set was attributed to corrosion product build up in the scribe, which could be clearly seen by this time.

6.6.1 SEM analysis of CM scribe corrosion product from NaCl immersion

The specimens tested in NaCl were prepared for SEM examination by the same process as the previous experiment. It can be seen in the micrograph in Figure 6.14 that the corrosion product is a porous and voluminous oxide. As such it offered little protection to the underlying substrate which was indicated by the low R_n values and visual appearance of the specimens.

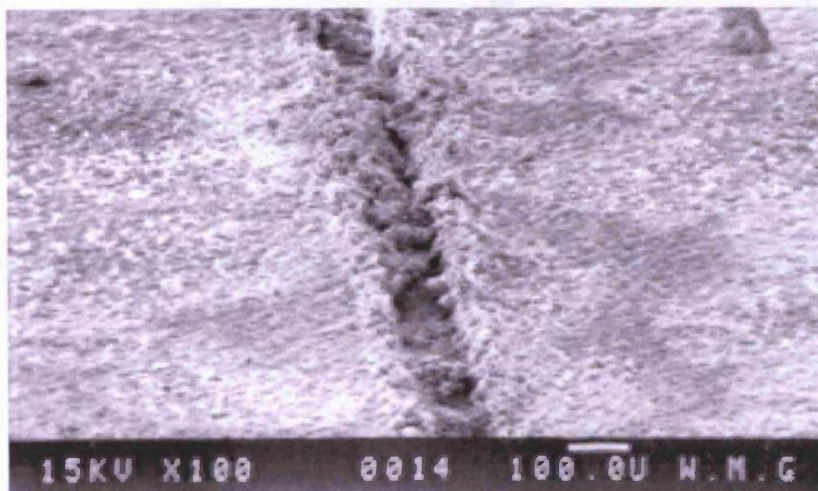


Figure 6.14 Corrosion product in NaCl solution

6.6.2 EDX analysis of CM scribe corrosion product from NaCl immersion

To verify the conclusions drawn that the ammonium in the Harrison's solution was the main factor in the morphology of the corrosion product EDX analysis was carried out on the voluminous product seen in the scribes of the samples exposed to the NaCl solution. Figure 6.15 shows the presence of high levels of iron and chloride in the scribe indicating that the product is ferric or ferrous chloride. The much smaller peaks of phosphorus and zinc appear to indicate that in this environment the mechanism does not involve phosphorus and it is this fact that has presented the stark contrast between the performance and morphology of the corrosion product formed in the scribes of the CM coating.

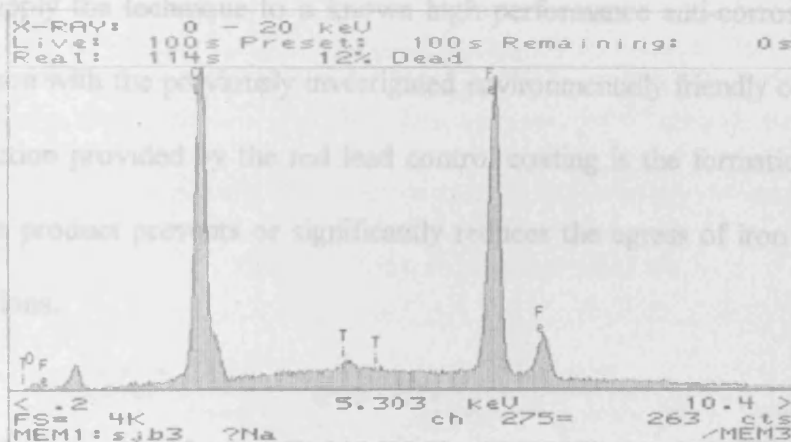


Figure 6.15 EDX analysis results of CM scribe corrosion product in NaCl solution

6.7 Conclusion

ENM has successfully registered the difference between the two mechanisms and an R_n value of around 5×10^4 ohm-cm² or higher appears to indicate that inhibition is present in the scribed area.

The findings of these experiments concerned the situation where a layer is formed on the substrate surface that impedes the migration of ions.

6.8 Investigation of scribed red lead

The following experiments aimed to investigate the situation where the surface of the exposed substrate is passive and despite the presence of aggressive ions remains bright.

Despite the fact that red lead is no longer commercially available for on-shore use in the UK it was decided that its unsurpassed performance in protecting underlying substrate at sites of coating damage would demonstrate if ENM could detect this type of behaviour. The aim then was to apply the technique to a known high performance anti-corrosive coating and have a comparison with the previously investigated environmentally friendly coating. The mechanism of protection provided by the red lead control coating is the formation of a lead soap. The corrosion product prevents or significantly reduces the egress of iron ions and the ingress of chloride ions.

6.8.1 Single coat red lead on Fe in 10% Harrison's solution

The coating was applied in one coat using a spreader bar to give approximately 80µm thickness. The bridge method was employed using new low aspect ratio cells which gave good visibility of the scribe area. The area of the cells was 7.5 cm² and the scribe area produced by the mechanical tool remained at 0.02 cm². Conditions for the ENM measurements also remained the same as for previous experiments at 2Hz data reading frequency over 150 seconds using at least two test runs. The data for the graphs presented in Figures 6.16 and

6.17 are contained in tables 6.4 to 6.5, appendix 3. Data is not corrected for the area of the scribe.

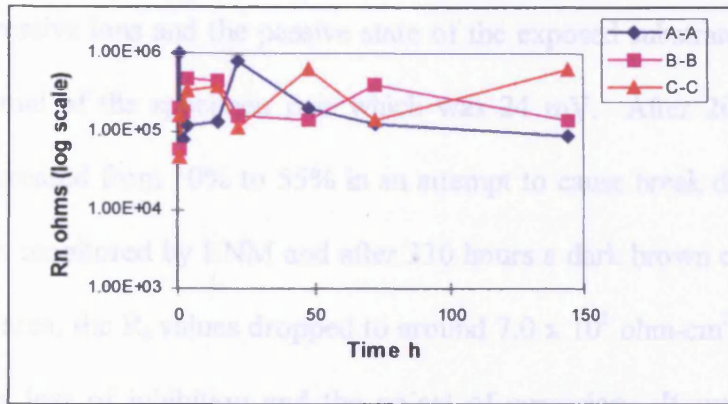


Figure 6.16 Scribed red lead in 10% Harrison's solution

Although R_n values remained reasonably high in this experiment all six samples showed some initial corrosion which appeared to stop at around four hours. The corrosion product formed then prevented further corrosion in much the same way as the CM coating with R_n remaining in the low to mid 10^4 ohm-cm². The aim of this experiment was to establish if R_n could detect inhibition where there was no corrosion. The approach used for the following result involved a pre-soak of the scribed coating in de-ionised water. Only one pair of samples were used as this was a preliminary check to establish if the technique would work.

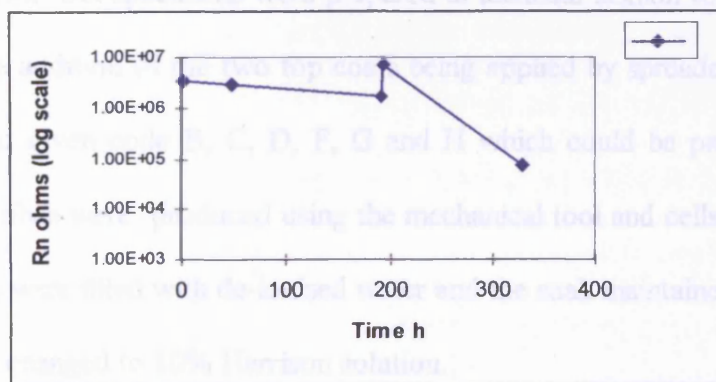


Figure 6.17 Scribed red lead soaked for 96 hours in de-ionised water prior to testing in 10% Harrison's solution

The pre-soaking of the coating for 96 hours prior to testing prevented any corrosion and the scribes remained bright. The method had enabled the formation of a protective oxide in the absence of aggressive ions and the passive state of the exposed substrate was reflected in the measured potential of the specimen pair which was 24 mV. After 200 hours the solution strength was increased from 10% to 55% in an attempt to cause break down of the protective oxide. This was monitored by ENM and after 330 hours a dark brown corrosion product had filled the scribe area, the R_n values dropped to around 7.0×10^3 ohm-cm² from 7.0×10^5 ohm-cm² indicating a loss of inhibition and the on-set of corrosion. It was postulated that the effective inhibition observed may be because of bulk diffusion of inhibitor from the coating into the solution. To check if this was the case it was further suggested that the experiment be re-run with scribed red lead which was sealed with a non-pigmented top coat. In this format the scribe could only be protected by inhibition from the red lead at the point of exposure along the sides of the scribe. The coating did eventually fail at the scribe in all cells because of disbonding. The R_n values dropped considerably into the low tens of kilohms indicating failure.

6.8.2 Single coat red lead sealed with non-pigmented alkyd

The red lead was sealed using two coats of alkyd top coat. The alkyd contained no anti-corrosive pigments. Six specimens were prepared in identical fashion to the previous tests on red lead with the addition of the two top coats being applied by spreader bar. Six specimens were scribed and given code B, C, D, F, G and H which could be paired using the bridge method. The scribes were produced using the mechanical tool and cells attached with silicon sealer. The cells were filled with de-ionised water and the soak maintained for 48 hours before the solution was changed to 10% Harrison solution.

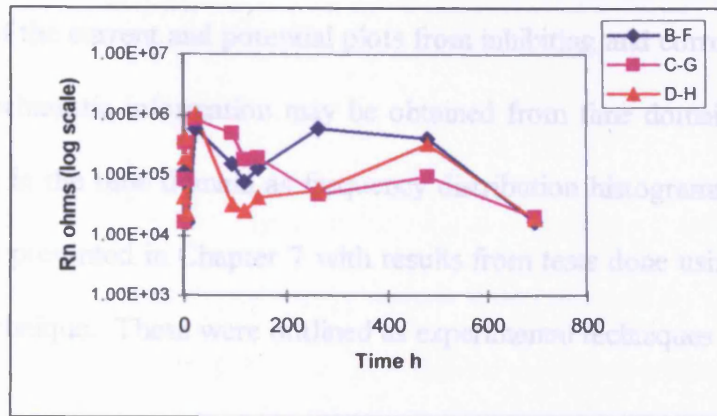


Figure 6.18 Sealed scribed red lead pre-soaked in de-ionised water prior to exposure to 10% Harrison's solution

It can be seen from Figure 6.18 that the R_n values are slightly lower than the sample R_n in Figure 6.17. However, there was sufficient leaching of pigment at the scribe for an oxide to form and the scribes remained bright. Additions of potassium ferricyanide to cells D and H also indicated that no Ferrous ions were being produced at the scribe and entering solution.

6.9 Interim conclusion on ENM for monitoring inhibition

This series of experiments show that ENM and in particular the parameter R_n has use in establishing if inhibition is present at a site of damage in a coating. This could be developed for investigating the effects of different environments on the effectiveness of inhibitive pigments as was seen with the results from the CM coating experiments. The technique could also be applied to testing new inhibitors and present a numeric value (see conclusions Chapter 8) for comparison against proven anti-corrosive pigmented systems.

6.10 Mechanistic information from data analysis

Data analysis of the current and potential plots from inhibiting and corroding systems indicates that further mechanistic information may be obtained from time domain data. The data sets were examined in the time domain as frequency distribution histograms. The findings of this area of work is presented in Chapter 7 with results from tests done using novel developments of the ENM technique. These were outlined as experimental techniques in Chapter 5.

CHAPTER 7

Results from New Techniques

7.1 Introduction

In an attempt to gain mechanistic information on the behaviour of anti-corrosive pigments at scribed defects in paint, time domain data analysis was performed on data collected from the experiments described in section 6.4 and 6.5. Where general corrosion was present the data plots of potential and current were seen to be of a Normal or Gaussian distribution. This was also found to be the case in conditions of successful protection by intact organic coatings verifying the assumptions in the literature (Bierwagen, 1994b)(Cottis and Turgoose, 1994) and giving R_n values that correlate with R_p and R_{dc} respectively. However, frequency distribution analysis of time domain data from scribed samples did not show this in all conditions and bi-modal and non-normal distributions were observed in the data which appeared to coincide with inhibitive processes beginning to break down or corrosion at the scribe.

The results presented in chapters 5 and 6 used established experimental set-ups: ie, the bridge and beaker methods described in Chapter 3. The success of ENM when applied to the two situations of intact and scribed organic coatings led to work which aimed to develop the ENM technique with a view of creating a portable test that could be of use to industry.

In addition to this, ENM was applied to detached samples of the same coatings used in chapters 5 and 6. The DC resistance (R_{dc}) method has traditionally been applied to detached coatings (Mills and Mabbutt, 1997) and recent work has been published, (Bierwagen, *et al*, 1994a) that used ENM to assess a detached solvent based marine coating. This work extends that by looking at a solvent based alkyd (RH) and epoxy (CM). Some preliminary results from the detached waterborne coatings investigated in Chapter 5 are also presented. The DC resistance method is used as a comparison to the ENM data.

7.2 Frequency Distribution Analysis of Time Domain Data Sets

The frequency distribution of electrochemical potential and current noise has been shown to be of a Gaussian distribution for intact coating systems (Mills *et al*, 1999). Figures 7.1 and 7.2 show potential and current frequency distributions of data sets obtained from the sealed red lead primer system used in Section 5.8. Experimental details of data analysis techniques are contained in Section 4.3 and explanations of the set-up for obtaining the ENM data are contained in Section 3.3.

The frequency distributions were plotted as histograms and fitted with a curve using the two point moving average technique. This common mathematical technique was found to give a good indication of the shape of the data distribution. For those data distributions appearing normal more accurate information can be obtained by calculation of skew and kurtosis values (4.3.2). It involves mathematically predicting the value of the next data point by calculating the difference between subsequent data points. For the purpose of this work the previous two points (hence 2 point moving average) was sufficient to give a smooth plot.

The use of the histogram alone tends to give a misleading impression because the columns only represent a total number of counts between two numerical limits. By contrast the moving average technique uses each individual data point of the data set to give a smooth and constant trend.

Where the frequency distribution plots indicated a Gaussian distribution the kurtosis and skew values were calculated using the formula in section 4.3, where the two measures of normality are explained. It has been shown that potential and current noise data of Gaussian distribution will produce Noise Resistance (R_n) values that correlate with the D.C. resistance value for an intact organic coating (Bierwagen, 1994b).

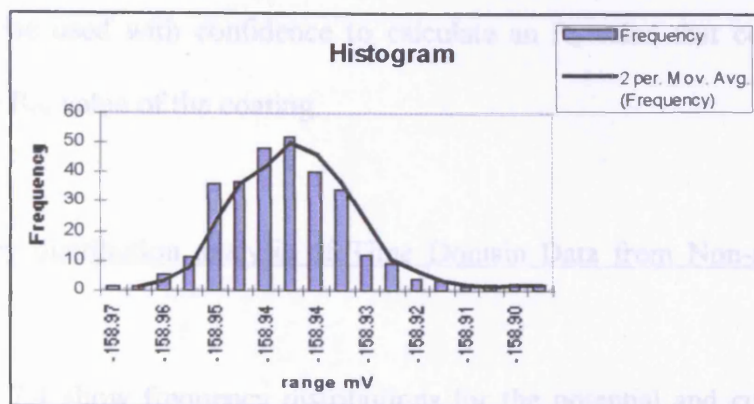


Figure 7.1 Potential frequency distribution from sealed red lead on Fe after 8 hours immersion

Kurtosis = 1.8

Skew = 0.7

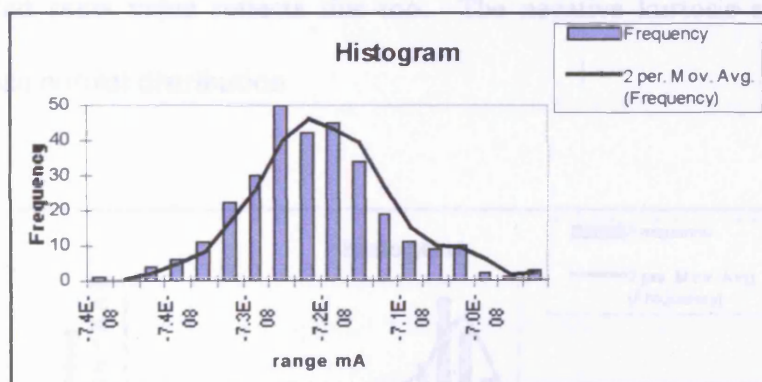


Figure 7.2 Current frequency distribution from sealed red lead on Fe after 8 hours immersion

Kurtosis = 0.59

Skew = 0.37

The kurtosis and skew values were calculated for the data sets used for the plots in Figures 7.1 and 7.2. These indicate that the distribution in both cases is close to a “perfectly” normal distribution where both values for Kurtosis and Skew would be close to zero. The positive kurtosis number indicates a slightly biased distribution of data values closer to the mean of the data set and this gives a more pronounced peak to the shape of the plot whilst still qualifying as a Gaussian distribution.

Thus, data may be used with confidence to calculate an R_n value that could be considered equivalent to the R_{dc} value of the coating.

7.2.1 Frequency distribution analysis of Time Domain Data from Non-pigmented Control Coating

Figures 7.3 and 7.4 show frequency distributions for the potential and current time domain data obtained from the control coating (152 - for details see section 6.4). This was an unpigmented epoxy which was scribed and exposed to Harrison's solution diluted to 10%. The coating offered no corrosion protection to the scribed area which showed general corrosion after 4 hours. The potential plot is skewed which reflects linear drift of the data set and the calculated skew value reflects this too. The negative kurtosis number indicates a slightly flatter than normal distribution.

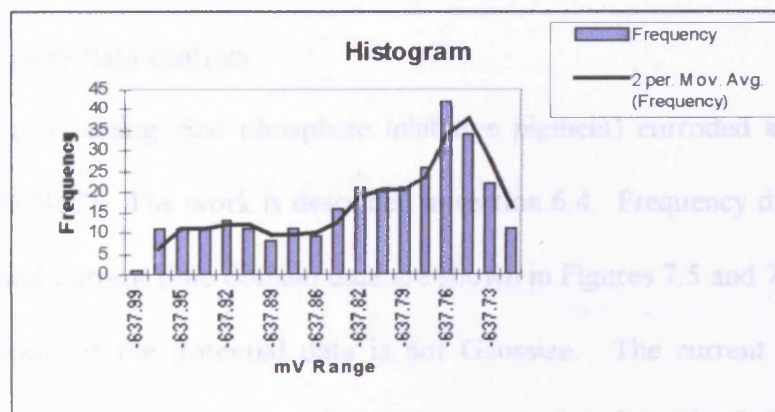


Figure 7.3 Frequency distribution of time domain potential noise - Corroding scribe in 152 unpigmented epoxy.

Kurtosis = -0.682

Skew = -0.662

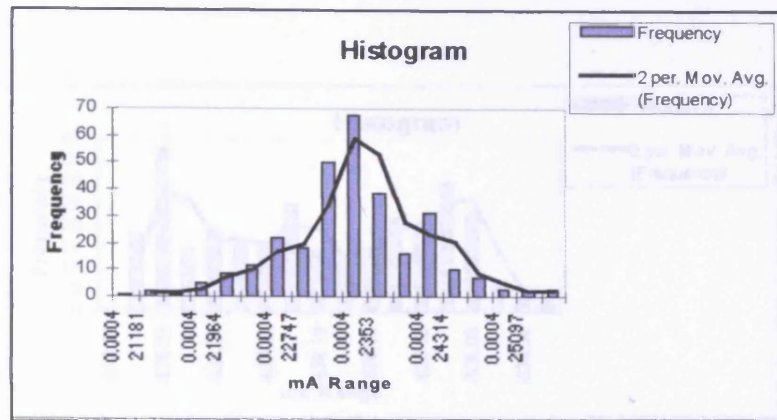


Figure 7.4 Frequency distribution of time domain current noise - Corroding scribe in 152 un-pigmented epoxy.

$$\text{Kurtosis} = 0.887$$

$$\text{Skew} = 0.03$$

The positive value of kurtosis indicates that the mA data had a slightly peaked distribution compared to a perfectly normal distribution. Skew on the current data was negligible.

7.2.2 Scribed epoxy data analysis

The CM epoxy (containing zinc phosphate inhibitive pigment) corroded at the scribe when exposed to 0.4 % NaCl. The work is described in section 6.4. Frequency distribution analysis of the potential and current time domain data are shown in Figures 7.5 and 7.6. It can be seen that the distribution of the potential data is not Gaussian. The current data is also non-Gaussian, possibly bi-modal as there appears to be a second peak on the data which is skewed. As explained in section 4.4, the mathematical values for Kurtosis and skew do not apply to non-gaussian or bi-modal data sets and as such no attempt is made to calculate these values for the scribed data from the pigmented coatings.

This pattern of distribution has been found to be common when frequency distribution analysis has been carried out on data from the scribed pigmented CM epoxy and red lead coatings used in section 6.5. The frequency distributions below demonstrate this.

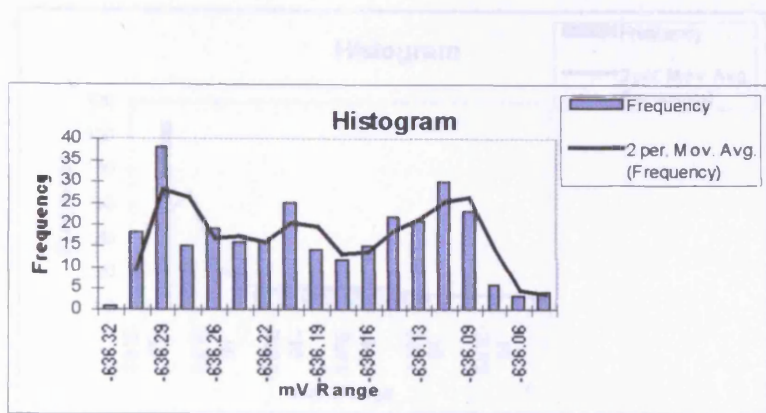


Figure 7.5 Frequency distribution of time domain potential noise - Corroding scribe of CML08 corrosion with voluminous product

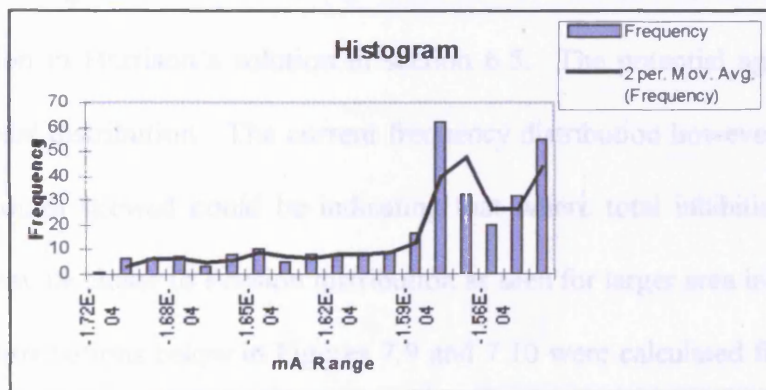


Figure 7.6 Frequency distribution of time domain current noise - Corroding scribe of CML08 corrosion with voluminous product

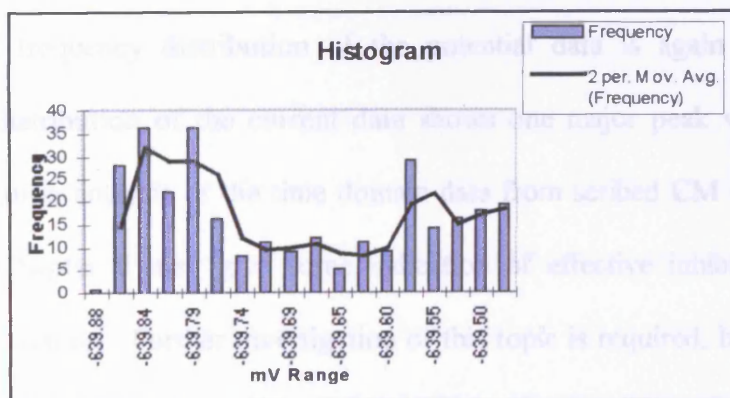


Figure 7.7 Frequency distribution of time domain potential noise - BF04 - inhibitive processes

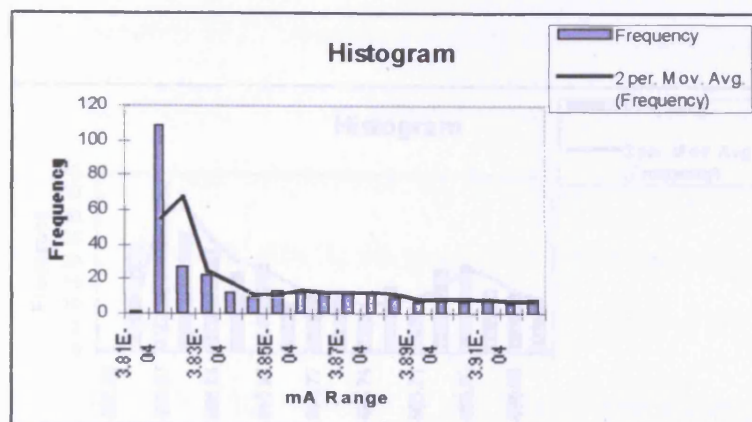


Figure 7.8 Frequency distribution of time domain potential noise - BF04 - inhibitive processes

The data used for Figures 7.7 and 7.8 was obtained from the scribed sealed red lead which inhibited corrosion in Harrison's solution in section 6.5. The potential again shows a non-normal or bi-modal distribution. The current frequency distribution however, only shows one peak which although skewed could be indicating that where total inhibition is present at a scribe the data may be closer to Poisson distribution as seen for larger area inhibition.

The frequency distributions below in Figures 7.9 and 7.10 were calculated from data obtained from the scribed CM epoxy that was exposed to Harrison's solution diluted to 10% and described in section 6.4. Corrosion at the scribed areas in this case was effectively reduced from further corrosion by a dense corrosion product: this was discussed and analysed in Chapter 6. The frequency distribution of the potential data is again non-Gaussian and interestingly the distribution of the current data shows one major peak with a smaller one. Frequency distribution analysis of the time domain data from scribed CM epoxy and red lead coating used in Chapter 6 may give some indication of effective inhibition at scribed or damaged areas of coating. Further investigation of this topic is required, but there does seem to be a link between a non-Gaussian distribution (particularly of the current data) inhibition at a scribe. Where effective inhibition is present the frequency distributions of the time domain data are closer to the single peaked or Gaussian distributions seen for effective protection by organic coating.

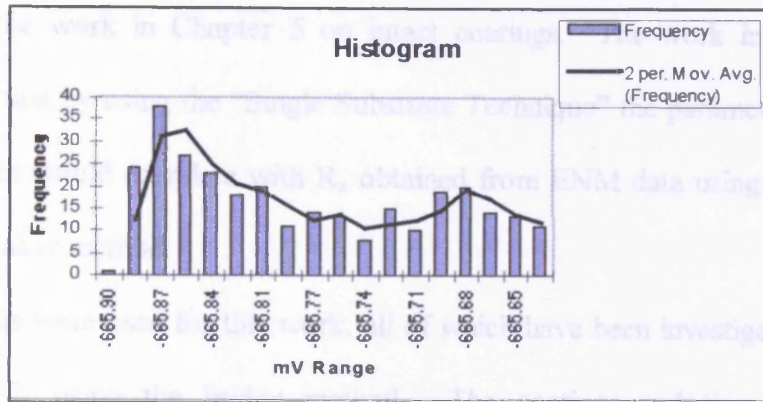


Figure 7.9 Frequency distribution of time domain potential noise - CMLB04 with dense corrosion product at the scribe

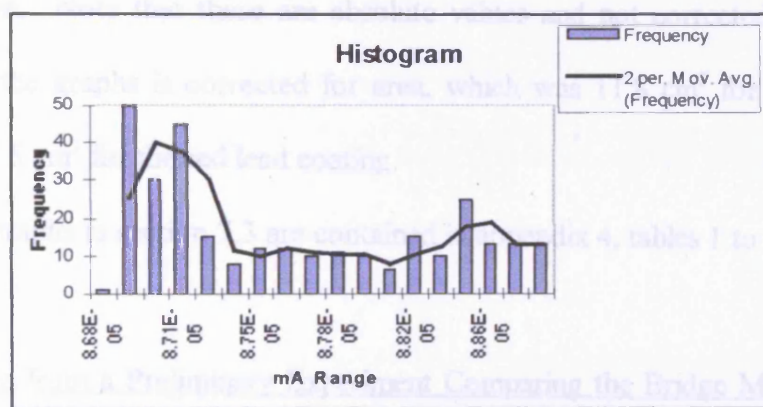


Figure 7.10 Frequency distribution of time domain current noise - CMLB04 with a dense corrosion product at the scribe

7.3 Results from using the Single Substrate Technique

The single substrate technique was developed in an attempt to create an experimental set - up that could be adapted to field applications of ENM or for faster testing in the laboratory.

The schematic circuit diagrams in section 4.4. show the test cell is electrically very similar to the traditional bridge method and beaker method. The advantage of the new technique is that two separate substrate elements are not required to make ENM measurements and this enables an ENM test to be done (theoretically) on any special area of coated substrate by using just one electrical connection.

Good correlation between D.C. resistance values and R_n has already been demonstrated throughout the work in Chapter 5 on intact coatings. The work in this section aims to demonstrate that by using the “Single Substrate Technique” the parameter R_n calculated from the ENM data would correlate with R_n obtained from ENM data using the traditional bridge method or beaker method.

Three coatings were used for this work, all of which have been investigated in the intact state in section 5.7. using the bridge method. The coatings and time period of the tests demonstrated the technique over the useful resistance range for intact anti-corrosive organic coating of $> 1 \times 10^9$ ohm-cm² for effective coating protection down to $< 3 \times 10^4$ ohm-cm² for low protection. Note that these are absolute values and not corrected for area. The data contained in the graphs is corrected for area, which was 11.8 cm² for the alkyd and epoxy coating and 7.5 cm² for the red lead coating.

Data for the graphs in section 7.3 are contained in appendix 4, tables 1 to 3.

7.3.1 Results from a Preliminary Experiment Comparing the Bridge Method and the Single Substrate Technique Using Solvent Based Alkyd

The first experiment using the Single Substrate (SS) technique as a comparison to the Bridge Method was carried out in 3% NaCl solution on the solvent based alkyd primer that was known to have high ionic resistance and very good protective properties.

7.3.2 Results from a Comparison of the Single Substrate technique and the Bridge Method using CM epoxy

The work carried out on the CM epoxy was a test that ran for almost 2100 hours. The coating proved to be very effective when immersed in Harrison's solution diluted to 10%, in both the intact and scribed conditions. It was considered that a proving test of the SS technique would be if the R_n values not only correlated with the Bridge Method but also tracked the performance of the coating over a period of time and range of resistance.

Three cells were attached to each coated steel panel. The coating was applied by spreader bar as described in Chapter 3. Two coats were applied to give a thickness of $120 \pm 10 \mu\text{m}$ and cells were attached using silicon sealer. Harrison's solution was used at 10% dilution. The data for the graph in Figure 7.12 is contained in appendix 4. The R_n values on the graph are averaged using the geometric mean from the three pairs used for the Bridge Method and the four separate combinations used for the SS technique.

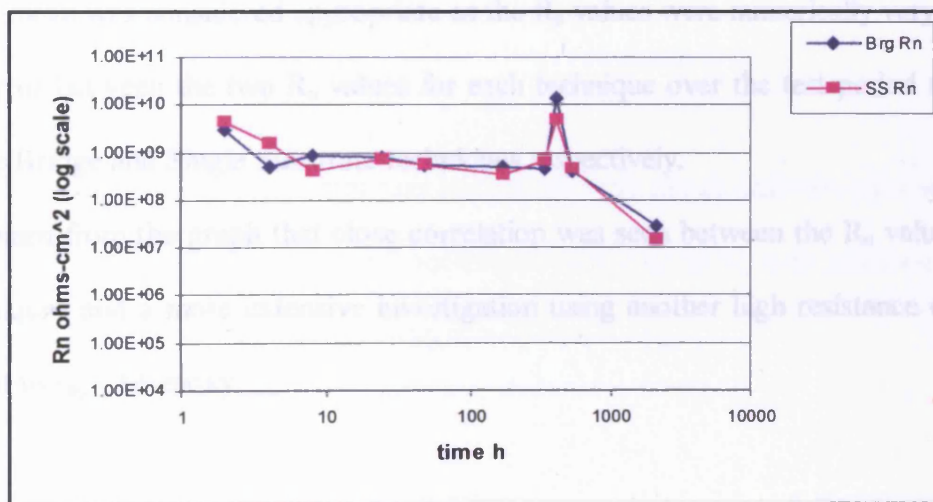


Figure 7.12 SS Technique and Bridge Method against time using CM epoxy on Fe in Harrison's solution diluted to 10%

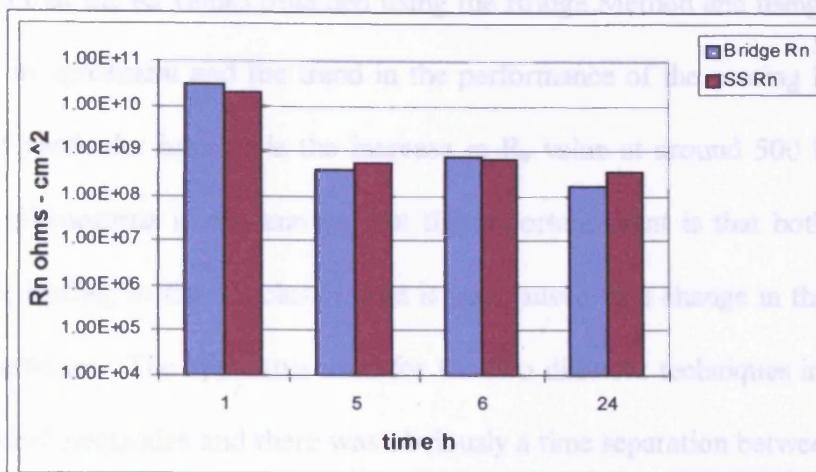


Figure 7.11 Preliminary results comparing the Bridge Method and the Single Substrate Technique.

Solvent based alkyd on Fe in 3% NaCl solution

Four cells, two on each panel were used for this test which by altering the formation of the test gave two pairs for each technique. The test was run for 24 hours and the ENM data used to obtain R_n values for each technique. For the histogram in Figure 7.11 the data from the two tests were averaged using the arithmetic mean to give one R_n value for each technique. The arithmetic mean was considered appropriate as the R_n values were numerically very close. The average error between the two R_n values for each technique over the test period was 0.7 and 0.5 for the Bridge and Single Substrate techniques respectively.

It can be seen from the graph that close correlation was seen between the R_n values from the two techniques and a more extensive investigation using another high resistance coating was carried out using CM epoxy.

It can be seen that the R_n values obtained using the Bridge Method and using the SS technique are generally in agreement and the trend in the performance of the coating is tracked by both methods. Of particular interest is the increase in R_n value at around 500 hours. The exact cause of this phenomena is not known, but the important point is that both techniques have indicated this, leading to the conclusion that it was caused by a change in the test cell and not an electrical artefact. The apparatus used for the two different techniques involved the use of different calomel electrodes and there was obviously a time separation between the tests.

The Single Substrate method has returned slightly higher values in the early part of the test and this is attributed to the fact that the SS technique is more stable during early measurements because SCE's are acting as working electrodes and have closer potentials as explained in chapter 4. The nature of the two tests also means that a direct and exact comparison cannot be made because the two cells that make up the pair can never be the same (see note) and this will obviously affect the values of R_n . In an attempt to minimise this effect the data for the graph was averaged from the three Bridge Method results and four SS technique results using the geometric mean.

Note: The nature of the two techniques necessitates the use of different pairs of cells for any combination. This is because the SS technique uses only those cells attached to one panel giving the combinations shown in the diagram (Figure 7.13).

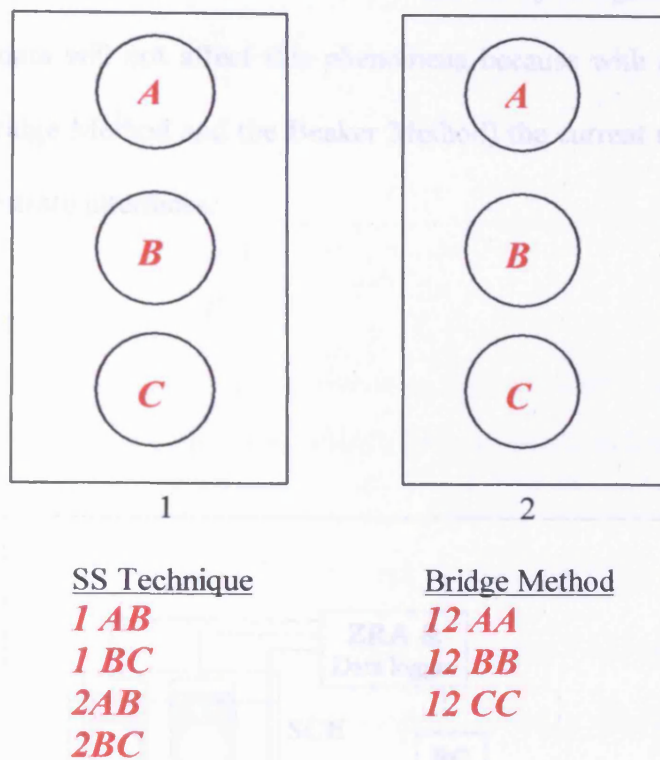


Figure 7.13 Schematic representation for the combination of cells giving pairs for the SS Technique and Bridge Method

7.3.2.1 Combinations of cells to identify failed coating area.

From diagram 7.13 it can be seen that a minimum of four combinations is required to give ENM data for all cells on each panel, whereas the Bridge Method can cover all cells in three combinations. The two individual cells which make up a pair can be altered to determine which particular cell has failed. This will manifest as a low R_n value, which by a process of elimination, using different cells to make-up the pair can be identified. This can be done of course with either technique and is based on the assumption that a low coating resistance in one cell will cause the R_n value to be low for that pair. This has been investigated (Bierwagen, 1994b) and the low R_n value is attributed to the (relatively) low potential noise that is produced between the failed cell and the reference electrode. Low current noise is still

characteristic due to the high impedance / resistance of the good coating between the two working electrodes. (See schematic of the ENM test set-up in Figure 7.14). The technique for obtaining ENM data will not affect this phenomena because with all three methods the (SS technique, the Bridge Method and the Beaker Method) the current noise is generated through two coating / substrate interfaces.

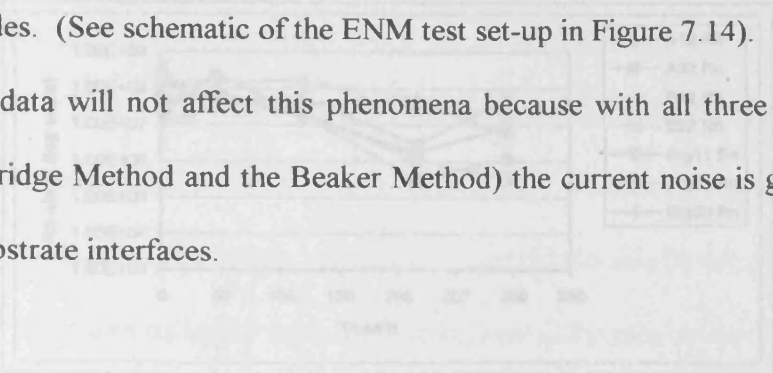


Figure 7.13 Data from individual cells using the Bridge Method and the SS Technique for RH Alkyd on Fe in Harrison's solution diluted to 10%

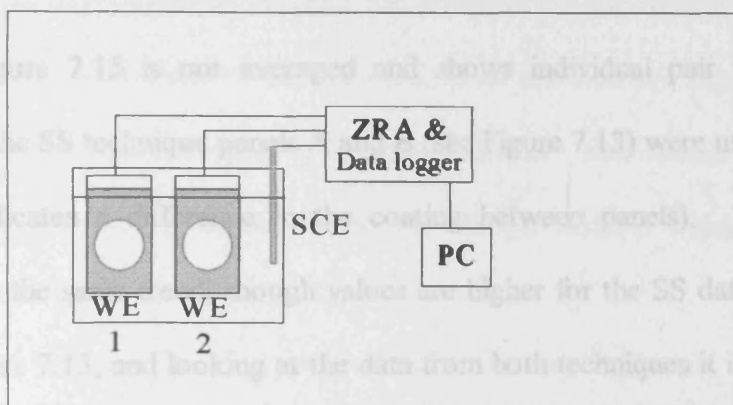


Figure 7.14 Schematic Beaker Method set-up

7.3.3 Results from the Single Substrate Technique compared to the Bridge Method using RH Alkyd

The third experiment in this section investigated the performance of the RH alkyd, which was characterised in section 5.7 as an intact coating on steel. Two coats applied by spreader bar gave a coating thickness of 90 +/- 10 µm and the solution used was Harrison's solution diluted to 10%. The conditions for the experiment and preparation repeated those used in section 5.7, but in this work the SS technique was used in addition to the Bridge Method for each test. The original data for the graphs in Figures 7.15 and 7.16 is contained in appendix 4, tables 3 and 4.

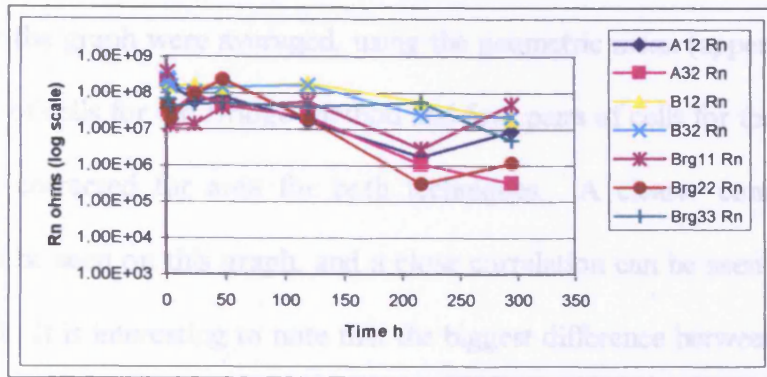


Figure 7.15 Data from individual cells using the Bridge Method and the SS Technique for RH Alkyd on Fe in Harrison’s solution diluted to 10%

The data on Figure 7.15 is not averaged and shows individual pair values without area correction. For the SS technique panels A and B (see Figure 7.13) were used. (The separation in R_n values indicates a difference in the coating between panels). The Bridge method generally follows the same trend, though values are higher for the SS data on panel B. With reference to Figure 7.13, and looking at the data from both techniques it is possible to identify a “weak” cell. E.g. Single Substrate - (A-32) and Bridge (22) are low at 300 hr’s, Single Substrate (B-32) is still high and Bridge (33) is still high. Conclusion – Panel A, Cell 2, has a coating breakdown. This data corresponded with blistering of cell A2 which despite this showed no corrosion beneath the coating.

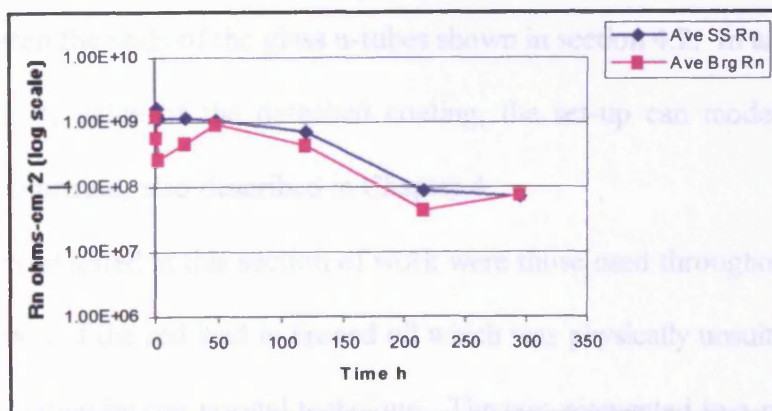


Figure 7.16 Averaged R_n values using the geometric mean for each technique. The R_n values are corrected for area

The values for the graph were averaged, using the geometric mean (appendix 4, table 4), over the three pairs of cells for the Bridge Method and four pairs of cells for the SS technique. The R_n values are corrected for area for both techniques. A clearer comparison of the two techniques can be seen on this graph, and a close correlation can be seen between the SS and Bridge method. It is interesting to note that the biggest difference between the two techniques is in the very early stages of testing where the data is less stable. Drift has not been corrected in this data in an attempt to show this advantage of the SS technique. In general less drift is evident using the SS technique because the potential of the two SCE's connected to the working electrode connections of the zero resistance ammeter are much more stable. More importantly the electrodes are closer to the same potential. This compares to the two substrate elements acting as working electrodes in the Bridge Method which may be at different potentials.

7.4 ENM Results on Detached Coatings

The results presented in this section are from experiments using coating detached from the substrate. The coatings were prepared on glass plates and removed by the methods described in section 3.2. The detached coatings were cut into small areas about 2 cm² in area for mounting between the seals of the glass u-tubes shown in section 4.2. In addition to being able to measure the R_n value of the detached coating, the set-up can model the situation of a coating on the substrate, also described in Chapter 4.

The coatings investigated in this section of work were those used throughout Chapters 5 and 6 with the exception of the red lead in linseed oil which was physically unsuitable for preparation as a detached coating by our normal technique. The non-pigmented two-pack epoxy, the CM two-pack epoxy and the RH solvent based alkyd were used. Some results are also presented

from detached water-borne coatings, acrylic and Haloflex, which were investigated in section 5.5.

7.4.1 Results from detached waterborne 152 compared to “on the substrate” values

The first two experiments in this section were a preliminary investigation of the waterborne unpigmented water based amine two-pack epoxy.

The Bacon, Smith and Rugg criteria is based on the premise that corrosion prevention by a coating is related to its ionic transfer resistance. This does not take into account the effect of chemical inhibition which has been shown to affect DC resistance (Mabbutt and Mills, 1997) and in previous chapters of this work R_n at the lower resistance end of the scale ($\sim 5 \times 10^4$ ohm-cm²). At higher values, in excess of 1×10^6 ohm-cm², the Bacon, Smith and Rugg criteria gives a good indication of protection ability using both the DC and R_n method. If the ionic resistance of the coating is responsible for the level of protection it follows that useful information can be gained about a coating by measurement of the detached coating.

Table 7.1 compares the values of R_n of 152 epoxy in the detached state and on the substrate, the coating thickness was 100 μ m. DC resistance was also used at intervals as a comparison for the detached samples when the resistance had dropped (after 90 hours). In this experiment DC resistance was not used earlier in the test because it was thought that the applied voltage from the electrometer might disturb the system. All values are corrected for area and are in ohm-cm².

Time h	R_n 152 on Fe	R_n 152 detached	R_{dc} 152 detached
24	4.75e8	1.33e8	
96	2.59e8	2.00e6	2.45e6
180	3.15e8	5.22e6	
430	1.55e8, DC= 3.2e8	1.01e6	1.93e6

Table 7.1 Comparison of Attached and Detached 152 epoxy in 3% NaCl

The data shows that initially the values of R_n and R_{dc} are very similar. However, by 96 hours there is a significant difference between the two. The DC value of the detached coating compares well with the R_n value which appears to indicate that ENM is measuring the same property as R_{dc} in the situation of a detached coating. The difference between the detached and attached values was attributed to the fact that water is being absorbed from both sides of the coating in the detached state as opposed to just one when it is on the substrate. This accounts for the more rapid drop off in resistance indicated by R_n and R_{dc} for the detached sample.

7.4.2 Results of detached and attached Pigmented CM epoxy in Harrison's solution

The following experiment used the pigmented CM epoxy and was checked with R_{dc} at periods during the test for both attached and detached coating. The tests were conducted in Harrison's solution diluted to 10%. The coating thickness was ~ 120 μm and the values for the substrate resistance were averaged over three pairs of samples using the arithmetic mean. The data tables for Figures 7.17 and 7.18 are contained in appendix 4.

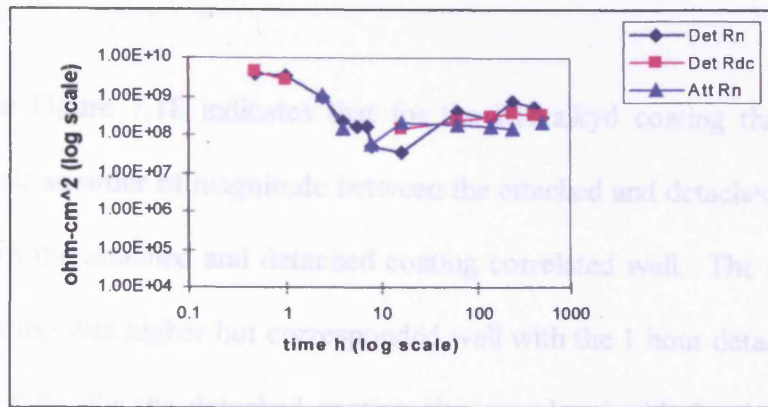


Figure 7.17 Detached and Attached CM epoxy in Harrison's solution

It can be seen in Figure 7.17 that the detached and attached R_n values correlate well and follow the downward trend in resistance with time. All values are corrected for area and are in ohm-cm^2 . The R_{dc} values are very close to the R_n values for the detached coating which agrees with the findings of the preliminary experiment in 7.4.1.

7.4.3 Results from detached and attached solvent based alkyd in Harrison's solution

Figure 7.18 shows detached R_n values for RH alkyd compared to the on substrate R_n values. The coating was $\sim 70\mu\text{m}$ thick produced by one coat. DC resistance values were taken at the beginning and end for the detached samples.

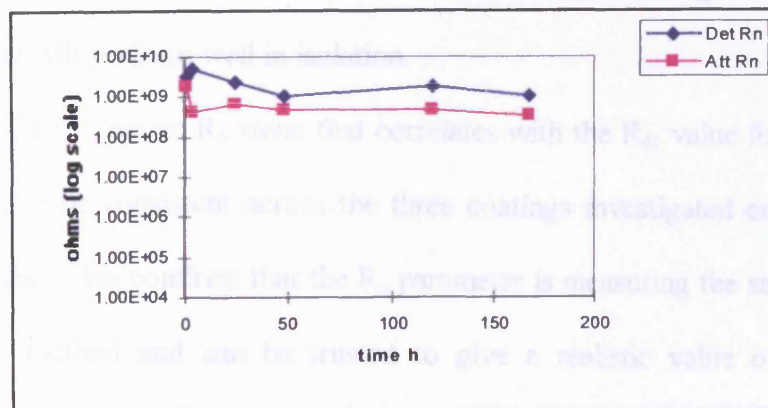


Figure 7.18 Detached and Attached RH alkyd in Harrison's solution

The graph in Figure 7.18 indicates that for the RH alkyd coating there is a difference on average of half an order of magnitude between the attached and detached values. Initial values of R_n for both the attached and detached coating correlated well. The initial R_{dc} value of the detached coating was higher but corresponded well with the 1 hour detached value of R_n . The final values of R_{dc} for the detached coating also correlated with the detached R_n value. The alkyd on the substrate failed by blistering before 200 hours and performed poorly from the early hours of the experiment indicated by the early fall off of R_n value. The RH alkyd was seen to perform poorly in the intact experiments in Chapter 5, and this appears to be because of water absorption.

7.4.4 General observations on detached coating investigation by ENM

The 152 unpigmented epoxy had a water based amine content and past work has shown [218], that water based coatings have a greater absorption rate than solvent based coating. The RH alkyd has also shown to have a higher water uptake. Both of these coatings differed in behaviour on the substrate compared to being investigated in the detached state and this was reflected in the R_n values. The solvent based CM epoxy performed extremely well on the substrate and the detached and attached data correlated well. Detached coating measurement can be of use for indicating the ionic resistance of a particular coating but it cannot be assumed that the coating will perform well in isolation.

The use of ENM to give an R_n value that correlates with the R_{dc} value for a detached coating has been seen to be consistent across the three coatings investigated and from high to low resistance values. This confirms that the R_n parameter is measuring the same properties as the DC resistance method and can be trusted to give a realistic value of resistance without imposing any external potential to the system.

CHAPTER 8

Conclusions and Further Work

8.1 Conclusions from Chapter 5

The experiments on the intact water-borne coatings gave initial findings that R_n is an indicator for the protection afforded by water-borne coatings in much the same way as D.C. resistance. The R_n parameter successfully ranked the water-borne amine, 2-pack epoxy and this correlated with visual and accelerated high temperature tests run to degradation.

Figure 5.9 in chapter 5 shows the range of coatings tested all on the same graph. Although solutions differed, conduction values were close and the difference in values of R_n are attributed to the resistance of the coating under investigation. This graph shows that ENM and in particular the parameter noise resistance (R_n) can be used with confidence to rank coating systems. This would make the technique a valuable tool in formulation, in quality control and in condition monitoring, as well as for laboratory applications in the study of inhibitors and new materials.

8.2 Conclusions from Chapter 6

Scribe production was improved by the use of laser ablation and then mechanically produced scribes using a special tool. Although slower to create the latter were of consistent area and gave reproducible results. Results from the laser produced scribes in the same CM epoxy coating correlated well with those from the mechanical scribes. This indicated that the laser method was not having an adverse effect on inhibitor performance in this coating.

ENM was successfully used to distinguish between inhibition provided by potassium dichromate to steel in sulphuric acid. The R_n value being, on average, of in excess of an order of magnitude higher at around 1×10^5 ohms-cm² compared to freely corroding steel in the same

molarity acid. This work was extended to leached inhibitor from Haloflex coating which was used to inhibit corrosion in equi-molar NaCl solution. Again ENM showed a difference in the R_n values, in this situation around half an order of magnitude between inhibition and freely corroding steel in equi-molar solution. Experiments on waterborne anti-corrosive coating (Neocryl and Haloflex) scribed through to the substrate produced R_n values averaging at low 1×10^4 ohms and little or no corrosion protection was seen. The CM epoxy and RH alkyd returned results of around 1×10^5 ohms and demonstrated some protection in Harrison's solution diluted to 10%. Because the alkyd showed signs of adhesion failure and red rust at the scribe further experiments were carried out on the CM in different environments against a control coating of non-pigmented 152 epoxy. The CM was seen to perform well in the Harrison's solution, forming a dense corrosion product, whereas the control coating corroded freely at the scribe. The R_n values reflected the difference in protection level between the two coatings with the CM producing R_n values in excess of 3×10^5 ohms and the control around 1×10^4 ohms.

In NaCl the CM coating did not inhibit the scribe and it was seen to corrode freely. In this instance the R_n value for the CM coating matched that of the freely corroding non-pigmented control coating 152.

Red lead in linseed oil was investigated in the scribed condition because of the proven success of this coating in preventing corrosion at scribes by inhibition. The red lead was found to perform well following a period of soaking in de-ionised water which allowed the inhibitor to become mobile and form a protective oxide before being exposed to the more aggressive Harrison's solution.

The findings of the scribe work in Chapter 6 have led to a criteria of R_n value which can be used to assess if a coating is providing protection at a scribe.

The values are contained in Table 8.1.

LEVEL OF PROTECTION	R_n value absolute- std scribe	R_n value ohms-cm ²
No Protection	$< 5 \times 10^4$	$< 1 \times 10^3$
Borderline Protection	$\sim 2.5 \times 10^5$	$\sim 5 \times 10^3$
Full Inhibition at Scribe	$> 2.5 \times 10^6$	$> 5 \times 10^4$

Table 8.1 R_n values for scribed coatings

It was considered useful to convert the values to Ohm-cm² so that the effects of inhibitor can be cross referenced to different dimension scribes.

Two assumptions are made for the conversion to ohms - cm² values presented here. Firstly, because the scribes are effectively bare metal, corrosion of the exposed area is taken to be uniform. This was seen to be the case for all of the scribes investigated in chapter 6. Secondly, because the corrosion is uniform the resistance is taken to have an inverse and linear relationship to the area exposed (Cottis and Turgoose, 1994).

Note: The “throw” of an inhibitor; the linear distance across the exposed substrate from the edge of the coating that will be inhibited will be a fixed parameter. Therefore the use of scribes of different dimensions must be used with this in mind and may not directly correlate with values corrected for area from 0.2 mm wide scribes.

8.3 Conclusions from Chapter 7

Data analysis was done on data sets obtained from intact coatings subject to ENM tests in Chapter 5. It was found that in accordance with the literature that the frequency distribution of the data was of a Gaussian or normal distribution (Bissell, 1990). When compared to frequency distribution plots from ENM data sets taken from scribed samples a distinct difference became apparent. It is probable that, in the condition where inhibitive or semi-inhibitive processes are functioning at the scribe, the data distribution deviates from a purely Gaussian form and exhibits what appears to be a bi-modal distribution in some cases. This may be of use in future work in determining mechanistic information about processes at scribes or other coating holidays without transforms into the frequency domain or other complex mathematical techniques.

Investigation of detached coating using specially built glass cells showed good correlation in performance of the coating and associated R_n values. This was backed up by DC resistance data. The anomaly of lower resistance in the early stages of testing is attributed to solution ingress into both sides of the coating while in practice this only occurs from one side.

The development of the Single Substrate Technique is believed to be a particularly successful feature of this work. The method has proven to give consistent results across the range of coatings investigated and across the range of resistance that result from extended testing in immersion conditions. The R_n values derived from ENM data obtained from the Single Substrate Technique correlate with the R_n values from the more traditional methods of testing and also with DC resistance values. It is worth noting the section (7.3.2) concerned with averaging the R_n values from the specimens. Because the two different techniques, by their nature, mean that the same two cells are never tested together using both techniques. This can be put to the advantage of the investigator as it enables an area of weak coating or a low resistance cell to be identified by a simple process of elimination which cannot be done by the Bridge Method alone.

8.4 Further Work

This project has not been exhaustive and there are still many areas of interest where questions need to be answered. It is hoped that what has been done in this work has contributed to the area of Electrochemical Noise Monitoring and re-enforced it as technique. The author, would from the findings of this research, use ENM and results from it with confidence.

The “pit fall” with ENM is still linear drift of the data sets. With confidence and familiarity this becomes less of a problem and it is believed that the protocol adopted of taking multiple runs gives consistent results that correlate with other electrochemical parameters. However, if ENM is to become a trusted addition to the electrochemical measurement techniques available, it is considered important that corrective procedures be built into the available operating software. This is in contrast to the present situation where the data is first corrected by one piece of software, but then the corrected data needs to be transferred to another software package to re-calculate R_p . A single procedure to perform these operations would be useful to assist ENM analysis.

Apart from the tying together of already available software the technique has scope for further development. With the production of better data manipulation it is believed that mechanistic information can be extracted from time domain data sets. Although localised corrosion was outside the scope of this project there may be advantages to data frequency distribution analysis in that area too.

The development of the Single Substrate Technique into a field application is an important direction for this work to go. This not only applies to coatings investigation but also to other areas of corrosion study. Some preliminary work in this area has already begun with the investigation of re-bar corrosion in concrete and initial findings have shown considerable promise in the technique for this type of application.

Another use of ENM as a non-intrusive monitoring technique has been suggested, whereby the condition of foodstuff containers or the polymer protective coating are monitored. By characterising the ENM response of “good” containers and foodstuff, it is thought that an indication of food condition or container damage may be able to be obtained by the chemical induced changes to the ENM data.

REFERENCES

Al Ansari, M. S. (1998) PhD thesis, UMIST. Manchester, UK

Al Ansari M. S. and Cottis, R. A. (1997) Proc.13th International Corrosion Congress, Melbourne, Australia, (pub.) Int. Corr. Council.

ASTM D4541 - 89 (1989) American Standards for Testing of Materials,
<http://www.asm.org.>, Philadelphia, Penn., USA.

ASTM D 1654 - 92 (1992) American Standards for Testing of Materials,
<http://www.asm.org.>, Philadelphia, Penn., USA.

ASTM D 2247 - 87 (1987) American Standards for Testing of Materials,
<http://www.asm.org.>, Philadelphia, Penn., USA.

Baboian, R. (1985) Electrochemical Techniques for Corrosion Engineering. Pub.
NACE, pp 73-79.

Bacon, B. C., Smith, J. J. and Rugg, F. M. (1948) Ind. Eng. Chem, Vol. 40, pp 161-167.

Bagley G. and Cottis, R. A. (1999) Proc. Corrosion'99 San Antonio, (pub.) NACE, Paper No. 1919.

Balfore, J. G. (1990) Reprinted from JOCCA, Vol 74, 12.

Balfore, J. G. (1996) Reproduced from Surface Coatings international. Vol.79,8, pp 362-366.

Barbucci, A. E. Pedroni & G. Cerisola, Paper from Advances in Corrosion Protection by Organic Coatings ii., pp 122-131, 1995

Bautista, A. and Huet, F. (1999) J. Electrochem. Soc., Vol. 146,5, pp 1730-1736.

Bentley, J. (1987) Chpt. 2, Paint and Surface Coatings theory and practice, (ed.) R. Lambourne, pp 50-51.

Bertocci, U. *et al.* (1997) J. Elec. Chem. Soc., Vol. 144, 1.

Bertocci, U. *et al.* (1997) ECS Meeting Abstracts, (pub.) Electrochem. Society, MA 97-1, No. 125, pp 146-147.

Betts, J. A., (1990) Block 5, Noise - T322 digital telecommunications, Technology: A 3rd level course, The Open uni. - Signal Processing, Modulation and Noise.

Betts, J. A. (1970) Unibooks, English Universities Press, SBN 340 05212 0, Noise, pp 79-95.

Bissell, C. (1990) T322 Digital Telecommunications Block 5 NOISE, The Open University, Technology: a third level course, pp 45 - 47.

Bierwagen, G. P., Mills, D. J. and Tallman, D. (1993) Proc.12th Int Corr Congress, Houston, Texas, (pub.) NACE, Vol 7, pp 4208-4218.

Bierwagen, G. P. (1994) J. Elec. Chem. Soc., Vol 141,11, pp 155-157.

Bierwagen, G. P. *et al.*, (1994a) Rep.-Characterisation of Corrosion Under Marine Coatings by Electrochemical Noise Methods. The Office of Naval Research, Grant No. N 00014-93-1-0013.

Bierwagen, G. P, *et al.* (1994b) Proc. from 1st Int. Symp. On Electrochemical Noise Measurement, (pub. NACE).

Bierwagen, G. P, (1995) Accepted for pub. Prog. Organic Coatings, Private Communication.

Bierwagen, G. P, *et al.* (1995) Proc. Symposium on Advances in Corrosion Protection by Organic CoatingsII, Pub. Electrochemical Society, Vol. 95, p13,

Blank,G. *et al.* (1977) J. Electroanal. Chem., Vol. 75, pp 97-124.

Camina, M. (1986) Complex vanadates as anti-corrosive pigments for one pack etch primers, Tech. Report TR/4/86, (pub.) Paint Research Association.

Camina, M. *et al.* (1990) The Mechanism of Action of Anti-corrosive paints, Final report C6R2, p 25, (pub.) Paint Research Association.

Campbell, D. and Thompson, I. (1994) *Corrosion Science*, Vol.36, 1, pp 187-198.

Carter, E. (1987) Proc. Symposium on anticorrosive pigments, binders and paints, London, (pub.) Paint Research Association (PRA), paper 2.

Chen, C. T. and Skerry, B. S. (1991) *Corrosion*, Vol. 47, pp 598-611.

Chen, J. F. and Bogaerts, W. F. (1995) *Corrosion Science*, Vol 37, 11, p 1840.

Cheng, Y. F., Wilmott, M. and Luo, J. L. (1999) *Corrosion Science*, Vol. 41, pp 1245-1256.

Colstee, E. H. and Waalwijk, B. V. (1997) *Protective Coatings Europe (PCE)*,7, pp.18-23.

Cook, M. I., Walker F. H. and Dubowik, D. A. (1999) *Surface Coatings International (JOCCA)*, Vol. 82,11, pp 528-535.

Cottis, R. A., and Loto, C. A. (1986) *Electrochemical Methods in Corrosion Research* (ed.) M. Duprat, *Mat. Science Forum*, Vol.8, pp 201-214.

Cottis, R. A., Al-Ansari, M. S. and Bagley, G., J. (1997) Electrochemical Soc., MA97-1, Abs 211, p261.

Cottis, R. A. and Turgoose, S. (2000) Corrosion Testing Made Easy: Electrochemical Impedance and Noise, ISBN 1-57590-093-9., (pub.) NACE, pp 56.

Cottis, R. A. and Turgoose, S. (1994) Proc. EMCR'94, Sesimbra, Portugal.

Cottis, R. A. *et al.* (1998) Materials Science Forum, Vol. 289, pp 741-754.

Darwin, A. B. and Scantlebury, J. D. (1995) Proc. of Symposium on Advances in Corrosion Protection by Organic Coatings II, Pub. Electrochemical Society, Vol. 95, pp 219-228.

Dawson, J. L. (1994) Electrochemical Noise Measurement: The Definitive in-situ Technique for Corrosion Applications, Proc. 1st Int. Symposium on ENM for Corrosion Applications, (pub.) NACE.

Dawson, J. L. (1996) Electrochemical noise Measurement for Corrosion Applications, ASTM STP 1277, pp 3-35.

Donohoe, C. J. (1995) Electrochemical Noise Behaviour of Temper Embrittled Steels, MSc Thesis, UMIST.

Eden, D. A., Hoffmann, D. and Skerry, B. A. (1986) ACS Symp. American Chem. Soc. Washington. (ed.) R. A. Dickie and Floyd, Serial. No. 322.

Eden, D. A. *et al.* (1986) Corrosion'86, (pub.) NACE, paper 274.

Fei, Z., Hudson J. L. and Kelly, R. G. (1994) J. Electrochem. Soc., Vol. 141,9.

Guruviah, S. J. (1970) J. Oil. Col. Chem. Ass., Vol 53, pp 669-679.

Gabrielli, C. (1990) Use and Applications of Electrochemical Impedance Techniques, (Technical report-Issue A : March), Private communication.

Geenen, F. M., De Wit, J. H. W. and Van Westing, E. P. M. (1990) Progress in Organic Coatings, Vol.18, pp- 299-312.

Gowers, K. R. and Scantlebury, J. D. (1983) Corrosion Science, Vol.23, 9, pp.935-942.

Gusmano, G., Montesperelli, G. and De Grandis, A., (1998) Electrochemical Methods in Corrosion Research VI, pt 2, (pub.) Trans Tech Publications Ltd., (ed.) P. L. Bonora and F. Deflorian, pp 763-770.

Haagen H. and W. Funke, (1975) J. Oil. Col. Chem. Ass. Vol. 58, pp 359-364,

Harrison, J. B. (1970) J. Oil and Col.Chem. Ass. [n.d].

Hernandez, L. S. *et al.* (1998) *Surface Coatings International (JOCCA)*, Vol.81, 1, pp19-25.

Hirozawa, T. and Turcotte, D. E. (1991) *Electrochemical Impedance - Analysis and Interpretation*, ASTM STP 1188, (ed.) Scully, Silverman and Kendig, pp 205-219.

Hladky, K. and Dawson, J. L. (1981) *Corrosion Science*, Vol. 21, 4, p. 317.

Howarth, G. A. (1998) *I.Corr / OCCA symposium*, SURFEX, Harrogate, 23 June.

Iverson, W. P. (1968) *Journal of the Electrochemical Society*, Vol. 115, 6, pp 617 - 618.

Jeffcoate, C. *et al.*, *Corrosion*, Pub NACE, Vol. 54, No. 10, pp 763 - 771, 1998

Jochems, P. A., Hotland and Bradley, S. (1999) Environmentally acceptable coating systems for use on overhead line towers, *Surface Coatings International (JOCCA)*, Vol. 82, 11, pp 544-545.

Jones, D. A. (1996) *Principles and Prevention of Corrosion 2nd Ed.* Chapter.5, pp 143-145.

Karrab, S. A. (1998) MSc Thesis, UMIST, Manchester, UK.

Kearns, J. R. *et al.* (1996) Electrochemical noise Measurement for Corrosion Applications, ASTM STP 1277, American Standards for Testing of Materials, Philadelphia, Penn., USA.

Kelly, R. G., Inman, M. E. and Hudson, J. L. (1997) Electrochemical noise Measurement for Corrosion Applications, ASTM STP 1277, pp 101-113,

Lambourne, R. (1987) Paint and Surface Coatings - theory and practice, (ed.) Lambourne, (pub.) Ellis Horwood, pp 29 - 32.

Leban, M. *et al.* (1998) Electrochemical Methods in Corrosion Research VI, pt 1, (pub.) Trans Tech Publications Ltd., (ed.) P. L. Bonora and F. Deflorian, p - 157.

Legat, A. J. *et al.* (1998) Materials Science Forum, Vol. 292, pp 807-812.

Legat A. and Dolecek, V. (1995) J. Electrochem. Soc., Vol. 142, 6.

Li, J. Jeffcoate, *et al.* (1994) Corrosion, Vol.54, 10, pp 763-771.

Loto C. A. and Cottis, R. A. (1987) Corrosion, Vol.43, 8.

Loto C. A. and Cottis, R. A. (1989) Corrosion, Vol. 45, 2.

Mabbutt, S. J. and Mills, D. J. (1997) Surface Coatings International (JOCCA), Vol. 80, 1, pp 18-25.

Mabbutt, S. J. and Mills, D. J. (1998) *British Corrosion Journal*, Vol. **33**, 2, pp 158-160.

Mayne, J. E. O. (1987) How paints protect metals from corrosion, Proc. Symposium on Anti-corrosive pigments, binders & paints, Paint Research Association, paper 1.

Mayne, J. E. O. (1990) *JOCCA*, Vol. **73**, p 413.

Mayne, J. E. O. and Burkill, J. A. (1995) *JOCCA*, Vol. **71**, p - 273.

Malo, J. M. and Velazco, O. (1996) Electrochemical Noise Measurement for Corrosion Applications, ASTM STP 1277, pp.387-397.

Mansfeld, F., Han, L. T. and Lee, C. C. (1996) *J. Electrochemical Soc.*, Vol. **143**,12, pp 286-289.

Mansfeld, F. and Lee, C. C. (1997) *J. Electrochem. Soc.*, Vol **144**, 6.

Mansfeld, F. and H. Xiao, (1996) Electrochemical Noise Measurement for Corrosion Applications, ASTM STP 1277, pp. 59-78.

Mendoza J. A. and J. M. Sykes, Mechanism of action of anti-corrosive paint, Paint Research Association (PRA), Final interim report - Section 7, Proj. ref. C6R2.

Meszaros, L. *et al.* (1996) *J. Electrochem. Soc.*, Vol. **143**, 11.

Metikis, M. *et al.* (1991) *Electrochemical Noise Measurements for the Evaluation of the Protective Properties of Organic Coatings in Marine Atmospheric Environments*, Available www.intercorr.com/intercorr/techsess [accessed May 1997].

Michael, C. *et al.*, (1981) *Conference Proc. Corrosion Control by Organic Coatings*, Lehigh, (pub.) NACE, pp 288-310.

Mickalonis, J. I. *Et al.* (1996) *Electrochemical Noise Measurement for Corrosion Applications*. ASTM STP 1277. pp 201-213.

Mills, D. J. (1974) PhD Thesis, University of Cambridge,

Mills, D. J. and P. J. Boden, (1993) *Corrosion Science*, Vol **35**, 5, pp 1311-1318.

Mills, D. J. *et al.*, (1993) *Proc. 12th Int. Corr. Congress*, Vol. **1**, pp 182 - 193.

Mills, D. J. *et al.* (1995) *Materials Performance*, Vol. **34**, pp 33 - 38.

Mills, D. J. and Mabbutt, S. J. (1997) *EUROCORR'97*, Proc. Event No. 208, pp 605-616.

Mills, D. J. and Mabbutt, S. J. (1998) *Advances in Corr. Protection by organic Coatings III*, pp 89 - 100.

Mills D. J. and Mabbutt, S. J. (1999) *Proc. 14 Int. Corr. Congress, Cape Town, S. Africa.*

Mills, D. J and Mabbutt, S. J. (1998) *Pigment & resin Technology*, Vol. **27**, 3, pp 168-172.

Mills, D. J. and Mayne, J. E. O. (1981) *Corrosion Control by Coatings (NACE)*, p 12.

Moon, M. and Skerry, B. (1995) *Journal of Coatings Technology*, Vol. **67**, pp 35 - 44.

Murray, J. N. (1997a) *Electrochemical Test Methods for Evaluating Organic Coatings on Metals: An Update part II, Progress in Organic Coatings.*

Murray, J. N. (1997b) *Electrochemical Test Methods for Evaluating Organic Coatings on Metals: An Update part III, Progress in Organic Coatings.*

Pistorius, P. C. (1997) *Corrosion (NACE)*, Vol. **53**, 4, pp 273-283.

Reck, E. and Richards, M. (1997) *Surface Coatings International (JOCCA)*, Vol. **80**, 12, pp 568-572.

Reichert, D. L. (1996) Electrochemical Noise Measurement for Corrosion

Applications, ASTM STP 1277, pp 79-89,

Reid, K. and Weidmann, G. (1990) Structural Materials, (ed) Weidmann, Lewis and

Reid, p 151.

Richter, W. (1991) The link between electrochemical noise and electrochemical

impedance measurements, [s.l.] Private Communication.

Scantlebury, D. (1984) Coatings and Surface Treatment for Corrosion and Wear

Resistance Ed. Strafford, *et al.*, Pub. Elsevier.

Scantlebury, D and Ho, K. N. (1979) J. Oil. Col. Chem. Assoc., **62**, pp 89-92.

Scully, J. R. (2000) Corrosion (NACE), Vol. **56**, 2, pp 199 - 218.

Skerry, B. S. and Eden, D. A. (1987) Prog. Org. Coat., **15**, pp 269-285.

Skerry, B. S. and Eden, D. A. (1989) Corrosion Protection by Organic Coatings, Proc.

Conference, Christs College, Cambridge, pp 373- 393.

Skerry, B. S. and Eden, D. A. (1991) Progress in Organic Coatings, **19**, pp 379-396.

Skully, J. R. (2000) Corrosion (NACE), Vol. **56**, 2, pp 199 - 218.

Souto, R. M. and Burstein, G. T. (1998) Materials Science Forum, Vol. **292**, pp 799-806.

Sykes, J. M. (1987) Extended Abs. from Symposium on Anti-corrosive pigments, binders & paints, Paint Research Association, paper 9, pp 33 - 35.

Thomas, J. G. N. and Bernie, J. A. (1987) Extended Abs. from Symposium on Anti-corrosive pigments, binders & paints, Paint Research Association, paper 14, pp 57 - 60.

Thompson, I. and Campbell, D. (1994) Corr. Sci., Vol **36**, 1, pp. 187-198.

Thompson, I. and Campbell, D. (1995) Corr. Sci. Vol. **37**, 1, pp 67-78.

Turgoose, S. and Cottis, R. A. (1991) Electrochemical Impedance - Analysis and Interpretation, ASTM STP 1188, pp 173-191.

Walter, G. W. (1981) J. Electroanal. Chem., Vol. **118**, pp 259 - 273.

Wittman, M. W. and Taylor, S. R. (1995) Advances in Corrosion Protection by Organic Coatings ii., pp 158-168.

Wormwell, F. and Brasher, D. M. (1949) Journal of the Iron and Steel Institute, Vol. **162**, pp 129-135.

Wranglen, G. (1972) *An Introduction to Corrosion and Protection of Metals*, Chpt. 4.3, pp 210 - 203, pub. Butler and Tamer Ltd.,

Xiao, H. and Mansfeld, F. (1994) *Journal of the Electrochemical Society*, Vol. **141**, No.9, pp 2332-2337.

H. Xiao, *et al.* (1997) *Corrosion*, (NACE), Vol. **53**, 5, pp, 412-422.

Appendix 1

Data Number	Positive Kurtosis set Numeric Value	Negative Kurtosis set Numeric Value
1	2	2.01
2	2	2.01
3	2	2.05
4	2	2.1
5	2	2.15
6	2	2.18
7	2.2	2.19
8	2.2	2.18
9	2	2.1
10	2	2
11	2	2
Kurtosis value	+ 2.037	- 1.857

Table 4.1 Data sets for positive and negative kurtosis

Time h	Specimen 1A	Specimen 1B	Specimen 3A	Specimen 3B
1	1.69E5	1.25E5	1.42E5	3.13E5
2	1.95E5	3.05E5	2.18E5	1.98E5
4	5.12E4	4.18E4	1.05E5	2.03E5
8	3.50E4	2.98E4	5.87E4	6.92E3
24	1.34E5	3.83E4	2.60E4	4.13E4
48	6.02E4	4.42E4	8.95E4	1.25E4
96	1.72E5	1.71E4	2.70E4	1.47E4
172	4.44E4	2.79E4	4.09E4	1.82E4

Table 4.2 Uncorrected data for scribed alkyd coating on Fe in 1% Harrison's solution

Time h	Specimen 1A	Specimen 1B	Specimen 3A	Specimen 3B
1	1.73E5	1.88E5	1.33E5	1.74E5
2	1.88E5	1.96E5	2.19E5	1.24E5
4	1.49E5	3.99E4	9.00E4	1.75E5
8	4.38E4	3.10E4	2.17E4	1.45E4
24	1.30E5	4.29E4	2.48E4	4.20E4
48	6.08E4	4.27E4	8.42E4	1.26E4
96	3.52E5	1.62E4	2.71E4	2.20E4
172	4.93E4	2.67E4	3.00E4	1.63E4

Table 4.3 Corrected R_n values for scribed alkyd results shown in table 4.2

Appendix 2

SAB1 - 3 pairs of cells 11.8 cm² on steel substrate

AAB1 - 3 pairs of cells 11.8 cm² on aluminium substrate

(S = steel substrate, AB = Cells A and B, 1 = sample 1)

Time hours	SAB1	SAB2	SAB3	AAB1	AAB2	AAC3
1	1.21E8	1.12E8	6.45E7	2.04E6	6.98E6	2.04E7
4	5.92E7	2.73E7	1.87E7	1.46E6	1.11E6	3.83E6
27	5.98E7	1.08E8	9.88E7	4.46E7	9.36E6	1.98E7
47	3.29E7	1.76E7	8.17E7	8.01E7	2.90E7	2.15E7
147	3.17E7	3.78E7	5.64E7	5.33E7	2.70E7	1.19E7
456	8.32E7	1.36E8	4.14E7	5.18E7	2.03E7	6.33E7
1990	4.30E8	2.72E8	1.09E8	5.33E8	3.94E8	8.30E7

Table 5.2 Intact R_n values for solvent based alkyd on Fe and Al

Time	Cell A	Cell A	Cell B	Cell B	Cell C	Cell C	Cell D	Cell D	A - C	B - D
h	R_{dc}	mV	R_{dc}	mV	R_{dc}	mV	R_{dc}	mV	R_n	R_p
1	8.50E8	50	9.00E8	80	9.50E8	90	1.1E10	70	7.76E8	1.93E8
4	1.90E8	100	2.10E8	100	2.30E8	110	3.20E8	90	7.73E7	3.58E7
24	9.00E7	130	1.0E8	110	1.10E8	100	1.20E8	110	3.06E7	6.73E7
48	3.50E7	110	7.00E7	120	6.80E7	110	6.70E7	110	1.43E7	2.34E7
168	3.00E5	140	7.00E5	100	8.00E5	130	5.00E5	120	7.78E5	2.90E6
436	5.00E5	140	6.00E5	110	7.00E5	120	1.00E6	110	4.89E5	8.72E5
604	6.00E5	-270	1.10E6	120	1.10E6	0	1.10E6	110	7.56E5	2.58E6
1017	1.20E6	-70	1.20E6	100	1.30E6	50	3.30E6	100	7.75E5	2.00E6
1201	2.00E6	-100	2.20E6	120	2.30E6	120	6.0E6	100	2.14E5	9.60E5

Table 5.3 R_n and R_{dc} values for Neocryl on steel in 10% Harrison's solution.

Time h	Cell A R_{dc}	Cell A mV	Cell B R_{dc}	Cell B mV	Cell C R_{dc}	Cell C mV	Cell D R_{dc}	Cell D mV	A - C R_n	B - D R_n
1	9.00E3	-550	1.00E4	-560	7.00E3	-570	7.00E3	-570	6.76E4	6.96E4
4	7.00E3	-630	6.00E3	-630	6.00E3	-630	6.00E3	-630	2.84E5	2.28E5
24	5.00E3	-680	6.00E3	-690	6.00E3	-680	5.00E3	-690	4.66E4	2.02E4
48	6.00E3	-690	7.00E3	-700	7.00E3	-700	7.00E3	-690	7.43E3	1.29E4
168	5.00E3	-700	5.00E3	-700	5.00E3	-710	6.00E3	-700	5.80E3	2.54E4
436	6.00E3	-700	7.00E3	-700	5.00E3	-710	5.00E3	-700	4.95E3	1.30E3
604	7.00E3	-700	7.00E3	-700	6.00E3	-710	6.00E3	-700	1.55E4	3.89E3
1017	8.00E3	-690	9.00E3	-710	7.00E3	-700	6.00E3	-700	5.13E5	7.46E3
1201	8.00E3	-700	1.00E4	-690	9.00E3	-700	7.00E3	-710	1.68E4	5.52E3

Table 5.4 R_n and R_{dc} values for Haloflex on steel in 10% Harrison's solution.

Time h	R_n 148 A-C	R_n 148 B-D	R_n 152 A-C	R_n 152 B-D
1	3.22E9	4.17E8	3.12E10	1.16E10
4	3.50E7	5.73E7	4.66E8	5.28E8
8	1.23E7	1.75E7	1.75E8	8.98E7
24	7.36E6	1.11E6	1.85E7	4.03E7
48	1.12E7	8.40E5	3.27E7	4.23E7
72	5.82E6	1.14E6	2.05E7	2.36E7
310	2.58E6	1.59E6	2.45E7	2.86E7
485	2.27E6	2.63E6	1.68E7	1.41E7
700	7.36E5	1.26E6	7.62E6	5.76E6
816	4.23E6	6.82E6	7.72E6	2.09E7
1200	6.73E6	1.69E6	2.77E7	1.57E7
3050	1.16E6	6.75E6	3.42E7	5.42E6

Table 5.5 Waterborne amine 2-pack epoxy, 148 R_n V 152 R_n .

Time h	R _n CM	R _n CM 7.5cm ²	R _n RH 11.8cm ²	R _n RH 7.5cm ²
	11.8cm ²			
0.5	2.09E9	8.88E8	7.00E6	5.96E6
1	3.48E9	5.03E9	3.25E6	1.65E7
2	1.65E7	6.35E9	3.52E7	4.02E6
4	2.00E8	3.39E8	1.09E6	9.30E5
8	6.82E7	8.16E7	1.62E6	1.18E7
24	1.55E7	1.33E7	7.84E6	1.63E4
48	6.20E5	3.46E7	8.29E6	3.63E4
96	1.34E6	8.57E5	9.70E6	1.31E7
100	2.01E6	1.02E7	3.02E6	2.34E6
168	6.63E5	6.34E6	8.30E7	1.71E6

Table 5.8 R_n values for solvent based (CM) 2-pack epoxy and (RH) alkyd.

Time h	Cells 1-1	Cells 2-2	Cells 3-3
2.0	3.99E8	3.45E8	1.13E8
4.0	4.97E7	2.60E7	4.97E7
8.0	1.85E8	1.88E7	1.25E8
24	2.11E8	2.90E7	5.24E7
48	9.56E7	3.41E7	2.97E7
168	3.90E7	3.16E7	6.55E7
336	3.86E7	2.55E7	5.87E7
408 dried /re-filled	2.18E9	7.75E8	1.04E9

Table 5.10 Further ENM of 2-pack Epoxy (CM)

Time h	R_n intact red lead
1	1.39E7
2	4.25E7
4	3.53E6
8	3.27E6
24	7.13E5
48	4.19E5
72	6.28E5
144	6.78E6

Time h	R_n Sealed intact red lead
1	5.99E7
2	7.25E7
4	2.45E7
8	1.38E7
24	2.39E7
96	7.86E7
120	2.20E7

146	7.69E7
264	4.24E7
480	1.51E8
696	1.03E7

Table 5.12 R_n values for intact and sealed intact red lead on Fe.

Appendix 3.

time h	Neo Rn1	Neo Rn2	Halo Rn1	Halo Rn2
1	1.78E+04	1.08E+04	1.82E+05	4.25E+04
4	2.91E+04	8.31E+04	5.84E+07	1.27E+08
24	2.76E+04	6.80E+04	6.80E+04	7.12E+03
100	4.01E+04	6.43E+03	9.60E+03	4.52E+03
200	2.07E+04	4.64E+03	1.07E+04	8.70E+03
300	4.52E+03	8.49E+03	1.05E+05	1.97E+03
650	1.60E+04	9.90E+04	4.58E+04	1.27E+04

Table 6.1 R_n data for scribed Neocryl and Haloflex in 10 % Harrison's sol.

Time h	CMLA	CMLB	CMMA	CMMB	RHLA	RHLB	RHMA	RHMB
1.0	1.03E5	1.26E5	1.05E5	4.60E4	6.93E4	6.13E4	1.52E5	6.02E4
2.0	1.36E5	5.87E5	4.04E4	4.15E5	3.97E4	1.72E4	2.23E4	1.67E5
4.0	9.60E4	2.09E5	5.29E4	2.88E5	2.64E5	2.86E4	2.24E5	8.77E4
8.0	1.13E4	1.24E5	5.52E4	4.52E4	1.19E4	7.02E4	4.50E4	2.40E4
24.0	1.08E3	6.11E4	3.88E4	1.08E5	4.54E4	9.42E3	1.48E5	9.15E4
48.0	8.29E3	6.53E3	7.47E4	1.93E5	2.16E4	5.03E4	5.45E4	4.56E4
120.0	5.75E4	2.32E4	8.94E3	6.71E4	4.52E4	2.35E4	7.34E4	9.22E4
220.0	2.99E4	3.09E4	4.06E4	6.07E5				
360	2.67E4	6.11E4	1.35E5	4.00E4				
360 R _{dc}	2.1E4	2.0E4	2.5E4	1.1E5				

Table 6.2 CM epoxy and RH alkyd scribed R_n values in 10% Harrison's sol.

time h	CMM Rn	CML Rn	NON Rn
0.5	4.97E+02	7.75E+02	7.85E+02
1	8.01E+02	1.05E+03	2.00E+03
2	1.55E+03	1.20E+03	1.57E+03
4	1.47E+03	1.34E+03	1.30E+03
6	1.19E+03	1.51E+03	4.13E+03
8	7.93E+02	1.17E+03	5.13E+02
24	9.40E+03	3.04E+04	1.03E+05
48	2.63E+04	1.61E+04	7.31E+03

Table 6.3 Scribed CM in 10% Harrison's sol. and 0.4% NaCl

Time h	A-A	B-B	C-C
0.5	9.72E+05	2.05E+05	1.63E+05
1	6.07E+04	5.94E+04	4.74E+04
2	8.15E+04	1.77E+05	2.30E+05
4	1.19E+05	4.81E+05	3.35E+05
15	1.34E+05	4.37E+05	3.70E+05
22	8.12E+05	1.60E+05	1.15E+05
48	2.04E+05	1.40E+05	6.27E+05
72	1.27E+05	4.03E+05	1.44E+05
144	8.72E+04	1.40E+05	6.27E+05

Table 6.4 Scribed Red Lead

Time h

1	3.45E+06
48	2.93E+06
192	1.62E+06
193	7.06E+06
330	7.18E+04

Table 6.5 Scribed Red Lead Soaked in De-ionised water before exposure to Diluted Harrison's solution

Time h	B-F	C-G	D-H
1	1.11E+05	8.44E+04	4.27E+04
2	8.12E+04	1.64E+04	4.17E+05
4	1.00E+05	3.40E+05	1.91E+05
8	1.62E+04	8.32E+04	2.22E+04
24	5.88E+05	8.29E+05	1.01E+06
96	1.54E+05	4.99E+05	3.20E+04
120	7.77E+04	1.80E+05	2.53E+04
146	1.29E+05	1.96E+05	4.27E+04
264	5.96E+05	4.73E+04	5.69E+04
480	4.04E+05	9.60E+04	3.26E+05
696	1.66E+04	2.01E+04	1.90E+04

Table 6.5 Scribed Sealed Red Lead Soaked in De-ionised water before exposure to Diluted Harrison's solution

time h	CMM R _n	CML R _n	NON R _n
0.5	4.97E+02	7.75E+02	7.85E+02
1	8.01E+02	1.05E+03	2.00E+03
2	1.55E+03	1.20E+03	1.57E+03
4	1.47E+03	1.34E+03	1.30E+03
6	1.19E+03	1.51E+03	4.13E+03
8	7.93E+02	1.17E+03	5.13E+02
24	9.40E+03	3.04E+04	1.03E+05
48	2.63E+04	1.61E+04	7.31E+03

Table 6.3 R_n V time for CM coating and 152 control coating scribed in 0.4% NaCl solution.

Appendix 4

time h	Bridge Rn	SS Rn
1	3.06E+10	2.04E+10
5	3.95E+08	5.18E+08
6	7.43E+08	6.51E+08
24	1.58E+08	3.63E+08

Table 7.1 CARRS Alkyd

Time h	Brdg 11	Brdg 22	Brdg 33	SS12A	SS32A	SS12B	SS32B	Ave Brg	Ave SS
2	3.99E+08	3.45E+08	1.13E+08	2.86E+08	5.76E+08	2.52E+08	4.24E+08	3.22E+08	3.94E+08
4	4.97E+07	2.60E+07	4.97E+07	4.18E+07	1.71E+08	8.84E+07	3.89E+08	2.09E+07	1.67E+08
8	1.85E+08	1.88E+07	1.25E+08	1.10E+08	3.76E+07	2.74E+07	1.31E+07	2.16E+07	2.49E+07
24	2.11E+08	2.90E+07	5.24E+07	9.75E+07	1.33E+08	2.58E+07	3.93E+07	1.97E+07	5.45E+07
48	9.56E+07	3.42E+07	2.97E+07	5.32E+07	7.26E+07	3.26E+07	3.99E+07	1.46E+07	3.99E+07

168	3.90E+07	3.16E+07	6.55E+07	4.54E+07	1.46E+07	1.46E+07	5.93E+07	6.32E+07	3.79E+07
336	3.86E+07	2.55E+07	5.87E+07	4.09E+07	4.97E+07	4.97E+07	9.73E+07	2.04E+07	5.43E+07
408	2.18E+09	7.75E+08	1.04E+09	1.33E+09	2.71E+08	2.71E+08	3.11E+08	4.09E+08	3.16E+08
530	1.24E+07	1.40E+08	2.60E+07	5.95E+07	2.92E+07	4.96E+07	2.09E+07	8.29E+07	4.57E+07
2088	3.92E+06	5.17E+06	7.35E+05	3.28E+06	4.78E+05	2.80E+05	5.52E+06	8.58E+06	3.71E+06

Table 7.2 CM Epoxy Not corrected for area.

Time h	A12 Rn	A32 Rn	B12 Rn	B32 Rn	Brg11 Rn	Brg22 Rn	Brg33 Rn
1	3.72E+07	2.19E+08	1.98E+08	2.49E+08	3.75E+08	4.66E+07	6.82E+07
2	1.37E+08	3.17E+07	1.93E+08	2.14E+08	4.55E+07	3.56E+07	6.56E+07
4	1.59E+08	2.78E+07	1.53E+08	1.53E+08	1.29E+07	1.97E+07	4.35E+07
24	6.08E+07	9.27E+07	1.66E+08	1.10E+08	1.36E+07	9.69E+07	4.97E+07
48	7.95E+07	4.55E+07	1.40E+08	1.47E+08	4.00E+07	2.39E+08	5.25E+07
120	1.68E+07	2.21E+07	1.89E+08	1.66E+08	5.80E+07	1.92E+07	4.17E+07
216	1.73E+06	1.09E+06	5.76E+07	2.49E+07	2.87E+06	3.18E+05	5.56E+07
295	8.72E+06	3.33E+05	1.80E+07	2.19E+07	4.99E+07	1.18E+06	4.93E+06

Table 7.3 RH Alkyd

Time h	A12 Rn	A32 Rn	B12 Rn	B32 Rn	Brg11 Rn	Brg22 Rn	Brg33 Rn	Ave SS Rr	Ave Brg Rr	Corr SS Rr	Corr Brg Rr
1	3.72E+07	2.19E+08	1.98E+08	2.49E+08	3.75E+08	4.66E+07	6.82E+07	1.42E+08	1.06E+08	1.67E+09	1.25E+09
2	1.37E+08	3.17E+07	1.93E+08	2.14E+08	4.55E+07	3.56E+07	6.56E+07	1.16E+08	4.74E+07	1.37E+09	5.59E+08
4	1.59E+08	2.78E+07	1.53E+08	1.53E+08	1.29E+07	1.97E+07	4.35E+07	1.01E+08	2.23E+07	1.19E+09	2.63E+08
24	6.08E+07	9.27E+07	1.66E+08	1.10E+08	1.36E+07	9.69E+07	4.97E+07	1.01E+08	4.03E+07	1.19E+09	4.76E+08
48	7.95E+07	4.55E+07	1.40E+08	1.47E+08	4.00E+07	2.39E+08	5.25E+07	9.29E+07	7.95E+07	1.10E+09	9.38E+08
120	1.68E+07	2.21E+07	1.89E+08	1.66E+08	5.80E+07	1.92E+07	4.17E+07	5.84E+07	3.59E+07	6.89E+08	4.24E+08
216	1.73E+06	1.09E+06	5.76E+07	2.49E+07	2.87E+06	3.18E+05	5.56E+07	7.21E+06	3.70E+06	8.51E+07	4.37E+07
295	8.72E+06	3.33E+05	1.80E+07	2.19E+07	4.99E+07	1.18E+06	4.93E+06	5.82E+06	6.62E+06	6.86E+07	7.81E+07

Table 7.4 Averaged RH Alkyd - Using the geometric mean. Data for Graph 7.16 corrected for area.

Time h	Det Rn	Det Rdc	Att Rn
0.5	4.03E+09	4.55E+09	0.00E+00
1	3.45E+09	2.80E+09	0.00E+00
2.5	9.03E+08	0.00E+00	1.00E+09
4	2.25E+08	0.00E+00	1.46E+08
5.5	1.65E+08	0.00E+00	0.00E+00
7	1.62E+08	0.00E+00	0.00E+00
8	4.83E+07	0.00E+00	5.81E+07
16	3.54E+07	1.40E+08	1.93E+08
64	4.31E+08	2.28E+08	1.86E+08
145	2.54E+08	2.80E+08	1.59E+08
240	7.28E+08	3.85E+08	1.43E+08

408 5.04E+08 3.33E+08 0.00E+00

511 2.76E+08 3.33E+08 2.08E+08

Table 7.5 Detached CM epoxy

Time h	Det Rn	Att Rn	Det Rdc
1	3.22E+09	1.92E+09	6.00E+09
4	5.25E+09	4.15E+08	
24	2.34E+09	6.30E+08	
48	9.87E+08	4.60E+08	
120	1.86E+09	4.72E+08	
168	1.05E+09	3.42E+08	7.70E+08

Table 7.6 Detached RH Alkyd.

Appendix 5.

Publications co-author by S. J. Mabbutt.
School of Design and Technology
UCN 1997-2000

REFEREED JOURNALS

1. Comparison of Two Electrochemical Techniques to Investigate Solvent and Water-Borne Anti-Corrosive Coatings, S. Mabbutt and D. J. Mills *Surface Coatings International* **80** (1) pp 18-25 (1997)
2. Novel Techniques for Investigating Anti-Corrosive Coatings, D. J. Mills and S. Mabbutt *Materials World* **8** No 3 (March) p 131-133 (1997)
3. Electrochemical Noise Measurement for Evaluating Anti-Corrosive Paints, D. J. Mills and S. Mabbutt, *Pigment and Resin Technology* **27** No. 3 pp 168-172 March 1998.
4. Novel Configurations for Electrochemical Noise Measurements. S. J. Mabbutt and D. J. Mills *British Corrosion Journal* **33** No.2 pp 158-160 (1998)
5. Electrochemical Noise Signals Method to detect Corrosion, D. J. Mills and S. J. Mabbutt *PPCJ (Polymer Paint Colour Journal)* **190** (April) No 4427 p 8-9 (2000)
6. Scientists intend to use Electrochemical Noise to detect Corrosion, D. J. Mills and S. J. Mabbutt *Asia Pacific Coatings Journal* **13** No 2 p 26-28 (2000)

SUBMITTED PAPERS TO JOURNALS

1. A Review of Recent Work using the Electrochemical Noise Method to Assess Anti-Corrosive Coatings, S. J. Mabbutt and D. J. Mills submitted to *Surface Coatings International*. Oct 2000

REFEREED CONFERENCE PROCEEDINGS/BOOKS

1. Electrochemical Noise Measurement in the Study of Surface Coatings. D. J. Mills and S. Mabbutt *Organic and Inorganic Coatings for Corrosion Prevention - Research and Experiences*, European Federation of Corrosion Publication, No. 20 pub. Institute of Materials (Papers from EuroCorr 96, Nice, France) pp 83-93 Pub. 1997.
2. Inhomogeneities in Organic Coatings - A Look at their Importance to Protection and at Ways of Detecting them, D. J. Mills and S. Mabbutt *Advances in Corrosion Protection by Organic Coatings III*, (proc. conf. Noda, Japan Oct 1997) Ed J. D. Scantlebury, M. Kendig and D. J. Mills Pub. The Electrochemical Society Vol No 97-41 pp 89-100 (1998).
3. Investigation into the Scribe Behaviour of Protective Organic Coatings investigated using SRET (Scanning Reference Electrode Technique) and ENM (Electrochemical Noise Technique), D. J. Mills, S. Mabbutt and R. Akid (Conf. "Advances in Corrosion Protection by Organic Coatings" Christ's College Cambridge Sept. 1999) *Journal of Corrosion Science and Engineering* **2** Paper 18 (2000)
4. Investigation of Defects in Organic Anti-Corrosive Coatings using Electrochemical Noise Method, S. J. Mabbutt and D. J. Mills (presented at Workshop *Application of Electrochemical Techniques to Organic Coatings*, Black Forest, Germany May 1999) *Progress in Organic Coatings* **39** 41-48 (2000)

CONFERENCE PROCEEDINGS

1. The effect of the Substrate on the Electrochemical Response of Protective Coatings D. J. Mills, S. Mabbutt, G. P. Bierwagen, Y. Pae and S. Berg Proc. *13th International Corrosion Congress* Melbourne, Australia paper 482 Nov. 25-29 1996
- 2 Use of Electrochemical Noise Method to study Protection by Anti-Corrosive Coatings and by Inhibitors, D. J. Mills and S. Mabbutt proc. *EuroCorr 97* (Trondheim ,Norway) Ed. E. Bardal (NTNU, Trondheim) Vol II p 605-616 (1997)
3. Use of Electrochemical Noise (ENM) and Other Techniques to Investigate Line Defects in Anti-corrosive Coatings, D. J. Mills, S. Mabbutt, S. Lyon and S. Badger, Proc. *14th International Corrosion Congress* Paper 86, Cape Town (S. Africa). Sept. 26 - Oct. 1 1999
4. Developments in the Electrochemical Noise Method to assess Anti-Corrosive coatings and Inhibitors, D. J. Mills and S. J. Mabbutt Proc. conf. EMCR 2000 (Electrochemical Methods in Corrosion Research) Ed E. Kalman Budapest May 2000
5. A Review of Recent Work using the Electrochemical Noise Method to Assess Anti-Corrosive Coatings, S. J. Mabbutt and D. J. Mills proc. *EuroCorr 2000* Queen Mary and Westfield College London Sept 2000 Coatings session paper 1 (also see submitted papers)

SUBMISSION TO CONFERENCES

- 1) D. J. Mills, N. Short and S. J. Mabbutt Electrochemical Noise Method applied to monitoring of rebar in concrete : comparison with LPR method to submit to EuroCorr 2001 (La Guardia Italy)